

DISS. ETH NO. 28123

**SPATIO-TEMPORAL ELUCIDATION OF THE
VACCINIA VIRUS-INDUCED HOST PROTEOTYPE**

A thesis submitted to attain the degree of
DOCTOR OF SCIENCES of ETH ZURICH

(Dr. sc. ETH Zurich)

presented by

FABIAN WENDT

M.Sc. in Biochemistry, Ruhr-Universität Bochum

born on 17.11.1989

citizen of Germany

accepted on the recommendation of

Prof. Dr. Bernd Wollscheid (examiner)

Prof. Dr. Jason Mercer (co-examiner)

Prof. Dr. Berend Snijder (co-examiner)

2022

Summary

Viral infections can cause severe health, societal and economic problems as we all witness currently on a daily basis during the ongoing pandemic. A molecular understanding of the underlying pathogenesis of viral infections provides a rational basis for the development of anti-viral strategies. Consequently, fundamental research of the last decades has led to antiviral drugs preventing virus propagation, as well as a new era of vaccination strategies. In this thesis, I investigate the molecular biology of the vaccinia virus (VACV) infection, a prototype of the poxvirus family, which includes variola virus, the causative agent of smallpox. Best known is VACV as a live vaccine, whose administration has led to the eradication of smallpox. Extant related zoonotic poxvirus infections, e.g. cow-, and monkeypox zoonoses are rare but can induce serious complications, and fear of spread is conceivable in our globalized world. Besides being a viral vector, VACV gained biomedical relevance as an oncolytic agent in anticancer therapy, as well as being a viral toolbox that aids to understand virus-host interactions.

Although VACV was and is extensively studied, knowledge about the engagement of the surfaceome in virus spread and immune evasion remains largely elusive. The surfaceome is defined as the cellular repertoire of extracellular-residing plasma membrane proteins and bridges extra- and intracellular signaling. Using chemoproteomic strategies enabled me to unravel the surfaceome proteotype following the VACV infection. More than 400 cell surface residing N-glycoproteins were tracked across the viral life cycle in a spatio-temporal fashion, revealing distinct quantitative changes within the surfaceome of VACV infected cells. Ephrin receptor signaling, growth factor receptors, and proteins with immunomodulatory potential, such as immune cell receptors and ligands are regulated upon infection. Moreover, VACV hijacks the human glycosylation machinery and repopulates the surfaceome with N-glycoproteins of viral origin. Spatio-temporal surfaceome analysis revealed that approximately 5% of the viral expressed ORFs localize to the cell surface, of which many are involved in VACV spreading and immune signaling. Upon VACV infection the surfaceome is certainly modulated and likely reorganized, supporting spread and immune evasion.

Immune signaling is orchestrated by soluble ligands and cell surface-residing receptors. The triggered cellular response depends on the signaling architecture affected by trans and cis interactions at the cell surface. Using a newly developed optoproteomic technology, I

contributed to, enabled me to discover the nanoscale organization of cell surface proteins. I investigated the interactome at the host cell surface of the detected VACV protein A40 with unknown function and immunomodulating phenotype. Using proximity-labeling technologies LUX-MS and SPPLAT I showed that A40 is embedded in a network of integrins and basement membrane proteins. One hypothesis is that hijacking these interactions through the C-type lectin-like A40 could help VACV to dysregulate the ECM-immune cell interaction at the infection site.

Together, I provide in this thesis intriguing molecular insights into viral-host pathogenesis with a focus on the VACV-induced modulation of the host surfaceome. Additionally, the data presented show systematically VACV hijacking the cell membrane through its repopulation with viral proteins. Further, surfaceome interactions might play a role in the successful propagation of viruses and should be considered for the development of new anti-viral strategies.

Zusammenfassung

Virusinfektionen können schwerwiegende gesundheitliche, gesellschaftliche und wirtschaftliche Probleme verursachen, wie wir derzeit tagtäglich in der Pandemie erleben. Ein molekulares Verständnis der zugrunde liegenden Pathogenese von Virusinfektionen bietet eine rationale Grundlage für die Entwicklung antiviraler Strategien. So hat die Grundlagenforschung der letzten Jahrzehnte zu antiviralen Medikamenten geführt, die die Virusvermehrung verhindern, sowie zu einer neuen Ära von Impfstrategien.

In dieser Arbeit untersuche ich die Molekularbiologie der Vaccinia-Virus (VACV) Infektion, einem Modellorganismus der Familie der Pockenviren, zu der auch das Variola-Virus, der Erreger der Pocken, gehört. Am bekanntesten ist VACV als Lebendimpfstoff, dessen Verabreichung zur Ausrottung der Pocken geführt hat. Verwandte zoonotische Pockenvirusinfektionen, z. B. Kuh- und Affenpocken, sind zwar selten, können aber schwerwiegende Komplikationen hervorrufen, und die Gefahr vor einer Ausbreitung ist in unserer globalisierten Welt durchaus denkbar. VACV ist nicht nur ein viraler Vektor, sondern erlangte auch biomedizinische Bedeutung als Lebendwirkstoff in der Krebstherapie sowie als viraler Werkzeugkasten, der zum Verständnis der Virus-Wirt-Interaktionen beiträgt.

Obwohl VACV ausgiebig erforscht wurde, ist das Wissen über die Rolle des zellulären Oberflächenproteinsystems bei der Virusausbreitung und der Umgehung des Immunsystems nach wie vor schlecht aufgelöst. Das Zelloberflächenproteom ist definiert als das extrazelluläre Repertoire an Plasmamembranproteinen und bildet die Brücke zwischen extra- und intrazellulärer Signalübertragung. Mit Hilfe chemoproteomischer Strategien konnte ich das Zelloberflächenproteom nach VACV-Infektion entschlüsseln. Mehr als 400 an der Zelloberfläche befindliche N-Glykoproteine wurden entlang des viralen Lebenszyklus räumlich und zeitlich verfolgt, wobei deutliche quantitative Veränderungen im Oberflächenproteom von VACV-infizierten Zellen festgestellt werden konnte. Ephrin-Rezeptor-Signalübertragung, Wachstumsfaktor-Rezeptoren und Proteine mit immunmodulatorischem Potenzial, wie Adhäsionsmoleküle und Immunzell-Liganden, werden bei einer Infektion reguliert. Darüber hinaus kapert VACV die menschliche Glykosylierungsmaschine, um danach das Oberflächensystem mit N-Glykoproteinen viralen Ursprungs neu zu besiedeln. Eine räumlich-zeitliche Analyse des Oberflächenproteomes ergab, dass etwa 5 % der von den Viren exprimierten ORFs an der

Zelloberfläche lokalisiert sind, von denen viele an der Ausbreitung von VACV und an der Immunsignalisierung beteiligt sind. Bei einer VACV-Infektion wird das Oberflächenproteom moduliert und wahrscheinlich reorganisiert, was die Ausbreitung und die Umgehung des Immunsystems unterstützt.

Die Immunsignalisierung wird durch lösliche Liganden und an der Zelloberfläche befindliche Rezeptoren gesteuert. Die ausgelöste zelluläre Antwort hängt von der Signalarchitektur ab, die durch trans- und cis-Wechselwirkungen an der Zelloberfläche beeinflusst wird. Mithilfe einer neu entwickelten optoproteomischen Technologie, zu dessen Entwicklung ich beigetragen habe, konnte ich die Organisation von Zelloberflächenproteinen und dessen Organisation aufdecken. Ich untersuchte das Interaktom des entdeckten VACV-Proteins A40 mit unbekannter Funktion und immunmodulatorischem Phänotyp. Mit Hilfe der Proximity-Labeling-Technologien LUX-MS und SPPLAT konnte ich zeigen, dass A40 in ein Netzwerk von Integrinen und Basalmembranproteinen eingebettet ist. Eine Hypothese besagt, dass das C-Typ-Lektin-ähnliche A40 diese Interaktionen manipulieren und so die Interaktion zwischen ECM und Immunzellen am Infektionsort deregulieren könnte.

Zusammengefasst biete ich in dieser Arbeit faszinierende molekulare Einblicke in die Virus-Wirt-Pathogenese mit einem Schwerpunkt auf der VACV-induzierten Modulation des Wirtsoberflächenproteom. Darüber hinaus zeigen die präsentierten Daten, dass VACV systematisch die Zellmembran durch ihre Neubesiedlung mit viralen Proteinen kapert. Die Wechselwirkungen mit dem Oberflächenproteome können eine Rolle bei der erfolgreichen Ausbreitung von Viren spielen und sollten bei der Entwicklung neuer antiviraler Strategien berücksichtigt werden.

Abbreviations

ACE2	Angiotensin-converting enzyme 2
ADAM17	A disintegrin and metalloprotease domain-containing protein 17
ADCC	Antibody-dependent cell-mediated cytotoxicity
AGC	Automatic gain control
AIDS	Acquired immune deficiency syndrome
ANTR1	Anthrax toxin receptor 1
AP-1	Activator protein 1
APC	Antigen-presenting cell
APEX	Engineered ascorbate peroxidase
APMS	Affinity purification mass spectrometry
AREG	Amphiregulin
AutoCSC	Automated cell surface capturing
AXL	Tyrosine-protein kinase receptor UFO
BAR	Biotinylation by antibody recognition
BST2	Bone marrow stromal antigen 2
CADA	Cyclotriazadisulfonamide
CCN1	Cellular communication network factor 2
CCN2	Cellular communication network factor 2
CCR5	C-C chemokine receptor type 5
CD	Cluster of differentiation
CFSE	Carboxyfluorescein succinimidyl ester
CITE-seq	Cellular indexing of transcriptomes and epitopes by sequencing
Co-IPMS	Co-immunoprecipitation mass spectrometry
COL12A1	Collagen type XII alpha 1 chain
COL1A1	Collagen type I alpha 1 chain
COL3A1	Collagen type III alpha 1 chain
COL4A1	Collagen type IV alpha 1 chain
COVID-19	Coronavirus disease 2019
COX-2	Prostaglandin-endoperoxide synthase 2
CR	Complement receptor
CRD	Carbohydrate-receptor domain
CSC	Cell surface capturing
CXCR4	C-X-C chemokine receptor type 4
DC	Dendritic cell
DC-SIGN	DC-specific intercellular adhesion molecule-3-grabbing non-integrin
DDA	Data-dependent acquisition
DIA	Data-independent acquisition
DMEM	Dulbecco's Modified Eagle Medium
DNA	Desoxyribonucleic acid
DOX	Doxycycline

ECM	Extracellular matrix
EDTA	Ethylenediaminetetraacetic acid
EGF	Epidermal growth factor
EGFR	Epidermal growth factor receptor
EGR-1	Early growth response 1
ELISA	Enzyme-linked immunosorbent assay
EMARS	Enzyme-mediated activation of radical sources
EPHA	Ephrin type-A receptor
EPHB	Ephrin type-B receptor
ER	Endoplasmic reticulum
ERK	Extracellular-signal regulated kinase
EV	Extracellular virion
FAT1	Protocadherin fat 1
FBLN	Fibulin
Fc	Fragment crystallizable
FCS	Foetal calf serum
FDA	Food and Drug Administration
FDR	False discovery rate
FGFRL1	Fibroblast growth factor receptor-like 1
FOSL1	Fos-related antigen 1
FRT	Flp recombination target
GAG	Glycosaminoglycan
GAS-6	Growth arrest-specific Protein 6
GPI	Glycosylphosphatidylinositol
GPR126	Adhesion G-protein coupled receptor G6
GPR37	Prosaposin receptor GPR37
GPR56	Adhesion G-protein coupled receptor G1
HAdV	Human adenovirus
HBV	Hepatitis B virus
HCD	High-energy collisional dissociation
HCMV	Human cytomegalovirus
HDV	Hepatitis D virus
HGP	Human Genome Project
HIV	Human immunodeficiency virus
HLA	Human leukocyte antigen
Hpi	Hours post infection
HRP	Horseradish peroxidase
HTLV-1	Human T-lymphotropic virus-1
IAV	Influenza A virus
ICAM	Intercellular adhesion molecule 1
IFN- γ	Interferon- γ
IFN- γ R	Interferon- γ receptor
IL-2	Interleukin 2
IL6RB	Interleukin-6 receptor subunit beta

JunB	Transcription factor jun-B
KIR	Killer cell immunoglobulin-like receptors
LAMC1	Laminin subunit gamma-1
LB	Lateral bodies
LC-MS	Liquid-chromatography mass spectrometry
LFA1	Lymphocyte function-associated antigen 1
LRC	Ligand receptor capture
LRP1	Low-density lipoprotein receptor-related protein 1
MAFF	Transcription factor MafF
MAFK	Transcription factor MafK
MCMV	Murine cytomegalovirus
MEK	Mitogen-activated protein kinase kinase
MEM	Modified Eagle Medium
MET	Hepatocyte growth factor receptor
MHC	Major histocompatibility complex
MIP	Macrophage inflammatory proteins
MOI	Multiplicity of infection
mRNA	Messenger ribonucleic acid
MS	Mass spectrometry
MTOC	Microtubule organization center
MV	Mature virion
MVA	Modified vaccinia ankara
MVB	Multivesicular bodies
MWCO	Molecular weight cut-off
N	Asparagine
NCAM1	Neural cell adhesion molecule 1
NCHL1	Neural cell adhesion molecule L1-like protein
NK cells	Neutral killer cells
NKG2A	NKG2-A/NKG2-B type II integral membrane protein
NTB-A	NK-T-B-antigen
NTCP	Sodium taurocholate cotransporting polypeptide
ORF	Open reading frame
PD-L1	Programmed-death ligand 1
PGE2	Prostaglandin E2
PM	Plasma membrane
PNGase F	Peptide-N-glycosidase F
PSM	Peptide spectra match
PTM	Post-translational modification
PTPRJ	Receptor-type tyrosine-protein phosphatase eta
QTV	Quantitative temporal viromics
REAP-seq	RNA expression and protein sequencing
RNA	Ribonucleic acid
RO52	E3 ubiquitin-protein ligase TRIM21
RPMI	Roswell Park Memorial Institute

RT	Room temperature
SARS-CoV	Severe acute respiratory syndrome coronavirus
SARS-COV-2	Severe acute respiratory syndrome coronavirus type 2
SDS-PAGE	Sodium dodecyl sulfate polyacrylamide gel electrophoresis
Siglec-1	Sialic acid-binding Ig-like lectin 1
SNAT1	Sodium-coupled neutral amino acid transporter 1
SOG	Singlet oxygen generator
SPPLAT	Selective proteomic proximity labeling assay using tyramide
TCEP	Tris (2-carboxyethyl) phosphine
TRIM	Tripartite motif
UBE2	Ubiquitin-conjugating enzyme E
UBE3	Ubiquitin-protein ligase E3
UV	Ultraviolet
VACV	Vaccinia virus
VGf	Viral growth factor
VPP2	V-type proton ATPase 116 kDa subunit a2
Vpu	Viral protein U
WGA	Wheat germ agglutinin
WHO	World Health Organization
WR	Western reserve
WV	Wrapped virion
ZIKV	Zika virus

Table of Contents

Summary	1
Zusammenfassung	3
Abbreviations	5
Chapter 1	11
1 Introduction.....	11
1.1 A brief history of infectious diseases	11
1.2 Proteomics to unravel the virus-host interaction.....	12
1.3 Vaccination defeats smallpox	14
1.4 Molecular background of vaccinia virus	15
1.5 Motivation of the Ph.D. thesis	19
Chapter 2	21
2 Elucidation of host-virus surfaceome interactions using spatial proteotyping	21
2.1 Abstract.....	22
2.2 The surfaceome is the host's cellular interface enabling viral entry, immune evasion, and viral spread.....	22
2.3 Mapping the surfaceome and its interaction network.....	24
2.4 Deciphering virus binding and entry strategies to guide rational design of antiviral strategies	31
2.5 Elucidation of virus-induced surfaceome dynamics	34
2.6 The surfaceome and its role in viral spreading	39
2.7 Perspective	41
Chapter 3	43
3 VACV hijacks the host surfaceome to gain control over extracellular signaling.....	43
3.1 Abstract.....	44
3.2 Introduction.....	45
3.3 Results.....	47
3.3.1 Temporal analysis of the total proteome changes upon VACV infection.....	47
3.3.2 VACV infection induces transcription factor expression, and leads to downregulation of extracellular matrix components	48
3.3.3 Temporal surfaceome analysis upon VACV infection reveals modulation of growth factor, adhesion, and immune-related cell surface proteins	49
3.3.4 VACV proteins repopulate the host cell surface	52
3.3.5 A14 and A40 are glycoproteins localising to the host cell surface.....	53
3.3.6 The C-type lectin-like A40 is embedded in a network of integrins and basement membrane proteins.....	55
3.4 Discussion	57
3.5 Methods	61
3.6 Figures and figure legends	74
Chapter 4	95
4 Contributions to collaborative projects	95
4.1 Light-mediated discovery of surfaceome nanoscale organization and intercellular receptor interaction networks.....	96

4.2	PCprophet: a framework for protein complex prediction and differential analysis using proteomic data	98
4.3	Diagnostics and correction of batch effects in large-scale proteomic studies: a tutorial.....	100
4.4	PIM1 phosphorylation of GBP1 guards bystander cells during infection.....	102
4.5	Finding cellular receptors for gastrointestinal viruses	104
4.6	Multiplexed interactome analysis reveals the molecular architecture of the human prefoldin network.....	106
4.7	ARTC1 enhances cancer cell proliferation through ADP-ribosylation and activation of c-MET, ErbB3 and IGF-IR signaling pathway	108
Chapter 5	111
5	Conclusions and Future Perspective	111
5.1	Refinement of the A40 interactome	111
5.2	Towards an <i>in vivo</i> resolved interaction network	112
5.3	Investigation of VACV-induced paracrine signaling.....	113
5.4	Utilizing extracellular viral proteins in immunotherapy	114
Chapter 6	117
6	References	117
7	Acknowledgment	139
8	Curriculum vitae	141

CHAPTER 1

Introduction

1.1 A brief history of infectious diseases

Mankind has been affected by infectious diseases throughout human history. Descriptions of plagues can be dated back to the beginning of written language (Morens et al., 2008; Piret and Boivin, 2020). In fact, ancient and medieval reports cover the spread of infectious diseases within their societies, although wrongly traced back in the miasma theory to harmful forms of “bad air” (Sterner, 1948). The first basic theories describing infectious microorganisms, “germs”, as the underlying cause of an illness have been hypothesized in the second millennium (Williamson, 1955). However, it was only until the 19th century that the germ theory of disease was fully accepted due to experimental evidence shown by Louis Pasteur and studies of Robert Koch converging in his postulates describing microbial pathogenesis (Gaynes, 2020). The germ theory of disease paved the way for modern infection biology with the aim to understand infectious diseases by investigating the host-pathogen interplay at a cellular and molecular level. Ever since, scientific discoveries led to a continuously evolving definition for pathogens, grouped into the classes of viruses, bacteria, protozoan, fungi, and parasites, that are capable of causing host damage (Casadevall and Pirofski, 1999; Janeway et al., 2001).

Pathogens have been a major cause of morbidity and mortality in endemics on a regional and global pandemic level. Major pathogen-caused pandemics of the past like plague, cholera, smallpox, or still progressing ones like flu, tuberculosis, human immunodeficiency virus (HIV), and severe acute respiratory syndrome coronavirus type 2 (SARS-COV-2) have been afflicting trillions of people, jeopardizing not only the individual health, but reshaping societies, and civilization dynamics (Morens and Fauci, 2020; Morens et al., 2004). Protection against contracting infectious diseases was limited to containment measures such as isolation and quarantine in the past and are still precautionary measures when diseases are unknown or pharmaceutical therapy options are rare (Wilder-Smith and

Freedman, 2020). Antibiotic and vaccine discoveries as well as their advanced developments have brought a medical revolution in the treatment and control of bacteria- and virus-caused illnesses (Fleming, 1929; Hsu, 2013; Hutchings et al., 2019; Jenner, 1798). Nevertheless, many pathogens still cause severe life-threatening diseases for humans around the world (based on World Health Organization's (WHO's) World health report 2004 & 2013, analyzed by (Morens et al., 2004)). Infectious diseases often cause an adverse effect on the health of the host at an organismal level. The characteristics of the disease are determined by its underlying molecular mechanism. Hence, elucidation of host-pathogen biology at a molecular level is indispensable in order to understand pathogenesis. The associated gain of knowledge supports the rationale design of pharmaceutical interventions for undefeated, ongoing, and future infectious diseases.

1.2 Proteomics to unravel the virus-host interaction

Viruses are obligate intracellular pathogens since they are dependent on the host's cellular resources for their propagation. Throughout the viral life cycle, the virus-host relationship is shaped by recurrent encounters, determining the fate of the infection and eventually the disease outcome. In particular, viruses enter cells and either lay latent or induce their productive infection by replication, multiplication and spread within the organism. In response, the host starts a multifaceted defense program, aiming at the clearance of the invading pathogen (Summers, 2009).

The underlying processes of the host-virus interactions are predominantly orchestrated by proteins, which represent biological macromolecules that are involved in all essential cellular processes (Berg et al., 2002a). The protein structure is encoded as sequenced information in genes composed of deoxyribonucleic acid (DNA) (Berg et al., 2002b). However, viruses represent a special case, as they carry either DNA or ribonucleic acid (RNA) to store their genetic code (Baltimore, 1971). The entire genetic information of an organism, referred to as the genome, is nowadays fully readable due to the endeavors of the Human Genome Project (HGP), which reported the full human genome in 2001 (Lander et al., 2001; Venter et al., 2001), and mapped the ~20,000 protein-encoding human genes (International Human Genome Sequencing Consortium, 2004). Cellular protein biosynthesis is started from DNA, which is transcribed into messenger RNA (mRNA) and the genetic code is eventually subsequently translated into the protein sequence composed of 20 different amino acid residues (Berg et al., 2002c). In fact, all present proteins of a

cell, tissue, or whole organism under a defined time and condition form the proteome (Wilkins et al., 1996). Whereas the genome is of static character with exceptions for DNA modifications during epigenetic control and undirected formation of gene defects, the proteome is of dynamic nature and can constantly alter its composition and abundance in response to stimuli (Carbonara et al., 2021). Adaptation of the proteome is achieved on various levels during and post biosynthesis. Alternative splicing of precursor mRNA leads to protein diversity (Nilsen and Graveley, 2010). Additionally, proteins are co as well as post-translational modified, and proteolytically altered. Furthermore, protein function is dependent on their interactions and localization. Therefore, a protein as a product of a single gene can appear in various structural and functional states, its proteoforms (Aebersold et al., 2018; Carbonara et al., 2021; Smith et al., 2013).

The comprehensive analysis of the proteome is feasible by the large-scale, systemic sequencing of proteins by mass spectrometry (Aebersold and Mann, 2003, 2016). In general, mass spectrometry-based proteomics can be divided into top-down and bottom-up applications. In top-down proteomics, proteins are analyzed directly in their denatured or native form, harboring the advantage to directly analyze and differentiate proteoforms in order to gain more insights into proteoform functionality. However, challenges in the separation of complex samples such as lysates and interpretation of complex spectra limit its analytical depth to single proteins and low complexity samples (Brown et al., 2020; Durbin et al., 2016). In contrast, in bottom-up proteomics, proteins are enzymatically digested into peptides, which then represent the analytical entity analyzed by liquid-chromatography tandem mass spectrometry. The peptide is first analyzed in its intact form, then isolated and fragmented, which facilitates the recording of the amino acid residue sequence of the peptide. Comparison between the experimental spectra with an *in silico* digested proteome enables the identification of the peptides and inference of proteins (Aebersold and Mann, 2003). Moreover, advanced data-dependent and independent acquisition techniques, as well as quantitative methodologies based on label-free, metabolic, and chemical labeling, enable monitoring of abundances on a proteome-wide scale (Bantscheff et al., 2007; Schubert et al., 2017). Bottom-up proteomics' peptide-centric approach inherently is challenged by the inference problem, that non-proteotypic peptides can be derived from different proteins leading to an ambiguous assignment (Nesvizhskii and Aebersold, 2005). Moreover, these peptide-centric data enable only a limited view on proteoforms due to incomplete sequence coverage. Nonetheless, coupled

with sophisticated sample preparation methodologies, bottom-up proteomics is powerful to extract protein abundances, decipher PTM patterns, elucidate subcellular localization, resolve structures, decode interactions, and activity states on a proteome-wide level for viral infections (Gerold et al. 2021).

1.3 Vaccination defeats smallpox

Up to date, two infectious diseases were declared eradicated by the WHO: smallpox in humans, and rinderpest in ruminants (Fenner et al., 1988; Njeumi et al., 2012). Smallpox disease was highly contagious and had often a severe disease progression with up to a 30 % fatality rate (Ellner, 1998). Although its origin is not fully resolved, cases of smallpox can be traced back thousands of years B.C. with smallpox pustules discovered on Egyptian mummies (Li et al., 2007). The oldest direct verification of genomic DNA from an ancient variola virus strain was found on a child mummy and is dating between 1643 and 1665 A.C. (Duggan et al., 2016). In fact, re-emerging smallpox epidemics with major outbreaks in the 18th, 19th and 20th centuries afflicted the world population with estimated 300 million deaths during the 20th century alone (Hopkins, 2002). Due to huge societal and political efforts by individual states culminating in a WHO-guided vaccination campaign, the last smallpox case in the US was reported in 1956 and worldwide in 1977. Subsequently, the WHO declared the eradication of variola virus, the causative agent of smallpox. Variolation with smallpox pustule-derived fluids for later protection against the disease was already described in Chinese and Indian reports (Boylston, 2012). However, the inoculation strategy with a less harmful variola virus-related species was postulated by the English physician Edward Jenner in 1798. Based on studies and observations, Edward Jenner hypothesized and experimentally proved that cowpox infection results in a life-long immunity against smallpox (Riedel, 2005). In contrast to Jenner's experiments, the WHO utilized a live vaccine based on vaccinia virus, which was introduced within the 19th century for inoculation. Noteworthy, the exact origin of the smallpox vaccine remains speculative and VACV is suspected to be rather a descendant of today's extinct horsepox than cowpox (Esparza et al., 2017). Poxviruses, often named based on the most infected host species, are immunologically related and belong to the Orthopoxvirus genus within the family of Poxviridae (King et al., 2012). Even though variola virus' host range was limited to humans, most other Orthopoxvirus species infect a broad range of hosts and spread within an animal reservoir (Reynolds et al., 2018). Thus, nowadays most infections

with Orthopoxvirus species are a result of zoonosis. Regularly, monkeypox infections of humans are reported, which face the danger of spreading in our globalized world (Di Giulio and Eckburg, 2004). Undoubtedly, smallpox was the cause of disaster for many generations and populations, but concurrently its eradication is a success story that stamps the beginning of modern vaccinology.

1.4 Molecular background of vaccinia virus

Fueled by the success of the smallpox vaccine, the application purpose of VACV has evolved from a live vaccine to a toolbox for biomedical and fundamental research (Jacobs et al., 2009; Volz and Sutter, 2017). Over time, different vaccinia virus strains were obtained with distinctive virulence patterns, ranging from a highly attenuated and limited replicative Modified Vaccinia Ankara (MVA) strain, the attenuated and replicative Lister, towards the more virulent Copenhagen and full virulent Western Reserve (WR) strains. Highly attenuated MVA strains are utilized as live viral vectors for a multitude of heterologous agents. Especially, their usage for respiratory diseases such as influenza was intensively characterized in preclinical and clinical studies (Altenburg et al., 2014). Likewise, viral MVA vectors expressing the SARS-CoV-2 spike protein are subject to clinical phase I trials (ClinicalTrials.gov IDs: NCT04569383, NCT04639466, NCT04895449). Moreover, VACV utilization as an oncolytic agent in cancer therapy harbors promise. A platform, based on VACV JX-594, was built to selectively infect and replicate in cancer cells, aiming at the lysis of tumor cells through transgene expression (Breitbach et al., 2011). In a later performed clinical trial, overall survival for lung cancer patients was increased in comparison to conventional treatment (Heo et al., 2013). Although the major breakthrough for VACV as a therapeutic agent has not arrived yet, its utilization as a viral transfection vector for gene delivery in research is widespread (Mackett et al., 1982). Furthermore, VACV represents an excellent model system to study host-virus biology. VACV can be easily cultivated, modified by genome editing and microscopically observed, which together with robust *in vitro* and *in vivo* infection models enabled scientists to establish fundamental concepts of virology (Moss, 2004).

VACV virions exist in different infectious forms, each with a distinct morphology, but the same genetic background. Most abundant during the viral life cycle is the single-membrane wrapped mature virion (MVs). Additional wrapping leads to virus particles enclosed by three membranes, usually called wrapped virion (WV). These can expel from the cell, then

forming the third infectious form of extracellular virions (EV). EVs carry a double-membrane and are either unattached or plasma membrane-associated (Moss, 2006). VACV MVs are brick-shaped with dimensions of approximately 360 x 270 x 250 nm (Cyrklaff et al., 2005). The envelope encloses a biconcave core, which contains the 200.000 base pair large genome as linear double-stranded DNA, encoding for more than 200 ORFs. The core is flanked by lateral bodies at each site, composed of a protein-rich, sphere-shaped structure (Condit et al., 2006).

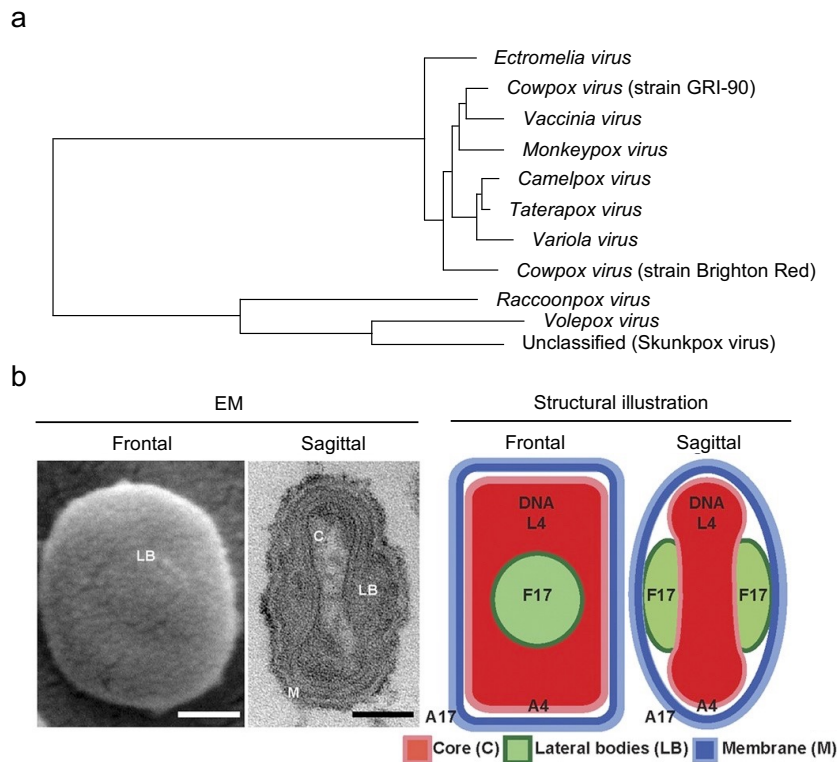


Figure 1: A. Phylogenetic relations in the Orthopoxvirus genus. Predictions are based on codon-alignment of nucleic acid sequences from nine conserved genes and topologies inferred by using Bayesian modeling. Modified from (King et al. 2012). **B. Structural features of VACV mature virion.** a) Electron microscopy image in frontal and sagittal projection. b) Illustration depicting the structural features of VACV. The viral membrane encloses the biconcave core, flanked by two lateral bodies. Modified from (Gray et al., 2016).

Most cell types are permissive for VACV infection (McFadden, 2005). The viral life cycle, described in detail by Bidgood and Mercer, is in contrast to most other virus families localized in the cytosol (Bidgood and Mercer, 2015). First, VACV attaches to the cell surface through binding to glycosaminoglycans (GAGs) (Chung et al., 1998; Hsiao et al., 1999). Attachment can be supported by interaction with the GAS-6-AXL complex

(Morizono et al., 2011). Subsequently, VACV triggers its cell entry by induction of protrusions, which leads to the endocytosis of VACV by macropinocytosis (Mercer and Helenius, 2008). Macropinocytosis is an unspecific internalization process engulfing extracellular fluids and residing components via the formation of large endosomes. Upon virus internalization, the virus envelope of MVs fuses with the endosomal membrane mediated by the viral entry-fusion complex in a low pH-dependent mechanism (Gray et al., 2019; Townsley et al., 2006). For extracellular virions (EVs), acidification leads first to the destruction of the outer membrane and subsequently to fusion with the endosomal membrane (Schmidt et al., 2011). In both cases, the core is released into the cytoplasm. Simultaneously, lateral bodies diffuse, and eventually proteins from LBs and core are released into the cytoplasm. In total, virions harbor approximately 80 proteins, involved in scaffolding, cell entry, early gene transcription, and counteracting the host defense measures (Chung et al., 2006; Resch et al., 2007). After the core release, immediate early gene expression is initiated and the core becomes uncoated. Many of the early gene products are antagonizing cell response mechanisms (Assarsson et al., 2008). Further, VACV productive infection is established through replication in large cytoplasmic viral factories (Cairns, 1960). Subsequent intermediate and late gene expression leads to the synthesis of proteins primarily involved in virus morphogenesis or intended to be packaged in newly formed virions (Assarsson et al., 2008). The virion assembly starts from crescents within the viral factories. These membrane discs develop in a stepwise process via immature virions into infectious MVs (Liu et al., 2014). MVs remain intracellular until cell lysis. Nonetheless, a fast spread of the infection is reached by the transformation of a small part of the MVs into WVs, which eventually enable VACV to egress. MVs get either wrapped with two Golgi- or endosomal-derived membranes or are packaged in multivesicular bodies (MVB). Both WVs and WV-MVB travel to the plasma membrane for their release by exocytosis (Huttunen et al., 2021). EVs either associate with the plasma membrane or induce actin tails, which catapult the EVs into the adjacent microenvironment (Smith and Law, 2004). In order to prevent the spread of the local infection, the host starts its defense on a cellular and organismal level. However, VACV uses approximately half of its proteins to counteract the host response to eventually establish a systemic infection (Bidgood and Mercer, 2015).

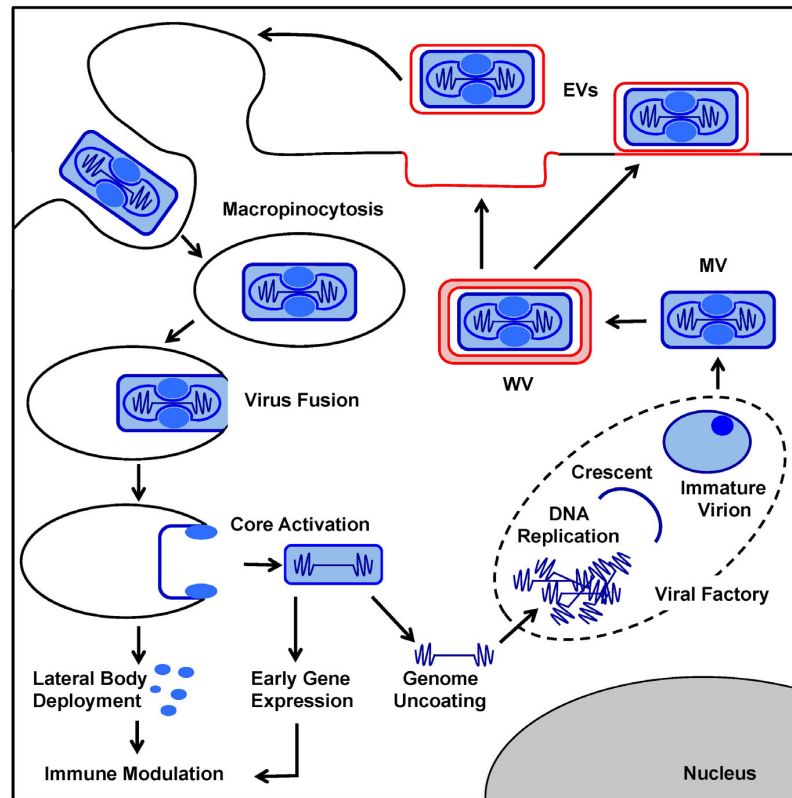


Figure 2: VACV life cycle. Initially, VACV enters cells by macropinocytosis. Once internalized, the core is released into the cytoplasm in a low pH-dependent fusion mechanism between the viral and endosomal membrane. In parallel, the LBs detach and brought along proteins released (Bidgood et al., 2020). During core uncoating, early gene expression starts. Replication is initiated and cytosolic viral factories are formed. Within these, replication, intermediate and late gene expression, as well as viral morphogenesis, takes place. Starting from crescents, MVs assemble via several intermediate immature forms. Most MVs stay intracellular until cell lysis. However, some MVs are wrapped and travel to the PM. By fusion with the PM, EVs egress, which stay either associated to the cell or are repelled by actin tails. Modified from (Bidgood and Mercer, 2015).

1.5 Motivation of the Ph.D. thesis

Viral infections threaten human health by causing often mild, but sometimes severe symptoms, and diseases without therapeutic options. Beyond the individual risk, societal health is compromised by the emergence and re-emergence of pathogenic viruses. Their spread in epidemics, and as currently being witnessed during a pandemic, is greatly accelerated in an interconnected, globalized world. A molecular understanding of the underlying biology of viral pathogenesis is a prerequisite for the rational development of drug-, and vaccine-based diagnostic as well as therapeutic strategies against viral pathogens.

The focus of my thesis is on the relationship between vaccinia virus (VACV) and its host. VACV, the prototype of the *Poxviridae*, was administered by the World Health Organization (WHO) to eradicate smallpox. Since then, it has found medical relevance as a live vaccine expressing foreign antigens for vaccination purposes, and as an oncolytic agent. Research on poxviruses over the past decades has helped to establish fundamental concepts of virology and by implication about host biology. Despite these great and productive investigative efforts, it is still not well understood how viruses, such as VACV, relatively simple with regard to their genome encoding for only ~200 ORFs, can fully hijack hosts effectively in no time and propagate themselves.

Critical to this is the question of how VACV spreads and how it evades the host defense response, in particular recognition of the immune system? Both processes involve proteins in the extracellular space, especially cell surface proteins. These proteins reside on the outside of the cell and transmit extracellular stimuli into intracellular signaling cascades, orchestrating cellular communication between infected and immune cells. VACV classifies as a master of manipulation. However, how VACV infection perturbs the cell surface protein composition and its organization remains mostly elusive but would give access to molecular details in the host immune response and knowledge for rational antiviral drug design.

With my thesis, I aim to elucidate the proteotype changes upon VACV infection with a focus on the spatio-temporal investigation of the host surfaceome of infected host cells. Moreover, I aim to gain knowledge about the importance of extracellular interactions during viral infection. Together, I would like to provide new molecular insights about the underlying viral pathogenesis, which might be helpful to understand poxvirus zoonoses, and other future viral threats.

CHAPTER 2

Elucidation of host-virus surfaceome interactions using spatial proteotyping

This chapter represents an unrefereed author's manuscript, which was later published as Chapter Four – Elucidation of host-virus surfaceome interactions using spatial proteotyping, by Elsevier Publishing Group in Proteomics Approaches to Unravel Virus – Vertebrate Host Interactions.

Fabian Wendt^{1,2}, Emanuela Sara Milani^{1,2}, and Bernd Wollscheid^{1,2}

Proteomics Approaches to Unravel Virus – Vertebrate Host Interactions

Advances in Virus Research

Volume 109, Pages 105-134, 12. April 2021

Edited by Gisa Gerold

DOI: 10.1016/bs.aivir.2021.03.002

1. Department of Health Sciences and Technology (D-HEST), ETH Zurich, Institute of Translational Medicine (ITM), Zurich, Switzerland
2. Swiss Institute of Bioinformatics (SIB), Lausanne, Switzerland

CRedit authorship contribution statement

Fabian Wendt: Writing - original draft, review & editing

Emanuela Sara Milani: Writing - original draft, review & editing

Bernd Wollscheid: Funding acquisition, Supervision, Writing - review & editing

Citations for this chapter are listed in chapter 6

2.1 Abstract

The cellular surfaceome and its residing extracellularly exposed proteins are involved in a multitude of molecular signaling processes across the viral infection cycle. Successful viral propagation, including viral entry, immune evasion, virion release and viral spread rely on dynamic molecular interactions with the surfaceome. Decoding of these viral-host surfaceome interactions using advanced technologies enabled the discovery of fundamental new functional insights into cellular and viral biology. In this review, we highlight recently developed experimental strategies, with a focus on spatial proteotyping technologies, aiding in the rational design of theranostic strategies to combat viral infections

2.2 The surfaceome is the host's cellular interface enabling viral entry, immune evasion, and viral spread

Proteins exposed at the exterior of the plasma membrane orchestrate the cellular communication with the extracellular environment. These cell surface residing receptors, transporters, channels, cell-adhesion proteins, and ectoenzymes are together referred to as the cell surface proteome or surfaceome (Almén et al. 2009; Bausch-Fluck, Milani, and Wollscheid 2019). In addition to the absorption of nutrients (Palm and Thompson 2017), cell surface proteins mediate information transduction from the outside environment to intracellular signaling networks (Bausch-Fluck, Milani, and Wollscheid 2019; Granados et al. 2018). As cellular gateway keepers cell surface proteins interact (trans) with soluble ligands (small molecules, peptides, proteins, microorganisms), extracellular matrix (ECM) proteins and surfaceome members of different cells enabling cell-to-cell communication (Armingol et al. 2021). Moreover, the transmission of extracellular signals depends on the lateral (cis) interactions of receptors with the adjacent surfaceome on the same cell, and intracellular effectors (Jacobson, Liu, and Lagerholm 2019). The dimensions of the lateral interaction network range from promiscuous heterodimerization, e.g. within the EGFR family (Kennedy et al. 2016), co-receptor dependencies, e.g. dictating HIV-tropism (Bozek et al. 2012), to the formation of functional protein nanoclusters in immunological synapses (Maity et al. 2015). Fluctuating external conditions cause cells to dynamically alter cell surface protein abundances that in turn lead to a context-specific interactome, adapting surface signaling capacity to allow subsequent rapid and efficient response (Bausch-Fluck, Milani, and Wollscheid 2019; Washburn 2016). All plasma membrane proteins with at least

one amino acid facing the extracellular space are considered part of the surfaceome (Bausch-Fluck, Milani, and Wollscheid 2019). This includes integral and extracellular peripheral membrane proteins, and also exterior lipid-anchored proteins such as glycosylphosphatidylinositol (GPI)-linked proteins. A mammalian cell-type specific screen cataloged over 1,500 cell surface proteins (Bausch-Fluck et al. 2015). This experimentally defined ground truth dataset enabled through feature extraction in combination with machine learning the prediction that approximately 2,900 proteins, from the roughly 20,000 UniProt annotated human protein entries, belong to the human surfaceome (Bausch-Fluck et al. 2018). Around 90% of the surfaceome members are N-linked glycosylated within their extracellular domain; which plays an important role in immunity (Maverakis et al. 2015). Moreover, the surfaceome and its organization reflects the identity and functional state of a cell and thus represents a valuable resource as a diagnostic and therapeutic target pool (Bausch-Fluck et al. 2018; Overington, Al-Lazikani, and Hopkins 2006; Yin and Flynn 2016).

As the plasma membrane delimits the cell, obligate intracellular viruses need to breach this barrier. For this task, viruses take advantage of the exposed localisation of cell surface proteins and non-proteinaceous, membrane-bound structures for initial attachment (Yamauchi and Helenius 2013) (**Figure 1**). Subsequently, the surfaceome is a critical interface for viral entry into the cell, immune evasion, virion release and spread (Doms and Trono 2000). During these steps of the productive infection cycle, the abundance, and organizational integrity of host cell surface proteins are modulated. Furthermore, viral proteins eventually also localize at the plasma membrane and become “foreign” surfaceome members, rewiring the cell surface signaling network leading to novel surfaceome functionality to promote viral propagation (Rodriguez Boulan and Pendergast 1980). Thus, the surfaceome plays a key role during viral infection, ultimately defining pathogenesis.

In this review, we describe recent technological advances that provided new insights into virus-host surfaceome interactions with a focus on mass spectrometry-based spatial proteotyping strategies. The highlighted strategies indicate great progress in the field of host-pathogen biology and show how information about molecular nanoscale organization opens up new theranostic opportunities to combat viral infection.

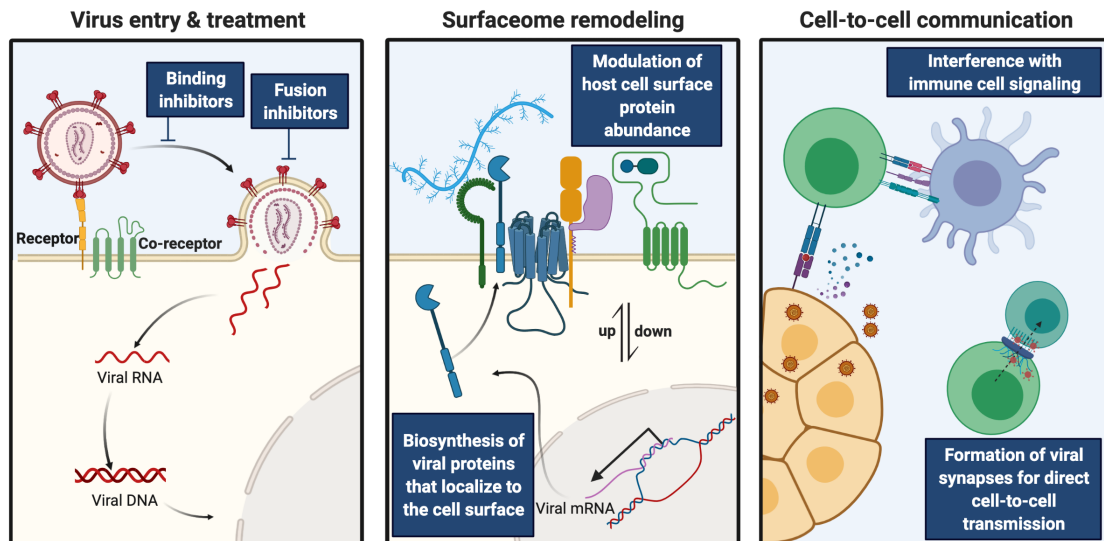


Figure 1: The surfaceome is the cellular interface enabling viral entry, immune evasion, and viral spread. The surfaceome is a critical molecular interface during the entire span of the viral life cycle. As an initial step during the infection cycle, viruses attach and bind cell surface proteins to invade host cells, which is targeted by antiviral treatments to inhibit the infection. During the course of infection (post virus entry), viruses modulate the abundance and the organizational integrity of host cell surface proteins to counteract the host response. Additionally, viruses synthesize and localize viral encoded proteins at the plasma membrane becoming “foreign” surfaceome members, changing the surfaceome functionality. Overall, viruses induce a reorganization of cell surface proteins in order to alter intercellular communication in immune signaling as well as promoting their spread through direct-cell-to-cell transmission.

2.3 Mapping the surfaceome and its interaction network

Over the past decade, mass spectrometry-based (MS) proteotyping strategies made significant strides forward facilitating the elucidation of fundamental biology and clinical phenotypes (Aebersold and Mann 2003; Bantscheff et al. 2007; Röst, Malmström, and Aebersold 2015; Aebersold and Mann 2016; Doll, Gnad, and Mann 2019). Substantial technological improvements in sensitivity and quantitative accuracy, but also the advancements in data acquisition strategies, and machine-learning-based computational data analysis have enabled comprehensive proteotype measurements (Kelstrup et al. 2018; Ludwig et al. 2018; Meier et al. 2020; Tyanova et al. 2016). The term proteotype is used to describe the acute composition and functional organization of the proteome associated with a specific phenotype.

In relation to the analysis of the composition of the proteotype, the quantitative analysis of up to 10,000 proteins from *in vitro* cultured cell lines, as well as quantitation of around 1,000 proteins from mammalian single cells have been reported recently (Muntel et al. 2019; Kelly 2020). Coupled with sophisticated sample preparation methodologies, mass spectrometry-based proteotyping is a powerful tool-box enabling the investigation of infectious diseases on the molecular level. Insights into virus-host biology were gained through the elucidation of the functional organization of the proteotype, including post-translational modifications, protein-protein interactions, and classification of subcellular proteome pools including spatial and temporal resolved surfaceome dynamics (Greco and Cristea 2017; Jean Beltran, Mathias, and Cristea 2016; Novy et al. 2018; Gordon et al. 2020; Weekes et al. 2014).

The MS-based spatially restricted elucidation of the cell surface protein pool is challenging due the fact that the plasma membrane represents only 1-2% of cellular membranes, the hydrophobicity of membrane proteins, their low abundance in contrast to intracellular proteins and the fact that cell surface are present at the cell surface, but can also reside in intracellular pools. Thus, whole cellular lysate-based proteotyping studies often only cover a small subset of the surfaceome and don't allow for making statements about the quantity and functional organization of proteins in a particular location, in this case the cell surface. Transcriptomic approaches are also utilized to impute protein quantities based on the measurable mRNA pool, but both strategies still fall short of reporting the actual identity and quantity of the surfaceome-residing pool of receptors, as these strategies can't report on spatially and functionally distinct receptor abundance information. Indeed, studies based on combined transcriptome sequencing with DNA-tagged identification of proteins (CITE-seq and REAP-seq) have shown that single cell relative mRNA abundances and corresponding surface protein abundances correlate weakly (Peterson et al. 2017; Stoeckius et al. 2017; Y. Liu, Beyer, and Aebersold 2016). However, contrasting studies have been published for selected surfaceome subgroups (Nusinow et al. 2020). Such neural network-based predictors of surfaceome abundance which are based on imputation from single cell RNA sequencing data showed early promising results for a set of 24 immunophenotypic markers, but did not prove system-wide prediction competence (Zhou et al. 2020). This shortcoming in the prediction accuracy is currently mainly due, as reported by the authors, to stochasticity in RNA processing, and lack of detailed knowledge/data about protein translation, protein transport, and proteostasis in very general terms. Therefore, tailored

surfaceome enrichment strategies and direct measurements are required to report accurately on the functionally relevant surfaceome proteotype across the viral infection process.

The spatial characterization of the surfaceome encompasses the mapping of the global cell surface receptor repertoire including receptor abundances, as well as the locally confined cell surface signaling microenvironments the receptors reside in, including the organisation of extracellular protein networks, and extracellular receptor-ligand interactions - which are eventually utilized during the viral life cycle. (**Figure 2**). In the past, methodologies such as proteolytic-cleavage of cell surface proteins by trypsin or proteinase K (Olaya-Abril et al. 2014), one-step plasma membrane purification by centrifugation (Lund et al. 2009), and silica bead coating-based affinity purification (Durr et al. 2004) were utilized in order to gain information about the surfaceome proteotype. However, these strategies typically suffer from protein contaminations, originating from cytosolic, intracellular plasma membrane attached or intracellular organelle membrane compartments. Thus, such strategies are only partially suited for the *bona fide* identification and quantification of only the functionally relevant pool of cell surface residing proteins. Alternatively, enrichment of cell surface proteins can be achieved by surfaceome-wide protein labeling/tagging methodologies (**Figure 2A**). These strategies typically rely on bi-functional, membrane-impermeable small molecules possessing affinity tags. Next to an affinity moiety (usually biotin), these reagents harbour a reactive group to covalently label/tag cell surface proteins. Extracellularly exposed proteins can be labeled with e.g. NHS-based chemistry on primary amines on accessible lysine residues or N-termini (Karhemo et al. 2012), or at their glycan structure with hydrazide- or aminoxy-based reactions (Wollscheid et al. 2009; Weekes et al. 2010). Chemical protein labeling approaches, partly combined with miniaturization and automation, were applied for surfaceome mapping of low-abundant receptors during cell differentiation, rare immune cell populations, and time-resolved dynamics in immune and neuronal signaling (Kalxdorf et al. 2017; van Oostrum et al. 2019; J. Li et al. 2020; Ravenhill et al. 2020; van Oostrum et al. 2020). Cell surface protein enrichment strategies and their molecular details were reviewed extensively in (Elia 2008; Elschenbroich et al. 2010; Kuhlmann et al. 2018; Y. Li, Qin, and Ye 2020).

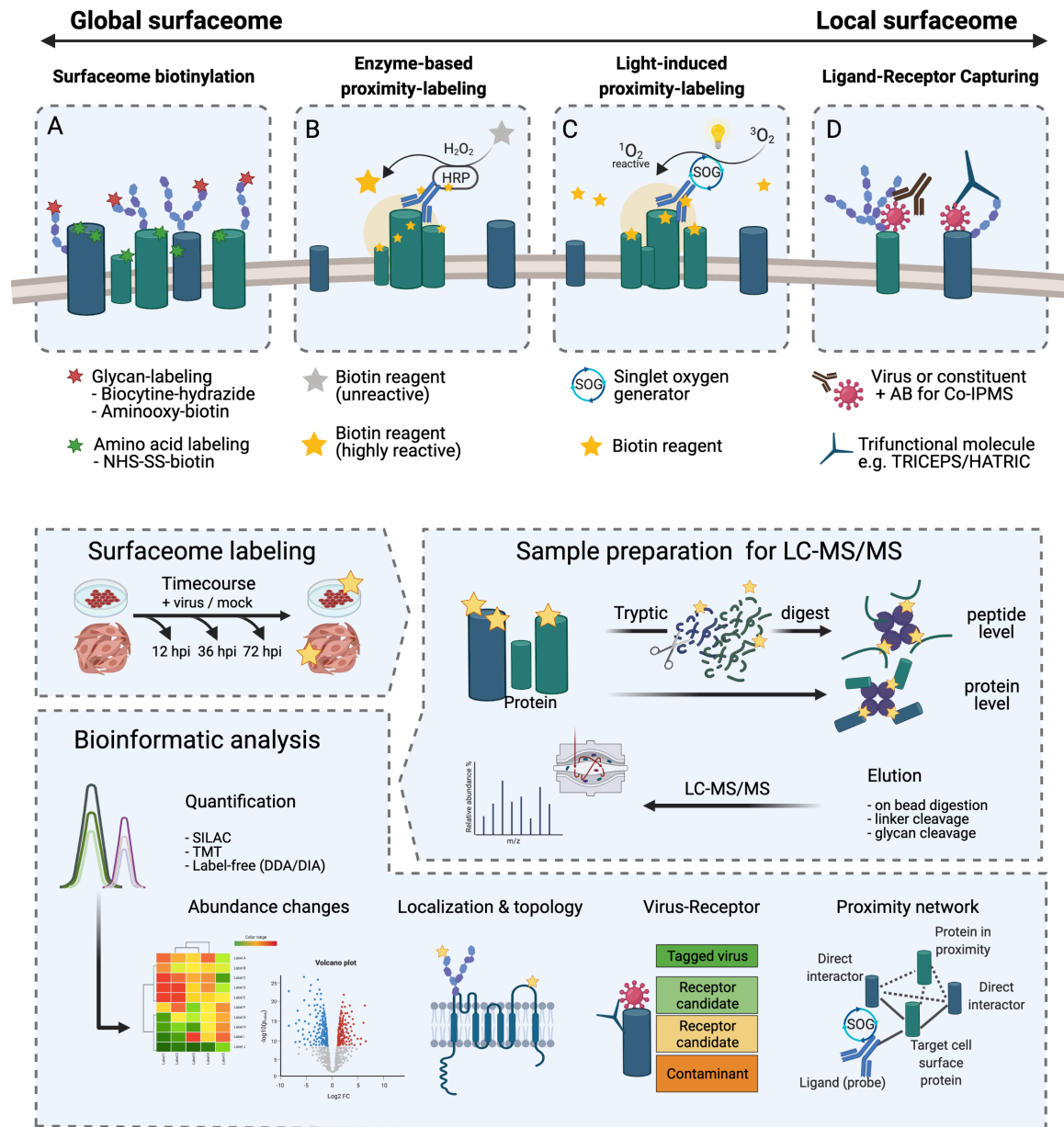


Figure 2: Molecular characterization of virus-induced surfaceome dynamics, interaction and organisation using spatial proteotyping strategies

The top panel illustrates exemplary labeling/tagging strategies (A) for global surfaceome biotinylation, (B, C) for proximity-based labeling of molecular microenvironments including interaction networks and (D) for the locally confined surfaceome analysis, e.g. direct ligand-receptor interactions (D). A. Extracellularly exposed proteins can be tagged at selected protein backbone amino acid residues with NHS-based chemistry or at their N- and O-glycosylation structures with hydrazide/aminoxy-biotin tags. B. Extracellular enzyme-based proximity-labeling strategies often utilize HRP-coupled antibodies against the target cell surface protein of interest. HRP catalyses the generation of highly reactive biotin-probes upon addition of H_2O_2 . Subsequently, the HRP-AB conjugate, protein of interest and adjacent proteins are labeled with biotin-tags. C. Light-induced proximity

labeling termed LUX-MS uses singlet oxygen generators (SOGs) coupled to antibody or ligands against the known or unknown target cell surface protein. Upon illumination, SOGs catalyzes the formation of highly reactive singlet oxygen ($^1\text{O}_2$). Singlet oxygen oxidizes biomolecules in close vicinity and activates amino acid residues for labeling. Subsequently, biocytin-hydrazide covalently reacts with these activated amino acid residues and biotinylates proteins in proximity. D. Extracellular receptors can be captured by Co-IPMS or with trifunctional crosslinkers, that (i) couple the ligand, (ii) crosslink with the receptors upon ligand binding on live cells, and (iii) enable affinity purification through a third moiety such as biotin.

The bottom panel shows schematically the proteotyping strategy for analysing the labeled/tagged cell surface proteins. Initially, the surfaceome of cells or tissue is tagged by the labeling strategies described above. Proteins are then extracted from the biological specimen and subsequently prepared for further proteotype analysis. Affinity purification of labeled/biotinylated species can be carried out at the protein- or peptide-level. Protein level: Undigested proteins are affinity purified exploiting the strong biotin/streptavidin binding. Upon stringent washing, proteins are eluted either by on-bead digestion, or through dissociation of cleavable linker molecules followed by in-solution digestion. Peptide-level: Proteins are digested by trypsin and biotinylated peptides are affinity purified with streptavidin. In case of NHS-based labeling, peptides can be eluted with harsh buffer conditions, and heating from streptavidin. Biotinylated N-glycopeptides can be enzymatically released with PNGase F. Release of formerly N-glycosylated peptides results in the deamidation of asparagine within the NXS/T consensus sequence, indicating surface localisation and glycosylation site. Eluted peptides are then analysed with liquid-chromatography mass spectrometry. Relative quantification of measured peptides/proteins can be computed based on the chosen quantitative strategy (TMT, SILAC, label-free DDA or DIA). Obtained quantitative matrices finally shed light on virus-induced surfaceome dynamics, interaction and organisation changes upon infection.

Whereas the described chemical labeling/tagging methodologies enable the global analysis of the surfaceome and the identity of cell surface proteins, these strategies do not allow for the investigation of the functional organization of cell surface proteins, e.g. the specific cell membrane microenvironments, and the receptor nanoscale organization, as for example relevant in immunological synapses upon viral infection. Here, proximity labeling methodologies can facilitate extracellular proteotyping in confined local areas at the cell surface (**Figure 2**) (Chen and Perrimon 2017; Bausch-Fluck, Milani, and Wollscheid 2019). These recently developed optoproteomic proximity-tagging strategies can be classified in enzyme-based and light-induced labeling technologies (**Figure 2 B, C**) which enable tagging of a cell surface-residing protein of interest, as well as its direct interaction

partners, transient interactors and proteins localizing in close proximity. The tagged cell surface proteins can then be affinity-purified under stringent conditions, as the affinity tag is covalently attached to the proteins which were in proximity of the bait. Genetically-fused engineered ascorbate peroxidase (APEX) or Pup ligase PafA were used for example to elucidate the interactome of growth factor signaling domains (Zhen et al. 2018), and T cell costimulatory receptor CD28 (Q. Liu et al. 2018), respectively. Likewise, a variety of technologies including EMARS (Jiang et al. 2012), split HRP (Martell et al. 2016), SPPLAT (Rees et al. 2015), and BAR (Bar et al. 2018) utilize horse-radish peroxidase (HRP), coupled to a probe (e.g. antibody, ligand) as baits, and have been applied to interrogate the lipid-raft composition, and B-cell receptor architecture, respectively.

Recently, two light-inducible optoproteomic proximity labeling technologies, termed μ Map and LUX-MS, were developed enabling the decoding of surfaceome signaling architectures (Geri et al. 2020; Müller et al. 2020). These proximity-tagging strategies utilize, instead of the larger enzymes mentioned before, small molecule catalysts, having likely also a smaller impact on the structure-function relationship upon coupling to the bait (**Figure 2C**). These catalysts were shown to be coupled to antibodies, ligands or in general terms affinity binders, targeting the cell surface protein of interest. Upon short illumination using selected light sources, these catalysts induce through chemical reactions modifications in backbone amino acids of cell surface proteins surrounding the target protein which can be subsequently identified upon affinity enrichment using MS-based technology. The μ Map strategy developed by the Mac Millan laboratory is utilizing a Dexter energy transfer-based mechanism for elucidation of protein interaction networks, such as shown for CD45, CD47 and CD20 on Jurkat cells, identifying both known and previously unknown interaction partners. Furthermore, μ Map enabled the dissection of the programmed-death ligand 1 (PD-L1) microenvironment on the surface of living lymphocytes (Geri et al. 2020). LUX-MS technology uses, in contrast, photosensitizers, namely singlet oxygen generators (SOGs), for decoding protein interactions on living cells (Müller et al. 2020). Using SOG-coupled probes, LUX-MS was able to decipher ligand-receptor interactions, and additionally surfaceome receptor nanoscale organizations. Furthermore, the immunological synapse formed between APCs and CD8+T cells was mapped successfully.

In summary, proximity-labeling strategies evolved into widely applicable technologies whose application space can be chosen and targeted to a particular microenvironment by the selected probe carrying the tagging functionality. Spatially confined probes such as

antibodies or ligands enable the deciphering of the extracellular local lateral nanoscale signaling interaction networks, and widely distributing probes even facilitate the global *in vivo* surfaceome analysis (J. Li et al. 2020).

Identified proteins in proximity-labeling methodologies are close to the targeted protein at the cell surface, but might not necessarily be direct interactors of functional relevance in the infection process (X. Liu et al. 2020). Nevertheless, to decode the direct ligand-receptor interaction, e.g. for the identification of the cognate virus receptor, several strategies were developed (**Figure 2D**). Well-established protein-protein interaction mapping technologies such as co-immunoprecipitation mass spectrometry (Co-IPMS) can help to decipher extracellular ligand-receptor interactions by antibody-based isolation of the whole or a virus constituent (Gerold, Bruening, and Pietschmann 2016). However, Co-IPMS for extracellular targets remains challenging, as the necessity of detergents to extract proteins from the plasma membrane can disrupt the often-labile ligand-receptor interactions. The transient character of interactions and, typically unknown, on and off rates can reduce the success rate of identifying such ligand receptor interactions at the surface of living cells (Martinez-Martin 2017). To overcome these drawbacks, the ligand receptor pair can be crosslinked on intact cells to stabilize the interaction prior to enrichment (**Figure 2D**). Technologies such as the TRICEPS- and HATRIC-based Ligand Receptor Capture (LRC) technologies, as well as the photocrosslinking-based approach by Srivastava et al., utilize this principle by exploiting three-headed small molecules that (i) bind the ligand, (ii) crosslink with the receptors, and (iii) enable affinity purification through a third moiety (Frei et al. 2012; Sobotzki et al. 2018; Srivastava et al. 2020). HATRIC- and TRICEPS LRC are leveraging quantitative chemical reaction differences in order to identify unknown receptor(s) of known ligands while Srivastava et al utilize UV exposure at different time points to generate quantitative differences, which enable the MS-based identification of the cognate receptors. Identification of ligand-receptor interactions on live cells by affinity-purification takes into account the native functional environment of the receptor, but can be a delicate task and thus restricted to a single or few ligands per experiment. Recently established large-scale platforms enable testing of binary extracellular ligand-receptor interactions in a straightforward manner, but require prior genetic engineering (Martinez-Martin et al. 2016; Galaway and Wright 2020; Husain et al. 2019).

In summary, the above-described technologies and strategies allow for the investigation of diverse spatially confined cell surface proteotypes. These applications show furthermore that mapping of global surfaceome dynamics during viral infection, decoding of

extracellular microenvironments, such as immunological or viral synapses and identification of locally confined ligand-receptor interactions e.g., cognate virus receptors can be approached successfully.

2.4 Deciphering virus binding and entry strategies to guide rational design of antiviral strategies

The interaction of viral particles with the cellular surfaceome plays an essential role during the first steps of the viral life cycle. It is the first contact/interaction point between the viral particle and the host cell, which sets the stage for viral entry, the initial step of the infection. Virus entry is initiated by the attachment of the virus to cell-surface receptors and leads ultimately to the delivery of the viral genetic content into the cell. The identification of host cell surface receptors is, therefore, fundamental for understanding the molecular processes involved in viral infection and virus tropism, as well crucial for the development of antiviral treatment to inhibit or interfere with successful viral infection.

With the recent evolution of MS-based proteotyping strategies, novel approaches have been developed to study different aspects of interactions between viruses and host cells including surfaceome interactions. A wide range of strategies have been developed over the years for the identification of viral receptors, extending from early biochemical and immunological strategies (Bass and Greenberg 1992) to genomic strategies, protein microarrays, high-throughput screening, gain-of-function and loss-of-function strategies, and MS-based strategies (Barrass and Butcher 2020). An extensive review describing the use of MS-based proteotyping technologies to map the host receptor space was written by Gerold et al. (Gerold, Bruening, and Pietschmann 2016). Here, we will describe a few prime examples highlighting the use of past and current MS-based approaches to identify host cell surface receptors for viral particles.

Co-IPMS and APMS are technologies widely used for the identification of protein-protein interactions. Co-IPMS was used for example to elucidate the receptor for SARS-CoV during the first SARS-CoV pandemic in 2003 (W. Li et al. 2003). The truncated soluble S1-domain of the viral spike glycoprotein was fused to the Fc domain of human immunoglobulin- γ 1. Immunoprecipitation allowed for the enrichment of the cognate receptor, which was subsequently identified by MS as the angiotensin-converting enzyme 2 (ACE2). Since SARS-CoV has very high homology with SARS-CoV-2, the cause of the

current COVID-19 pandemic, ACE2 was also recently confirmed to play an essential role in SARS-CoV-2 entry (Hoffmann et al. 2020; Ou et al. 2020).

In combination with the above-mentioned affinity-purification strategies a chemical cross-linking strategy was utilized to discover the receptor of hepatitis B virus (HBV). In 2012, the Li group used a “zero-distance photo-cross-linking” approach coupled to tandem affinity purification and MS to identify sodium taurocholate cotransporting polypeptide (NTCP), a multipass transmembrane transporter predominantly expressed in the liver, as the HBV receptor (Yan et al. 2012). In this study, a synthetic viral peptide based on a viral protein modified with photoreactive amino acid analogs and biotin was used. Irradiation with UV light enabled the direct covalent crosslinking to amino acids within the corresponding HBV-binding receptor, which was then purified using the biotin moiety. Cross-linking was essential to stabilize the HBV-receptor interaction and only enabled in this way the subsequent identification of NTCP by MS. Further experimental validation of the results showed that inhibition of NTCP expression blocked both HBV and HDV infection of liver cells. The discovery of NTCP as HBV entry receptor not only allowed the development of new HBV-sensitive cell lines that better phenocopied the complete life cycle of the virus but also enabled the further development of myreludex B (Volz et al. 2013), a synthetic N-acylated preS1 lipopeptide-based inhibitor of HBV and HDV entry, currently used for the treatment of chronic HDV (Bogomolov et al. 2016) or dual infection of HBV and HDV (Blank et al. 2016; Donkers et al. 2017).

An alternative affinity capture approach is the above mentioned HATRIC-LRC, which was implemented to shed light on the complex interaction between Influenza A virus (IAV) and the surface of the host cell (Sobotzki et al. 2018). This chemoproteomic technology employs a tri-functional linker, termed HATRIC, that enables attachment of a ligand, covalent binding to the glycosylated receptor, and click-chemistry based enrichment. HATRIC was first coupled to the intact Human IAV H3N2 virus. Upon binding to the A549 cell surface, receptors in close proximity were crosslinked to the virus and enriched through the azide affinity handle. Mass spectrometry was used to identify candidate receptors, and the list was further refined to six potential host entry facilitators for IAV by validating their impact on viral entry.

Srivastrava et al. used likewise a trifunctional chemical probe, but with different chemical properties to identify the entry receptor for Zika virus. The multifunctional chemical probe was first conjugated to the surface of the intact ZIKA virus particle, the photoreactive second group cross-linked to the cell surface receptor on the host cell upon UV exposure,

and the third moiety, a biotin, enabled the purification of the cross-linked complex. The use of the whole viral particle, instead of a truncated soluble domain of a viral protein, to capture natural *bona fide* virus entry, enabled the identification of NCAM1 as the Zika virus receptor (Srivastava et al. 2020).

The progress achieved in the field of quantitative MS-based proteotyping has enabled the discovery of virus entry receptors shedding light on the mechanisms viruses exploit to enter the cells. The elucidation of viral entry mechanisms raises the opportunity for targeted development of therapeutic interventions that block the viral entry process. Currently, around 66% of all pharmaceutical drugs in the DrugBank target cell-surface proteins (Bausch-Fluck, Milani, and Wollscheid 2019). In the field of antiviral treatments an opposite trend has been observed. Classically, host-targeting antiviral strategies have focused on inhibiting intracellular proteins crucial for virus replication and/or immune modulation. However, new classes of antiviral drugs affecting cell-surface proteins have gained a foothold as an antiviral strategy.

The first antiviral agent of this class to be approved by the US Food and Drug Administration (FDA) in 2007 was maraviroc, a prime example for the importance of spatial knowledge about the lateral interaction network of receptors. Maraviroc inhibits the interaction between the host chemokine receptor CCR5 and the HIV-1 viral protein gp120, thereby inhibiting the entry of HIV into the host cell (MacArthur and Novak 2008; Dorr et al. 2005). CCR5 was discovered by Alkhatib et al, as a co-receptor essential for HIV entry into CD4+ T lymphocytes (Alkhatib et al. 1996). Treating cells with the MIP-1a, MIP-1b, or RANTES, the natural ligands of CCR5, significantly inhibited HIV virus entry. This discovery raised great interest in the pharmaceutical industry, and the efforts to screen for drugs targeting CCR5 led to the development of maraviroc.

Once the cell surface receptors exploited by viruses are identified, antibodies can also be developed against these specific receptors to block viral binding. A strategy established along with these recent developments is immunochemical engineering, a technology based on anchoring receptor specific antibodies to the plasma membrane in order to enhance local concentration and efficiency with which virus attachment to the surfaceome is blocked. This strategy was used to effectively render cells insensitive to human rhinovirus and HIV-1 (Xie et al. 2017). In the context of rhinovirus, a phage-displayed combinatorial human antibody library was screened for antibodies that bind to ICAM-1, the known receptor of rhinovirus (Greve et al. 1989). Selected ICAM-1 specific antibodies were anchored to the

plasma membrane to inhibit binding between the rhinovirus and its receptor at a higher efficiency compared to free circulating antibodies. The same surfaceome-targeting approach was used to render cells resistant to HIV infection by targeting the CD4 receptor, thereby opening the possibility of curing the infection. An alternative treatment approach is based on the principle that the inhibition of the entry receptor synthesis will result in a reduction of the abundance of the receptor at the plasma membrane. A strategy that hinders virus attachment and subsequent infection. A prime example for such an approach is the antiviral agent cyclotriazadisulfonamide (CADA), which lowers CD4 abundance and subsequently leads to reduced binding and infection by HIV-1 and human herpesvirus 7 (Vermeire et al. 2002).

In summary mapping of the cell surface receptor repertoire, and more generally the complex host-virus nanoscale interactions, is of critical importance for understanding the mechanisms by which viruses infect host cells. The progress achieved in the MS-based proteotyping field has enabled the discovery of cell surface receptors with high sensitivity in smaller subpopulation of cells. In the future, further elucidation of virus-induced surface remodeling is expected to guide the development of new antiviral strategies that will not only block virus entry and reduce the spread of the virus, but also selectively target cells that are already infected for the treatment of persistent infections.

2.5 Elucidation of virus-induced surfaceome dynamics

Invading viruses are under constant pressure to escape the host immune system. Among the viral countermeasures, viruses modulate cell surface residing and secreted proteins to their advantage (Alcami and Koszinowski 2000). For example, HIV infection of T cells or antigen-presenting cells (APCs) leads to a decrease in the cell surface abundance of complement receptors CR1, CR2, CR3, C5aR, major histocompatibility complex (MHC) - class I and II proteins, entry receptors CD4, CXCR4, CCR5, and T cell activating receptors CD3 and IL-2R (Speth and Dierich 1999; Landi et al. 2011). These abundance modulations of selected cellular receptors, and in turn their signaling functions, enable the virus eventually to evade the host immune response. The well-studied effects of HIV infection illustrate the diversity of modulated processes belonging to the innate and adaptive immune system occurring during virus infection. Interestingly, many virus families have evolved similar strategies to target immune signaling. To avoid clearance of infected cells by T cell

mediated cytotoxicity viruses such as HIV, human cytomegalovirus (HCMV), Influenza A and bovine papillomavirus modulate MHC-class I and II antigen presentation. Viruses suppress the cell surface abundance of antigen presenting proteins by altering their expression, their localizations at the cell surface, or their turnover (Petersen, Morris, and Solheim 2003; Forsyth and Eisenlohr 2016; Koutsakos et al. 2019). As a counter effect, this loss renders cells susceptible to cytotoxicity mediated by natural killer (NK) cells (Kärre et al. 1986). NK cells are among the first line of defenders and function prior to the induction of the adaptive immune response. NK cells express the two major inhibitory receptor classes KIR and the CD94-NKG2A heterodimers, that sense the presence of MHC class I proteins on cells (Pegram et al. 2011). Deficiency in MHC class I proteins prompts activation of NK cells, ultimately leading to pathogen clearance (Vivier et al. 2008). Viruses have developed numerous mechanisms to evade NK-based immune surveillance (Orange et al. 2002). Members of the retrovirus, poxvirus, herpesvirus, papillomavirus, and flavivirus families evade the NK cell response mainly by modulation of surface receptors and/or ligand secretion to interfere with NK cell receptor recognition. HCMV encodes a MHC class I homolog named UL18 (Beck and Barrell 1988) that blocks NK cytotoxicity despite the absence of host MHC class I (Reyburn et al. 1997; Cosman et al. 1997). As UL18 has been reported to have both inhibitory and activating effects on the NK cell response (Prod'homme et al. 2007; Leong et al. 1998), further experiments are needed to elucidate its function in more detail. Studies based on murine CMV support the notion that multiple class I MHC viral homologs exist (Smith et al. 2002). Other viruses overcome the cytotoxic responses emanating from T and NK cells by specifically modulating only the expression of certain MHC class I alleles. Viruses reduce surface HLA-A and HLA-B molecules, which are efficient at presenting viral peptides to cytotoxic T lymphocytes, whereas they spare HLA-C and HLA-E, well-known ligands for NK-cell inhibitory receptors (Schust et al. 1998; Lopez-Botet, Llano, and Ortega 2001).

Apart from its immune modulatory function, the host surfaceome also plays a role in confining the spread of virions. For instance, the INF-induced antiviral host restriction factor Bone marrow stromal antigen 2 (BST-2, also named Tetherin) blocks the release of diverse mammalian enveloped viruses, e.g. HIV (Homann et al. 2011), filoviruses (Jouvenet et al. 2009), arenaviruses (Sakuma et al. 2009) and herpesviruses (Mansouri et al. 2009), by tethering virions to the plasma membrane. This mechanism hinders virion release towards the extracellular space and therefore limits the spread of the infection (Neil, Zang, and Bieniasz 2008; Van Damme et al. 2008). This strategy is counteracted by the

HIV protein Vpu, which promotes in turn the downregulation of BST-2. Interestingly, downregulation of BST-2 by Vpu also protects HIV-infected cells from antibody-dependent cell-mediated cytotoxicity (ADCC) (Alvarez et al. 2014; Arias et al. 2014). However, it was reported that INF α and/or small-molecule inhibitors of BST-2 antagonists promote elimination of productively infected cells by broadly neutralizing antibodies (Pham et al. 2016). Therefore, BST-2 antagonists are explored towards the effective treatment of infections caused by enveloped viruses.

The selected examples described above represent only a few of numerous mechanisms, which viruses developed during co-evolution with cellular hosts to evade the immune system. Nevertheless, the examples also illustrate the importance of studying the surfaceome and its virus-induced qualitative, quantitative and organizational changes. The analysis of surfaceome perturbations that occur upon infection is, therefore, imperative to shed light on the ever-improving strategies viruses use to escape the host immune system, as well as the rational basis for the development of new antiviral therapeutics. In this regard, several MS-based studies provided qualitative and quantitative data on surfaceome dynamics upon virus infection (Berro et al. 2007; Gudleski-O'Regan et al. 2012; Stergiou et al. 2013; Weekes et al. 2014; Hsu et al. 2015; Matheson et al. 2015; Viswanathan et al. 2017; Ersing et al. 2017; Zhang et al. 2019; Soh et al. 2020). Here, we will focus and describe in more detail two viruses and associated studies exploring surfaceome dynamics, in the context of human cytomegalovirus (HCMV) infection, as a prime example for DNA viruses, and a second study focusing on human immunodeficiency virus (HIV) infection, as a prime example for RNA viruses.

HCMV is an enveloped, double stranded DNA virus belonging to the herpesvirus family. A high percentage of the world population is actually infected with HCMV, albeit this pathogenic virus has the ability to lie dormant, causing typically life-long latency. Nevertheless, HCMV infection can lead to severe issues in immunosuppressed individuals and preterm infants (Mocarski et al. 2013). Gudleski-O'Regan et al. analysed the surfaceome of HCMV infected fibroblasts in order to gain insights into HCMV molecular pathogenesis (Gudleski-O'Regan et al. 2012). Cell surface residing proteins were tagged with sulfo-NHS-SS-biotin, a primary amine-reactive reagent enabling tagging of lysine residues and N-termini in protein amino acid backbones, which can subsequently be enriched by affinity purification strategies using the biotin handle with subsequent analysis by MS-based quantitation. Over the course of the viral infection, 500 annotated cell surface proteins were quantified at 6, 24 and 72 h post infection. While in the early phase only 8%

of the surfaceome was classified as differentially abundant, the ratio of regulated to unregulated cell surface proteins increased with progression of infection to 24% at 72 h post infection. These cell surface proteins were involved in apoptosis (e.g., CD99), cell adhesion (CSPG4, VCAM1), immune response (CD55, CD59), metabolism (LRP1, GLUT4), transport (Na⁺/K⁺-transporting ATPase-subunits), and signaling (ephrins). Further validation of LRP1 demonstrated that its increased abundance during the early phases of infection reduced intracellular cholesterol levels and altered the lipid composition of virion envelopes, resulting in lower infectivity due to inefficient fusion of the virion envelope with the plasma membrane.

In a second study, Weekes et al. applied a quantitative temporal viromics (QTV) (Weekes et al. 2014) approach to characterize the surfaceome and in parallel the cellular proteotype during HCMV infection. Cell surface proteins were enriched through chemical labeling using aminoxy-biotin, which can be used to covalently attach biotin to aldehyde or ketone groups on polysaccharides/glycoproteins, with subsequent affinity purification. In total, about 1,200 cell surface annotated proteins and >8,000 intracellular proteins were quantified by using an MS3-based TMT data acquisition strategy with seven time points starting from 6 to 96 h post infection. By integrating both datasets the regulation of several known, as well as potentially new cell surface residing NK and T cell ligands, were reported. Among these, protocadherins were exceptionally strongly reduced in their cell surface abundance as protein family, indicating a potential role as immunomodulators. Besides the quantitation of host proteins, 29 viral glycoproteins were identified as surfaceome members. Apart from known members of the virion envelope, which appear only at the plasma membrane during later stages of infection, a high correlation between expression and cell surface abundance for viral proteins was observed for many glycoproteins. The temporal resolution enabled the classification of the delayed appearing UL119 as a potentially new envelope protein (Weekes et al. 2014). The dataset from Weekes et al. was subsequently used to validate the isolation quality of the plasma membrane fraction in an elegant cell-wide organelle separation approach by Beltran et al., enabling insights into molecular infection processes on the subcellular level upon HCMV infection of human fibroblasts (Jean Beltran, Mathias, and Cristea 2016). Cellular organelles were separated in a two-step centrifugation approach up to 120 h post infection with five time points post infection in order to establish a spatio-temporal resolved proteotype during infection with compartmental/subcellular resolution. Isolated proteins were classified in spatially distinct plasma membrane-residing, cytosol, ER, Golgi

complex, lysosome, mitochondria, and peroxisome clusters. The plasma membrane fraction reached >80 % agreement in the localisation assignment with the QTV analysis (Weekes et al. 2014). Beltran et al. further reported an early reduction of plasma membrane abundance of proteins involved in adhesion, cell junction, and antigen presentation, together with a global reorganisation across the secretory pathway, plasma membrane, and mitochondria. Interestingly, Beltran et al. could show the dynamic localisation switch of the viral protein UL13 between the plasma membrane/cytoplasm at 24 h post infection, to the mitochondria at 72 h post infection, and again to the plasma membrane and ER/Golgi late in infection (Jean Beltran, Mathias, and Cristea 2016). The multi-localizing viral protein UL13 may also have different functional relevance in its distinct environments, which still remains elusive. In addition to the temporal analysis of surfaceome dynamics, MS-based proteotyping can be used as a tool to dissect the contribution of individual proteins to molecular mechanisms. The viral HCMV proteins US3, US6, US11 and US2 were individually overexpressed in THP-1 cells. Subsequently, the surfaceome was analysed by aminoxy-biotin-based chemical labeling. The HCMV proteins US3, US6 and US11 were found to specifically downregulate MHC class 1 proteins, as predicted from the literature. Besides that, expression of US2 in THP-1 had a broader impact and played the role of a mediator. Through triggering the proteasomal degradation of five distinct integrin chains, CD112, the interleukin-12 receptor, PTPRJ via the cellular E3 ligase TRC8, US2 ultimately affected integrin signaling, cell adhesion and migration (Hsu et al. 2015).

HIV causes, since the early 1980s, an ongoing pandemic and has infected an estimated 65 million people worldwide. HIV infection eventually leads to the acquired immunodeficiency syndrome (AIDS), which resulted in approximately 25 million deaths to date according to the Joint United Nations Programme on HIV/AIDS (UNAIDS) 2006 report on the global AIDS epidemic. Over the course of an HIV-infection, the surfaceome is described as a “combat zone” (Doms and Trono 2000). The surfaceome was shown to play multiple critical roles in the infection of HIV beyond the initial binding and uptake of the HIV particle itself (Abbas and Herbein 2014). Viral adhesion, viral spreading and cellular apoptosis are additional aspects in which the surfaceome plays a role in HIV pathogenesis. (Speth and Dierich 1999).

In an interesting study by Matheson et al., the HIV infection of T cells was temporally analyzed during the first 72 h of the infection using the above described QTV approach (Matheson et al. 2015). The proteomic data confirmed the previously reported reduction in cell surface abundance of CD4, HLA-A, CCR7, CD28, NTB-A, SELL, and the tetraspanins

CD37/53/63/81/82, as well as controversially discussed proteins such as CD71, CXCR4, and CCR5. In total, more than one hundred host surfaceome members were differentially regulated in their cell surface abundance. Many of these detected quantitative protein abundance changes were associated with cell surface receptors involved in immune functions, but others such as in case of SNAT1, were interestingly associated with amino acid transport and therefore further validated. It was subsequently found that Viral protein U (Vpu), an accessory protein that in HIV is encoded by the *vpu* gene, mediates the depletion of amino acid transporter SNAT1 from the surfaceome pool by triggering its proteasomal-degradation. The resulting data revealed a mechanism showing that SNAT1 depletion results in limited alanine uptake and reduced intracellular free alanine pools in CD4⁺ T cells. This mechanism ultimately leads to decreased alanine-dependent CD4⁺ mitogenesis and consequently to reduced T cell activation. The authors propose therefore a unique paradigm of HIV interference with immunometabolism (Sugden and Cohen 2015; Matheson et al. 2015).

In summary, the above-described MS-based surfaceome analysis strategies enabled the characterization of dynamic surfaceome changes during the course of viral infection and, more importantly, contributed to a deeper mechanistic understanding of the molecular mechanisms underlying the interactions between viruses, the host surfaceome and the immune system.

2.6 The surfaceome and its role in viral spreading

During the final stage of the viral life cycle, newly generated viral particles egress the cell at spatially confined cell membrane locations. Viruses typically spread in between host cells through the release of viral particles in the extracellular space surrounding the initially infected cell. However, several viruses have developed alternative mechanisms to spread in a direct cell-to-cell fashion. These alternative strategies facilitate a rapid viral dissemination and avoid immune recognition of extracellular virions. Viruses achieve cell-to-cell dissemination through a variety of mechanisms as reviewed by Sattentau (Sattentau 2008): some viruses hijack intracellular protein complexes, like for example the recruitment of actin- or tubulin-containing structures that project the virus towards neighbouring cell, strategy commonly used in poxviruses, herpesviruses and retroviruses infection, whereas others induce a surfaceome reorganization in order to engage cell-to-

cell contacts. An illustration is the formation of virological synapses at the surface of immune cells. Virological synapses are highly molecular organized cellular surfaceome junctions formed between communicating infected and uninfected cells, with a partial functional homology to immunological synapses (Igakura et al. 2003; Bayliss and Piguet 2018). The formation of virological synapses between infected and uninfected T cells has been observed in numerous viruses, including the human T-lymphotropic virus-1 (HTLV-1) and HIV-1. HTLV-1 takes advantage of the additional engagement of intercellular adhesion molecule 1 (ICAM1) on the infected cells of the ligand lymphocyte function-associated antigen 1 (LFA1) to stabilize virological synapses. This process initiates an intracellular relocation of the microtubule organization center (MTOC) in a Tax-dependent fashion inducing a polarization of viral assembly and budding towards the synaptic cleft of the virological synapses (Barnard et al. 2005; Nejmeddine et al. 2005; Nejmeddine and Bangham 2010). Additional studies have shown that HIV-1 exploits the same strategy to form virological surfaceome synapses between infected and uninfected T cells to facilitate cell-to-cell transmission (Jolly et al. 2011; Jolly, Mitar, and Sattentau 2007; Vasiliver-Shamis et al. 2009). Beside cell-to-cell transmission between T cells, HIV-1 also takes advantage of the interaction between dendritic cells (DC) and T cells during lymphocyte activation for the early transmission of viral particles between the mucosal tissue and the secondary lymphoid tissue. HIV-1 virions are “trapped” at the surface of DC cells by alternative HIV-1 receptors. Upon interaction with the T-cell a virological synapse is formed which recruits virions and the cognate receptors CD4, CXCR4 and CCR5 on the T-cell facilitating cell-to-cell spread. Several alternative receptors have been identified as HIV-1 binding factors, including: DC-SIGN (DC-specific intercellular adhesion molecule-3-grabbing non-integrin) which binds the viral protein gp120 (Geijtenbeek et al. 2000; Arrighi et al. 2004; Curtis, Scharnowske, and Watson 1992) and Siglec-1 (sialic acid-binding Ig-like lectin 1, CD169) which mediates HIV-1 trans-infection by interacting with viral membrane gangliosides. The molecular, spatial and temporal organization of virological synapses and their molecular mode of action is currently not completely understood.

Viral synapses, and functionally similar mechanisms supporting cell-to-cell (or trans) infections are significant strategies for viruses to achieve high infectivity in order to escape the immune system response. Therefore, it is essential to understand at the molecular level the nanoscale reorganization of the surfaceome of infected cells and their respective communicating cells in order to be able to inhibit further viral dissemination. With the

recent advancements in spatial MS-based proteotyping strategies described above the more detailed elucidation of such processes within virological synapses becomes feasible now.

2.7 Perspective

Proteotyping technologies considerably contributed to the identification of viral receptors and the elucidation of virus-induced surfaceome changes, thereby providing mechanistic insights and expanding our knowledge about viral pathogenicity. Temporally-resolved analysis of surfaceome abundance changes provide direct insights into the cellular host response towards viral intruders and enable the determination of virus-hijacked signaling networks. Surfaceome abundance changes can also be tell-tale signs as extracellular markers for intracellular signaling network changes and provide additional mechanistic insights into the molecular mode of action during the stages of successful infection and viral propagation. Twenty years after the human genome was sequenced, new technologies enable virologists now to go beyond genomics and elucidate the spatial molecular (surfaceome) organisation influencing viral propagation. The analysis of protein-protein interactions, functional nanoclusters and receptor cross-talk are taking center stage in recognition that these submembrane signaling domains are playing key roles in viral propagation, immune signaling and pathogen clearance (Mattila, Batista, and Treanor 2016). Recently established large-scale platforms enable now high-throughput testing of binary extracellular receptor interactions in the context of host-pathogen interactions (Martinez-Martin et al. 2016; Galaway and Wright 2020; Husain et al. 2019). Martinez-Martin et al. mapped the extracellular host-virus interactome of recombinant Human Adenovirus HAdV-E3 proteins versus 1,500 single host transmembrane proteins. The Genentech team identified 51 new interaction pairs and validated them using complementary technologies (Martinez-Martin et al. 2016). While these approaches have great potential to decode extracellular interactions, complementary technologies are needed to also probe the native environment of receptors and their nanoscale organization. Here, recently developed proximity-tagging strategies can fill this gap and together these technologies can provide a systems virology understanding and perspective on the molecular nanoscale organization necessary for successful viral propagation. Among these new proximity-tagging strategies for decoding surfaceome nanoscale organization are the recently developed light-induced proximity labeling approaches μ Map and LUX-MS. Both

MS-based optoproteomic technologies were shown to enable the discovery of molecular nanoscale architecture in a spatio-temporal manner from receptor interaction networks to intercellular communication within immunological synapses (Geri et al. 2020; Müller et al. 2020). The application of light-induced proximity-tagging strategies in the context of viral infection will likely lead to new molecular mechanistic insights about the spatial organization and development of virological synapses. Moving from a protein-centric view in the context of viral infection to a proteoform-centric view will further be critical to bridge the current gap and quest in determining the cellular phenotype upon infection from the genotype. As scientists/virologists, we have the unique opportunity now to appreciate the complexity which resides within co-existing (surfaceome) proteoforms decorated with specific subsets of post- and co-translational modifications guiding functional molecular interactions with viruses uncovered by the latest (MS-)technology advancements. This newly gained knowledge can in turn be leveraged now to combat viral infections using innovative pharmaceutical strategies, targeting not only proteins residing within the drug-accessible surfaceome, but rather host proteoform-centric complexes - as the mediators of viral infection.

Acknowledgements

B.W. acknowledges generous support from ETH Zurich and D-HEST (BMPP). This work was also supported by a Swiss National Science Foundation Grant (grant 31003A_160259) to B.W. and by the Personalized Health and Related Technologies (PHRT) strategic focus area of ETH (to B.W.). Figures were created with a licensed version BioRender.com (to B.W.), partially by adaptation of BioRender templates, retrieved from <https://app.biorender.com/biorender-templates>. The authors would also like to acknowledge the Wollscheid lab (wollscheidlab.org) for critical feedback on the manuscript.

Conflict of interest statement

The authors declare no conflicts of interest, competing interests or financial interests.

CHAPTER 3

VACV hijacks the host surfaceome to gain control over extracellular signaling

This chapter represents a draft of a manuscript in preparation about my main Ph.D. project.

Fabian Wendt^{1,2}, Moona Huttunen^{3,4}, Jason Mercer^{3,4}, Bernd Wollscheid^{1,2}

Manuscript in preparation

1. Department of Health Sciences and Technology (D-HEST), ETH Zurich, Institute of Translational Medicine (ITM), Zurich, Switzerland
2. Swiss Institute of Bioinformatics (SIB), Lausanne, Switzerland
3. Medical Research Council-Laboratory for Molecular Cell Biology, University College London, London, UK
4. Institute of Microbiology and Infection, University of Birmingham, Birmingham, UK

Contribution

Fabian Wendt conceived the project, designed research, and conducted all experiments. He wrote the original draft and edited the manuscript. He performed experiments including design, sample preparation, data acquisition, data analysis and interpretation.

3.1 Abstract

Control over extracellular signaling is critical for pathogens, such as vaccinia virus (VACV), to evade the immune response and effectively spread within the host. VACV is known to encode more than 200 viral proteins, of which one-third are estimated to combat the human immune system. However, underlying mechanisms at the cell surface, the interface of extracellular signaling, and the engagement of the cell surface residing proteome (surfaceome) during infection are largely unknown. Using spatial chemoproteomic strategies enabled us to unravel the surfaceome proteotype across the VACV life cycle and revealed a distinctive quantitative modulation of adhesion, ephrin, and growth factor receptors as well as proteins with immunomodulatory potential. The abundance reduction of NK and T cell ligands from the cell surface supports the evasion of VACV from cellular cytotoxicity. Moreover, VACV proteins repopulate the host cell surface, of which many are thought to be involved in virus spread and immune signaling. Approximately 5 % of the encoded viral proteome localizes to the cell surface during the infection, including previously not reported viral protein A14, and proteins with an unknown function such as A40. Intrigued by the immunomodulatory phenotype of A40 *in vivo*, we decoded the extracellular interactome using proximity-labeling technologies. We found A40 to be embedded in a network of integrins and basement membrane proteins, which may cause a dysregulation of ECM-immune cell interactions. Together, the presented data reveal that VACV hijacks the surfaceome by modulation of host protein abundance and localization of viral proteins at the cell surface to gain control over extracellular signaling.

3.2 Introduction

Vaccinia virus (VACV) is best known for the eradication of smallpox's causative agent variola virus (Fenner et al., 1988). Beyond its intended use as a live vaccine, the investigation of host-VACV biology led to the discovery of fundamental concepts in virology and host-virus biology (Yang et al., 2021). As an obligate intracellular parasite, VACV depends on the infection of a host for its replication. To achieve favourable replication conditions, beneficial pathways like the MEK/ERK pathway are exploited, while simultaneously the host defense response is counteracted to evade cell death, and the immune system (Bonjardim, 2017; Haga and Bowie, 2005; Veyer et al., 2017). As a large DNA virus, VACV encodes more than 200 ORFs, and packages around 80 proteins within the virion (Resch et al., 2007). Many viral proteins interfere with the host proteome on transcriptional, translational, and post-translational level, driving a host shut off (Dhungel et al., 2020). Moreover, VACV selectively modulates the abundance, PTM profiles, interaction space, and subcellular localisation of host proteins (Kleinpeter et al., 2019; Mercer et al., 2012; Novy et al., 2018; Soday et al., 2019).

Initially, VACV passes the plasma membrane (PM) barrier and enters cells by macropinocytosis (Mercer and Helenius, 2008). The subsequent virus replication is localised exclusively cytosolic. Nevertheless, the PM remains a crucial interface during the viral infection. Next to representing a physical barrier separating the cell from its environment, the PM harbours the cell surface residing proteome (surfaceome), which orchestrates the bidirectional information transfer bridging the extra- and intracellular space (Bausch-Fluck et al., 2019). At the infection site, cell surface proteins process immune signaling of the inflammatory interferon (IFN)-mediated response and intercellular communication with macrophages and NK cells, important for the innate immune response, and with T and B cells, involved in the adaptive immune system and eventually responsible for virus clearance. Therefore, many viruses such as human cytomegalovirus (HCMV) and human immunodeficiency virus (HIV), hijack surfaceome-mediated signaling to achieve favourable replication conditions and to evade the immune system (Wendt et al., 2021). Likewise, it was reported that VACV engages with the surfaceome to its advantage. VACV triggers receptor-mediated signaling promoting critical steps of the viral life cycle such as replication and spread by e.g. EGFR-mediated signaling (Beerli et al., 2019; Silva et al., 2006). Additionally, VACV proteins operate in the extracellular space. For instance, viral proteins were identified at the cell surface

accelerating the infection kinetics, avoiding superinfection and suppressing immune signaling (Alcamí et al., 2000; Doceul et al., 2010; Turner and Moyer, 2008). The regulation of immune cell ligands such as HLA-E upon VACV infection perturbs the cell-mediated cytotoxicity (Brooks et al., 2006). However, VACV spreading and immune evasion mechanisms are not fully understood. The role of the surfaceome and its engagement in the VACV infection post virus entry remains elusive. Knowledge of host cell surface modulation is sparse and a systematic picture of viral proteins at the PM, their engaged interactions and functional relevance in this localisation need to be investigated to understand viral propagation.

To resolve the role of the surfaceome during the VACV infection, we investigated the spatial proteotype upon VACV infection by integration of the full proteome and the surfaceome protein profiles with high spatio-temporal resolution. Overall, we tracked > 5600 proteins in the whole cell lysate and > 400 cell surface residing N-glycoproteins by mass spectrometry-based chemoproteomics across the VACV life cycle. In line with reported findings, we observed the strong regulation of the MEK/ERK pathway as well as the downregulation of Ephrin signaling, and extracellular matrix constituents (Soday et al., 2019). Furthermore, we report two processes, by which VACV hijacks the PM and the surfaceome. On the one hand, VACV exploits the plasma membrane as a scaffold, observed by the repopulation of the cell surface with viral proteins, from where they can interfere with extracellular signaling. On the other hand, VACV infection leads to the regulation of adhesion molecules, growth factor receptors, and immune-relevant signaling proteins, aiding its replication and evasion from the immune system. Surprisingly, some viral proteins such as VACV A40 were already present at the cell surface in the early phase of the infection. Thus, we further investigated the immunomodulatory phenotype and unknown function of A40, by characterising its interaction space at the cell surface using the strength of proximity-labeling technologies. We found A40 embedded in a network of integrin and basement-membrane proteins and hypothesize that A40 may dysregulate ECM-immune cell interactions.

3.3 Results

3.3.1 Temporal analysis of the total proteome changes upon VACV infection

To investigate the host-VACV interaction, we first elucidated the total proteome across the life cycle of VACV. For this purpose, we selected experimental timepoints covering all essential steps of the infection (Fig 1a). The first experimental timepoints at 1 and 2 hours post infection (hpi) represent the early events subsequent to cell entry during VACV core uncoating and activation. The following time points at the intermediate and late stage of the infection between 4, 6 and 8 hpi cover the genome replication and virion assembly in cytoplasmic viral factories as well as cell egress of extracellular virions (EVs). The tremendous intracellular accumulation of mature virions (MVs) at 24 hpi represents the study endpoint (Fig. 1a and Supplementary Fig 1a). The VACV cell egress by host cell lysis is observed in a noticeable later time point after approximately 72 hpi and was not considered in this study (Bidgood and Mercer, 2015). We infected HeLa CCL2 cells with VACV Western Reserve (WR) at a high multiplicity of infection of MOI = 10 to reach synchronous cell infection. Subsequently, the total proteome was quantified at 1, 2, 4, 6, 8 and 24 hpi against the Mock-infected control by utilizing a global DIA-based proteomic approach (Fig. 1b). Quality control by principal component analysis and hierarchical clustering allows sample separation based on their abundance variability. Application to our dataset verified that the individual samples for the same time point cluster closely together and that the conditions delineate from each other (Supplementary Fig. 1b, c). Overall, we quantified > 5600 proteins across all conditions with 627 proteins being differentially regulated at a minimum of one timepoint post infection compared to the mock-infected control (Fig. 1c). Next to the host proteome changes, our mass spectrometry-based approach enabled us to characterize the virus-originated proteome, the entirety of all viral proteins synthesized within the viral life cycle. According to the UniProt Knowledgebase, VACV WR encodes 230 ORFs (Identifier: 10254 /VACCV). For 77 % of these we identified the gene product at the protein level and were able to quantify 151 viral proteins across the VACV life cycle (Fig. 1d). By studying the protein abundance changes longitudinal, we observed, as expected, the staggered appearance of viral proteins with advancing infection. In contrast, significant host proteome changes during the first 8 hpi are moderate and mostly appear between 8 and 24 hpi (Fig. 1f). At 24 hpi we found approximately 440 host proteins being significantly down- and 33 host proteins being significantly upregulated (Fig. 1e). The overall abundance of the host proteome decreased

slightly but non-significantly after 8 hpi. This observation correlates with the transcriptional and translational host shutdown induced by VACV and was also observed with complementary technologies, such as transcriptomics and ribosome profiling (Dai et al., 2017).

3.3.2 VACV infection induces transcription factor expression, and leads to downregulation of extracellular matrix components

Only a minority of regulated host proteins was found to increase in abundance upon VACV infection. Striking, among these upregulated proteins many transcription factors are accumulated. In line with previous reports, we detected the upregulation of the transcription factors EGR-1, and c-Jun, which are expressed downstream upon activation of the MEK/ERK pathway (Fig. 2b) (Leite et al., 2017; Silva et al., 2006). C-Jun is the main component of the AP-1 transcription factor and can form homo Jun-Jun dimers, or heterodimers with proteins of the Fos family (Karin et al., 1997). Moreover, we also observed the upregulation of further AP-1 components, JunB and FOSL1, as well as the associated transcription factors MAFK and MAFF, which follow the same kinetic abundance pattern (Fig. 2b). Interestingly, the expression of COX-2, known to be regulated by AP1, is strongly upregulated alongside.

The majority of regulated proteins lose abundance with advancing VACV infection. To obtain further insights into their functionality, we performed a gene ontology analysis on the differentially regulated proteins. The significantly overrepresented categories reveal enrichment of proteins that are involved in the response to DNA damage stimulus, cellular stress response, cell cycle, DNA metabolic processes and proliferation as well as most prominently proteins modulating or belonging to the extracellular space (Fig. 2a).

The downregulated protein cluster of the extracellular space contains fibrillin-1 and -2, fibulin family members FBLN1, -3, and -5, as well as collagen family members, COL1A1, COL3A1, COL4A1, COL12A1. Moreover, several laminin members were found lower in abundance. The modulation of the ECM, in particular collagens, was previously reported for DNA viruses such as HCMV and VACV (Soday et al., 2019). However, the underlying processes are unknown. Interestingly, we observed the temporary upregulation of ECM remodelling proteins CCN1 and CCN2 between 2 and 6 hpi which might play a role in the downregulation of the ECM components.

Furthermore, ubiquitin regulating enzymes are strongly enriched among the regulated proteins. Many ubiquitin-conjugating E2 enzymes, such as UBE2 -T, -K, -S, -N, -A, -C are

downregulated late during the infection, which might be a protection mechanism against the degradation of viral proteins, without impairing early necessary proteasomal degradation. Moreover, UBE3 ligases such as UBE3C and ubiquitin ligases belonging to the tripartite motif (TRIM) family members were found to be regulated. Whereas TRIM21 (RO52), -32 and -47 abundance increased, we detected TRIM25 to be less abundant upon infection. Interestingly, next to the catalysis of polyubiquitination, TRIM proteins are involved in the regulation of innate and adaptive immunity (Yang et al., 2020).

Besides the host proteome, we quantify two-thirds of the viriome upon infection. The time-resolved data enabled us to define temporal classes for the synthesis of VACV proteins using soft-clustering (Mfuzz). In accordance with earlier findings (Croft et al., 2015), we can report four temporal classes of viral protein synthesis by unbiased clustering (Fig. 2c). We named our synthesis classes in accordance with previous reports, immediate early, early, intermediate, and late class and applied a literature-guided annotation of the protein function based on the transcriptomic study of Yang et al. and the total proteome study of Soday et al. (Soday et al., 2019; Yang et al., 2010). Proteins synthesized in the early time points of the infection are involved in the interaction with the host, followed by proteins necessary for DNA replication and the VACV transcription machinery. The predominant majority of late synthesized VACV proteins are associated with the virus morphogenesis, and constituent of the virion (Fig. 2c). The temporal order of synthesized proteins is following the necessary function for the individual phases of the VACV life cycle, which manifest the biological relevance of our data.

3.3.3 Temporal surfaceome analysis upon VACV infection reveals modulation of growth factor, adhesion, and immune-related cell surface proteins

Due to the strong enrichment of extracellular proteins among the regulated clusters, we investigated the cell surface proteome (surfaceome) in more detail. For this purpose, we took quantitative snapshots of the surfaceome in a temporal fashion across the viral life cycle using our recently published automated cell surface capturing (autoCSC) strategy (van Oostrum et al., 2019). AutoCSC enables a comprehensive view of the N-glycoproteome at the cell surface, which encompasses ~90 % of all cell surface residing proteins, by selective labeling, enrichment and elution of integral and from the outer leaf associated cell membrane proteins. The quantitative autoCSC data draw a spatially-resolved map of cell surface N-glycoproteins during infection. Moreover, the detected peptides give access to protein topology information (Supplementary Fig. 3a). In order to

directly integrate our total proteome and surfaceome data, we followed the same experimental timepoints for the autoCSC experiment (Fig. 3a). Overall, we quantified more than 400 cell surface residing proteins across the VACV life cycle of which 230 overlapped with the total proteome data (Fig. 3b). A cellular compartment analysis of the quantified proteins verified that these predominantly belong to the cell surface and are mostly integral components of the plasma membrane confirming the specificity of the enrichment by our autoCSC methodology (Supplementary Fig 3b). Across all timepoints, we found approximately 80 proteins differentially regulated of which 30 increased and 50 decreased in abundance upon infection (Fig. 3c).

A full overview of significant differentially regulated proteins is given in a heatmap displaying the scaled log₂ cell surface abundance (Fig. 3d). Strikingly, among the upregulated proteins, a group of proteins has ambiguous cellular localisation annotation. Although annotated to localise to the cell membrane, many of these are also annotated as membrane proteins present on intracellular membrane organelles. Primarily on membranes, derived from endosomes, lysosomes, Golgi and a few also from the endoplasmic reticulum (ER). The quantification of e.g. the endosomal and cell surface membrane protein VPP2 in the total proteome and surfaceome dataset revealed that its overall expression does not change, but its cell surface abundance increases after 6 hpi (Fig. 3d). It is conceivable that these proteins with ambiguous membrane localisation might get co-transported to the plasma membrane during exocytosis of VACV.

Similarly to the total proteome, we also observed the upregulation of MEK/ERK signaling cascade proteins. Amphiregulin (AREG), an EGFR ligand, increases in abundance early upon infection. AREG is shedded by ADAM17 into the extracellular space and is able to activate EGFR by binding with its EGF-like domain (Hosur et al., 2018). However, we are limited in the discrimination between the membrane-residing and the shedded, but EGFR-interacting species.

A similar temporal abundance increase was observed for FAT1 at the cell surface. Comparison with the total proteome data leads to the conclusion that the higher cell surface abundance is caused by its upregulated expression. In contrast to our results, FAT1 was shown previously to get slightly downregulated upon VACV infection in keratinocytes (Soday et al., 2019). The contrary findings might be due to cell-type specificity. Nevertheless, its regulation is highly interesting, as it localizes to lamellipodial protrusions and interacts with Ena and VASP, both proteins involved in the modulation of the actin skeleton during VACV infection (Krause et al., 2004).

Next to the upregulated proteins, we identified approximately twice as many downregulated proteins using autoCSC. Among these are growth factor receptors, ephrin receptors, adhesion and immune-regulatory cell surface proteins. We observed the abundance decrease of growth factor receptors EGFR, FGFR1 and MET at the cell surface. In contrast, a significant downregulation of EGFR or MET in the total proteome pool was not observed. In addition, FGFR1 was not identified in the total proteome. Therefore, their abundance decrease at the cell surface might be a result of internalisation caused by growth factor binding. Furthermore, we observed a decrease of several ephrin receptors EPHB2, EPHA3 and EPHA5 at the cell surface during the course of the infection. A fourth quantified receptor EPHA2 did not change in abundance. Ephrin receptors as well as their corresponding Eph ligands are involved in immune-related signaling and serve as entry receptors for many viruses. Comparison with the total proteome revealed that EPHB2 and EPHB4 are also downregulated in the total proteome data set. Thus, the cell surface abundance decrease might not be due to Eph ligand binding or virus binding and subsequent internalization events, but rather due to an abundance decrease of the total pool in the course of infection. Indeed, recently the VACV-induced proteasomal degradation of Ephrin receptors was discovered (Soday et al., 2019).

Additionally, VACV infection led to the downregulation of many immune-regulated proteins from the cell surface. We observed the abundance reduction of the non-classical MHC class I HLA-E. HLA-E is recognized by a subset of NK and T cells, and can inhibit NK cells through interaction with the inhibitory CD94/NKG2A receptor complex or activate NK cells by binding to CD94/NKG2C (Pietra et al., 2009). Interestingly, the CD94/NKG2A-mediated killing was described before (Brooks et al., 2006). We did not quantify the classical MHC class I HLA-A, -B and -C abundance in our screen. However, classical MHC class I regulation was reported with diverging results upon VACV infection. Whereas in an antibody-based flow cytometry analysis total MHC class I cell surface abundance was not regulated, a MS-based quantification showed in the total proteome a downregulation of HLA-A, -B- and C (Brooks et al., 2006; Soday et al., 2019). Further immunomodulatory proteins regulated in our screen are T and NK cell ligands. Interestingly, we detected the reduction of CD83 abundance at the cell surface. CD83 is an immune checkpoint regulator and allows additionally the classification of mature dendritic cells (Grosche et al., 2020). Its expression in epithelial HeLa cells was validated by the human cell atlas (NX = 8.3, Human Cell Atlas, retrieved 20/2021). In line with our result, VACV-infected dendritic cells show a decreased expression of CD83, CD86 and CD25

during the maturation process (Engelmayer et al., 1999). Membrane-bound CD83 receptor expression in mature dendritic cells leads usually to T cell activation and thus downregulation by VACV could counteract the adaptive immune response. Moreover, we have discovered the downregulation of ICAM1 early in the infection, a costimulator of NK cells, and Nectin-1, whose interaction with CD96 leads to NK cell activation (Holmes et al., 2019). Furthermore, several proteins involved in cell adhesion such as adhesion G-protein coupled receptors GPR56, GPR37 and GPR126, membrane-residing adhesion proteins anthrax toxin receptor 1 (ANTR1) and neural cell adhesion molecule L1-like protein (NCHL1), are less abundant late in the infection, which might affect the migration and motility of infected cell in the late phase of the infection.

3.3.4 VACV proteins repopulate the host cell surface

Interestingly, using our surfaceome approach we detected twelve viral proteins localizing at the cell surface at 24 hpi. A33, B18, A40, A14, A56, F5, SPI3, A34, A28, A38, B5, and A43 gradually appeared to be identified in our temporal resolved autoCSC data set (Fig. 3d). The staggered appearance with the advancing viral infection indicates that the viral cell surface-residing proteins are rather newly translated gene products, than proteins brought along with the entering virions. Integration of topology and signal peptide information from the UniprotKB and Phobius predictor tool via Protter revealed that ten of these proteins harbour a transmembrane structure. The other two proteins B18 and SPI3 carry a signal peptide for secretion and might attach to the plasma membrane upon secretion (Supplementary Fig 3.2b). Identification of the protein N-glycosites allowed them to determine the protein orientation and revealed the viral proteins face the extracellular space (Supplementary Fig 3.2b).

The very first viral proteins that localize to the cell surface during the early infection timepoints are A33, B18 and A40. Indeed, A33 was found to be early expressed and localizes together with A36 to the cell surface, promoting the fast kinetics of VACV spread (Doceul et al., 2010). The reported reverse orientation of these two proteins, with A33 facing the extracellular space and A36 the cytoplasm, explains why A36 was not identified in our screen. Early expressed proteins during VACV infection often fulfill immunomodulatory functions. B18 is known to be an IFN decoy receptor, diminishing host inflammatory signaling. Interestingly, B18's function relies on its tight binding to the plasma membrane via interaction with glycosaminoglycans (GAGs) (Alcamí et al., 2000).

Moreover, A40 is also thought to be an immunomodulatory protein, but its function and clear phenotype remain elusive. It was previously suggested that A40 localizes to the ER, or at the plasma membrane (Palacios et al., 2005; Wilcock et al., 1999). Using an antibody-free approach, we confirmed by detecting its labeled peptide features, that A40 localizes early to the plasma membrane and is a type-II transmembrane glycoprotein facing the extracellular space with its C-terminus. The proteins F5, A56, A14 and SPI3 are appearing in the intermediate phase of the infection during the formation of cytoplasmic factories. For Δ F5-VACV infection a reduced plaque size is reported, but mechanistically insights are largely unknown (Dobson et al., 2014). Interestingly, the membrane protein A56 and secreted SPI3 interact extracellularly and prevent the superinfection of the cell and thus accelerating vaccinia virus spread (Turner and Moyer, 2008). VACV protein A14 is a component of the MV membrane and was previously classified as a phosphorylated and glycosylated protein of which the non-glycosylated form is residing in the virion envelope (Mercer and Traktman, 2003). Here, we confirmed that glycosylated A14 localizes to the plasma membrane. Interestingly, the retrieved topology information by analysing the detected glycosylation site revealed that the orientation within the virion and in the plasma membrane is inverted. Furthermore, we identified another MV membrane component A28, a major constituent of the entry-fusion complex. A38 and A43 are late expressed proteins and were described previously at the plasma membrane, but their function remains elusive (Parkinson et al., 1995; Sood and Moss, 2010). The proteins, which localize latest to the plasma membrane, are B5 and A34 and are packaged into the mature virion (Resch et al., 2007).

3.3.5 A14 and A40 are glycoproteins localising to the host cell surface

We further investigated the molecular details of A14 and A40 in HeLa CCL2 cells, due to their largely unknown function, but interesting immunophenotype. For this purpose, we stably transfected HeLa CCL2 cells with STREP-HA-(SH)-tagged ORFs of the viral proteins under a doxycycline-inducible tet promoter (Supplementary Fig. 4a). In order to verify our expression system, we characterised the viral proteins using SDS-PAGE (Supplementary Fig. 4b). Expression of A40 in HeLa CCL2 cells revealed two distinct migration patterns: a faint signal at 100 kDa and a strong broad signal centering around 37 kDa. Both of these signals are higher than the expected size of SH-tagged A40 protein at 25 kDa. Whereas the high migrating signal corresponds most likely to multimeric A40s,

the strong signal constitutes the glycosylated protein form. To verify the altered migration pattern, we performed a deglycosylation assay using PNGase F, which cleaves off the innermost glycan moiety from the amino acid asparagine. Upon deglycosylation the broad signal at 37 kDa collapsed to a narrow band at the predicted height of ~25 kDa, confirming the N-glycosylation of A40. A comparable analysis was conducted for A14 in HeLa CCL2 cells. SDS-PAGE analysis of A14 revealed the detection of two strong signals, corresponding to the approximate migrating heights of the monomeric and dimeric SH-tagged A14. Additionally, both bands show a faint signal right above the monomer and dimer, which disappears upon PNGase F treatment. These results are in line with previous reports characterizing VACV A14 and A40 proteins (Mercer and Traktman, 2003; Pérez et al., 2020; Wilcock et al., 1999). As reported, we identified and confirmed the glycosylation site of A40 on N136 and A14 on N83 using the mass spectrometry-based autoCSC approach.

To verify the localization of A14 and A40 at the cell surface during VACV infection, we induced the expression of either A14 or A40 in HeLa CCL2 cells and subsequently performed flow cytometry analysis under non-permeabilized conditions (Fig. 4a). For both proteins, we could confirm the cell surface localization upon induction. Furthermore, immunofluorescence analysis of untreated or doxycycline-induced A14 or A40 expressing HeLa CCL2 cells revealed the colocalization of cell surface glycosylation by generic staining with the glycan binding lectin wheat germ agglutinin (WGA) with our proteins of interest targeted by their SH-tag, indicating that both A40 and A14 reside in the plasma membrane facing the extracellular space (Fig. 4b). The composition of the surfaceome is tightly regulated and can be selectively modulated by expression of single proteins (Chen et al., 2021). Thus, we investigated potential protein changes by selectively expressing either A14 or A40 in HeLa CCL2 cells. Quantification of the proteome and surfaceome data sets revealed almost no changes in protein abundance. For A14 expressing HeLa CCL2 cells no proteins, except the viral protein itself changed significantly in abundance. Similar results were obtained for A40 expressing HeLa CCL2 cells. Only the surface abundance of LAMC1, a protein belonging to the extracellular matrix, was seen to increase in abundance. Nevertheless, these results reveal that the overexpression of neither A14 nor A40 lead to large changes in the proteotype and supports that the phenotype does not change upon expression.

3.3.6 The C-type lectin-like A40 is embedded in a network of integrins and basement membrane proteins

In vitro infection characteristics of the Δ A40-VACV WR deletion strain did not differ from the full WR strain. Neither the reduction in replication efficacy nor plaque morphology changes have been observed *in vitro*. However, inoculation of mice with Δ A40-VACV WR in an intradermal infection model exhibited an increase in lesion size (Wilcock et al., 1999). Together, with the cell surface localization early during the infection, this pinpoints that A40 is a virulence factor involved in the immune modulation of the infection. Interestingly, A40 exhibits a C-type lectin-like domain, similarly to NK and T cell ligands and receptors. A sequence similarity comparison with human proteins revealed a 60 % similarity with NK cell receptor NKG2A. NK receptor signaling is dependent on coreceptor CD96. Moreover, immune cell regulation is dependent on the formation of immunological synapses. These are composed of a complex nanoscale architecture of receptors. In order to retrieve potential details of a molecular mode of action, we characterized the interaction space of A40 at the cell surface. For this purpose, we mapped the protein proximity of the viral protein in its cell surface localization using SPPLAT and LUX-MS, both proximity labeling technologies with mass spectrometry-based readout. Since the underlying labeling chemistry is different for both approaches, confidence can be gained and methodology bias circumvented by combining the results. Moreover, in order to exclude nonspecific bystanders at the cell surface, we mapped the protein proximity of A40 in contrast to the control cells expressing A14. Enriched candidate proteins, derived from the proximity labeling experiments are summarized in the volcano plot (Fig. 5b). Next to the enrichment of our viral proteins, we enriched around 40 protein candidates in the vicinity of A40. The majority of these proteins are cell surface and extracellular matrix proteins. Interestingly, 17 proteins form a highly interconnected network based on deposited literature data (STRING) (Fig. 5d). The network consists of four integrins at the cell surface and the hepatocyte growth factor receptor (MET), which interact with a collagen and laminin cluster as well as a cluster of heparan sulfate proteins of the basement membrane. For A14 we did not observe enriched candidates being annotated to localize to the extracellular space. Thus, it is conceivable that A14 may act alone and glyco-shields the infected immune cell.

Due to the similarity of A40 to NK and T cell C-type lectin-like receptors and ligands, we elucidated the effect of cell surface residing A40 on NK cells. NK cell activation is

described by IFN- γ secretion, and granulation (Paul and Lal, 2017). Hence, we co-cultured human NK-92 with HeLa CCL2 cells expressing A40 and uninduced control cells. To exclude a bias caused by the expression of a cell surface protein itself, we controlled the experiment with A14-expressing HeLa CCL2 cells. After 12 h co-culture, we analysed the secreted IFN- γ concentration. While we observed an increase in IFN- γ secretion for both cells expressing A14 and A40 compared to the uninduced control, the difference was only significant for the co-culture with HeLa CCL2 cells expressing A40 (Fig. 5e).

Furthermore, we studied the NK cell cytotoxicity towards viral protein expressing HeLa CCL2 cells by flow cytometry upon co-culture for 12 hours. To increase our assay resolution, different effector to target cell concentrations have been studied. For doxycycline-induced A14 expressing HeLa CCL2 cells, no difference in the NK killing assay compared to non-induced HeLa CCL2 cells was observed (Fig. 5d). In contrast, doxycycline-induced A40 expression on HeLa CCL2 cells enhanced the cytotoxicity of NK cells compared to the non-induced control for the 1:5 as well as 1:10 HeLa CCL2:NK92 condition. Surprisingly, and in contrast to our hypothesis, we observed the activation of NK cells by expression of A40 on the cell surface of HeLa CCL2 cells, instead of their inhibition.

3.4 Discussion

Our study provides valuable insights into the spatio-temporally resolved proteotype upon VACV infection. Next to the total proteome, we investigated systematically how the surfaceome is perturbed by the viral infection. Applying a surfaceome-specific approach does not only increase the cell surface protein coverage in the analysis, but more importantly reveals spatial information about the true abundance of proteins at the cell membrane. A prediction of cell surface abundance from transcriptomics or total proteome data is imprecise since the total, and cell surface pool cannot be differentiated. This advantage is in particular depicted in our data while studying the upregulation of endosomal and Golgi-derived membrane proteins at the cell surface, such as VPP2. Its abundance in the total proteome data stays constant, but its cell surface abundance increases after 6 hpi. Interestingly, this correlates well with the exocytosis of infectious extracellular virions (EVs), which starts at 6 hpi and is responsible for the fast spread of VACV. Upon assembly of infectious mature virions (MVs), a fraction is wrapped with two additional membranes, which originate from early endosomes, Golgi or multivesicular bodies, resulting in egress-ready wrapped vaccinia virus (WV) (Huttunen et al., 2021). These triple-membrane virions then fuse with the plasma membrane and leave behind the outermost membrane with inverted orientation to release the infectious EVs into the extracellular space. Hence, the accumulation of the intracellular derived membranes at the cell surface may lead to the abundance increase of these proteins. Many of these proteins are involved in pH and ion homeostasis. Thus, accumulation may lead to perturbed cellular hemostasis, which could affect the viral infection.

Similarly, we observed a significant 2-fold decrease of EGFR from the cell surface, but only a slight non-significant change in the total proteome, pinpointing to the internalization of EGFR. Indeed, the VACV encoded growth factor VGF, an EGFR ligand, is early expressed during infection, as our and other data suggest. It was reported that VGF binding leads to the internalization of EGFR (Morgis et al., 2021). VACV hijacks paracrine VGF/EGFR signaling to direct the cellular motility of infected cells (Beerli et al., 2019). Furthermore, VGF-mediated EGFR stimulation leads to the full activation of the MEK/ERK pathway. VACV activates the MEK/ERK pathway to control favourable conditions for its replication (Andrade et al., 2004). In line, we detect the known downstream regulated expression of EGR-1 and AP-1 transcription factors. Interestingly, we can also report enhanced COX-2 expression, which is known to be regulated by the AP-

1 component Jun. COX-2 is involved in the catalysis of prostaglandin E2 (PGE2). Both have been described as negative as well as positive innate immunity modulators, whose function is cell-type and virus family specific (Sander et al., 2017). Further, we also observed the increased abundance of the growth factor amphiregulin (AREG) at the cell surface, which can induce AP-1 expression itself through EGFR binding (Fang et al., 2013). Interestingly, the loop of amphiregulin stimulating COX-2 expression during MCMV infection was reported (Melnick et al., 2011). However, for MCMV infection NF- κ B signaling is critical, which in contrast is strongly inhibited by VACV (Ember et al., 2012). COX-2 expression and its catalyzed product PGE2 were increased upon MVA infection, but its expression was found to be NF- κ B independent (Pollara et al., 2012). Therefore, a cell surface receptor stimulated signal transduction pathway through AREG/EGFR/??/COX-2 axis might be induced during VACV infection and the missing connecting link needs to be further investigated.

VACV evolved many intracellular mechanisms to evade the host immune response. Thus, we wondered if evasion pathways are transferred to the regulation of cell surface proteins. Indeed, downregulation of proteins known to be NK cells ligands such as NECT1, ICAM and T cell ligands e.g. CD83 was observed using the surfaceome approach. Modulating the abundance of these proteins helps VACV to evade the innate and adaptive immune system and to establish the productive infection. Besides the regulation of host proteins, the repopulation of the cell membrane with viral proteins is striking. To be picked up by our autoCSC strategy, the enriched proteins need to be N-glycosylated. Glycosylation is a co- and post-translational modification that occurs in the ER and Golgi. Proteins traversing these organelles within the secretory pathway are mostly determined to localise to the extracellular space. VACV hijacks the host glycosylation machinery for its protein modification (Hassan et al., 2021). Conversely, non-glycosylated proteins such as WR encoded and secreted VCP, which is known to bind to A56 extracellularly like SPI-3, is undetectable in our approach (Dehaven et al., 2011; Meseda et al., 2014). We identified approximately 5 % of the viral proteome localizing to the plasma membrane. This is a rather small fraction of VACV proteins in relation to VACV proteins with transmembrane domain. Thus, this finding pinpoints to a selective translocation of these viral proteins to the cell membrane. Therefore, we conclude that VACV hijacks the cell membrane as a scaffold for viral proteins. Their localization at the cell surface supports the hypothesis that these viral proteins function in viral spread and immune modulation. Interestingly, viral proteins can have a multitude of functions at the cell surface. For example, A56 interacts

with SPI3 to prevent superinfection, simultaneously it is involved in immune signaling with NK cells (Jarahian et al., 2011; Turner and Moyer, 2008). Although, VACV is the best-studied poxvirus, the cell surface localization-induced phenotype and molecular mode of action are largely unknown for some of the viral proteins.

In particular interesting is the viral protein A40, since it harbours an immunomodulatory phenotype in the intradermal murine infection model and deletion from VACV strain MVA increased the immunogenicity for a MVA-B-based HIV vaccine candidate (Pérez et al., 2020; Tschärke et al., 2002). But, the underlying molecular mode of action for the immune modulation by A40 remains elusive. Based on the observed phenotype, its localization and C-type lectin structure, similar to T and NK cells ligands and receptors, we and others hypothesized that A40 might be involved in immune cell interactions. Signaling between infected and immune cells is orchestrated by secreted ligands and cell surface residing receptor-receptor interactions, leading to inhibitory or activating intracellular signaling cascades. Many of these interactions are supported by co-receptors, interacting lateral on the cell surface of the same cell. Therefore, we investigated the lateral interaction network of A40 on the infected cell using proximity labeling technologies SPPLAT and LUX-MS. Interestingly, we observed in the vicinity of A40 the functional cluster of integrins and extracellular matrix proteins of the basement membrane. Putative interaction with these candidate proteins could be mediated through A40-protein binding, or mediated through the carbohydrate-receptor domain (CRD) and be based on A40-glycan binding. Although A40's CRD domain is only partially conserved, glycan binding cannot be excluded (Wilcock et al., 1999). Interestingly the ECM is largely involved in the modulation of the immune response. Remodeled ECM structure could cause altered immune cell migration. The high similarity of A40 with NK cell ligands and receptors led us to further investigate A40's signaling potential towards NK cells. Due to the smaller lesion size upon infection with Δ A40-VACV in the intradermal murine model, we hypothesized an inhibitory effect of the innate immune cells. In contrast to our hypothesis, we found a slight upregulation of about 15 % in NK cytotoxicity upon expression of A40 in HeLa CCL2 cells compared to the non-induced control. An effect induced by the expression itself was controlled with A14 expression, which did not alter the NK cytotoxicity. Although the effect size is rather small, we assume A40 functions in NK cell modulation. This might be caused by interactions of A40 to stimulating receptors on NK cells.

The previous impairing immune modulatory effect of A40 was studied in a murine intradermal model. Contrary, we established an *in vitro* assay using human NK cells.

Whereas the adaptive immune B and T cell biology is well conserved between humans and mice, recent findings have shown differential mechanisms of NK cell biology for these two species (Colucci et al., 2002). Furthermore, how the result translates to a more complex *in vivo* model system with full infection is unknown, but might be critical, as NK cell cytotoxicity is the sum of balanced inhibitory and activating signals. Interestingly, VACV encoded protein A56 binds to NK receptor NKp46, stimulating NK cytotoxicity, but also interacting with NKp30, blocking NK cell activity. But, studies with Δ A56-VACV infection resulted eventually in an overall inhibitory effect of A56 towards NK cytotoxicity (Jarahian et al., 2011). Taking this finding into consideration, the VACV infection in absence, or with overexpression of A40 would give access to a more comprehensive picture.

In summary, we provide a valuable resource about the perturbation of the surfaceome upon VACV infection with high temporal resolution. Our data present on the one hand, how VACV hijacks the cell membrane as a scaffold for localising viral proteins towards the extracellular space for intercellular communication. On the other hand, we report VACV counteracting the immune response by decreasing the cell surface abundance of immune signaling competent proteins. Future work will enclose the investigation of the underlying mechanisms leading to the downregulation of immunomodulatory proteins from the cell surface. Furthermore, our proximity-labeling data indicate the importance of extracellular interactions, which should be taken into consideration for antiviral therapy.

3.5 Methods

Material

All chemicals were purchased from Sigma Aldrich, if not otherwise stated. Purified vaccinia virus Western Reserve (WR) was kindly provided by Prof. Jason Mercer. Antibodies were used in the following concentrations:

Table 1 Antibodies

Antibody	Concentration	Vendor
anti-HA Tag (2-2.2.14) for WB	1:3000	Invitrogen #26183
anti-HA TAG-AF647	1:500	Invitrogen #26183-A647
anti-WGA-AF488	5 µg / ml	Invitrogen #W11261
anti-Phalloidin-AF647	1:400	Invitrogen #A22287
Peroxidase AffiniPure Goat Anti-Mouse IgG (H+L)	1:10000	Jackson ImmunoResearch
StrepTactin-HRP	10 µg / sample	IBA LifeSciences

Cell culture

HeLa CCL2 cells were grown in full growth media, consisting of Dulbecco's Modified Eagle Medium (DMEM, Gibco) supplemented with 10 % Foetal Calf Serum (FCS) and 1x Penicillin-Streptomycin (PenStrep) (Invitrogen) at 37 °C in 5 % CO₂ atmosphere. NK-92 cells were grown in Modified Eagle Medium(MEM) without nucleosides, 12.5 % FCS, 12.5 % horse serum, 0.2 mM inositol, 0.02 mM folic acid, 0.1 mM b-mercaptoethanol, 1 x PenStrep and 10 mM IL-2 at 37 °C in 5 % CO₂ atmosphere.

Viral infection

Hela CCL2 cells were grown in full growth media, consisting of Dulbecco's Modified Eagle Medium (DMEM, Gibco) supplemented with 10 % Foetal Calf Serum (FCS) and 1x Penicillin-Streptomycin (PenStrep) (Invitrogen) at 37 °C in 5 % CO₂ atmosphere. Hela CCL2 cells were grown to 80 % confluency and full growth media was changed to DMEM without FCS, and PenStrep, containing Vaccinia Virus (VACV) Western Reserve (WR). Cells were infected with VACV WR at a multiplicity of infection (MOI) of 10. The mock-infected control was not infected, but equally treated with unsupplemented DMEM. After one hour, the infection media was changed back to full growth media.

Immunofluorescence imaging

For immunofluorescence imaging, HeLa CCL2 cells were grown in full growth media on coverslips. For the VACV infection time course, cells were infected or mock-treated at 50 % confluency following the above described infection protocol. Sampling was conducted at 1, 2, 4, 6, 8 and 24 hours post infection (hpi) by fixation. For co-localisation experiments, HeLa CCL2 cells were fixated 24 h after starting the protein expression with 1 µg/ml doxycycline at 50 % confluency. Samples were fixated in 4 % formaldehyde for 30 min at room temperature (RT) and afterwards permeabilized in 0.1 % Triton-X100 for 5 min in PBS at RT. Samples were washed thrice for 5 min with 3 % BSA in PBS. Afterwards, samples were incubated with primary antibodies for 1 h in the dark at RT and subsequently washed thrice for 5 min with 3 % BSA in PBS. Then, samples were incubated with secondary antibodies for 1 h at RT and afterwards washed thrice for 5 min with 3 % BSA in PBS. After buffer aspiration and through sample drying, coverslips were mounted onto microscope slides with a DAPI-containing mounting medium. Subsequently, immunofluorescence analysis was performed using a confocal microscopy setup and raw images adjusted for brightness and contrast using FIJI. For all images within one experiment the same acquisition and image processing settings were applied.

Glycosylation analysis

Deglycosylation was conducted as suggested by New England Biolab PNGase F protocol. Expression of viral proteins was induced by 1 µg/ml doxycycline in HeLa CCL2 cells. 24 h after protein expression, HeLa CCL2 cells were harvested by scraping. Control samples were mock-treated without doxycycline. HeLa CCL2 cells were lysed in the Glycoprotein denaturing buffer and heated up to 95 °C for 10 min. Full lysis was supported by 2 x 30 s (A: 80 %, C: 80%) sonication using a VialTweeter (Hielscher Ultrasonics). Cooled cell lysate was supplemented with Glycobuffer 2 and 1 % NP-40 final concentration. 3 µl PNGase F was added to 20 µg of lysate and incubated overnight for 16 h at 37 °C. Deglycosylation was verified by SDS-PAGE followed by immunoblotting.

Immunoblot analysis

For immunoblot analysis of glycosylation analysis, cells were harvested by scraping after 24 h of doxycycline-induced protein expression. Cells were lysed in RIPA lysis buffer containing 150 mM NaCl, 1 % Triton X-100, 0.5 % sodium deoxycholate, 0.1 % SDS, in 50 mM TRIS, pH 8.0 at 95 °C for 5 min. Full lysis was supported by 2 x 30 s (A: 80 %, C:

80%) sonication using a VialTweeter (Hielscher Ultrasonics). Protein concentration was determined using bicinchoninic acid assay (Micro BCA™ Protein Assay Kit, Thermo Scientific), following the manufacturer's guidelines. Protein concentration was normalized accordingly and cell lysate was mixed with 4 x NuPAGE LDS Sample Buffer (Invitrogen) (no DTT), boiled at 95°C for 5 min. Proteins were separated on a NuPAGE 4-12 % Bis-Tris SDS-PAGE-gel (Invitrogen) by electrophoresis. Afterwards, proteins were transferred onto a nitrocellulose membrane (Trans-Blot Turbo, Bio-Rad). A40 and A14 expression was verified by anti-HA-tag antibody (Invitrogen, 1:3000)/horseradish-peroxidase (HRP)-coupled goat anti-mouse IgG antibody induced chemiluminescence with a Fusion FX camera setup (Vilbert).

Surfaceome analysis

Cell surface capturing (CSC) was conducted on living HeLa CCL2 cells, constantly incubated at 4 °C during the experiment. First, cell surface glycans were mildly oxidized for 20 min with Oxidation buffer (OB) containing 2.34 mM NaIO₄ in PBS, pH 6.5. HeLa CCL2 cells were washed twice with PBS, pH 7.4 and subsequently cell surface glycoproteins were biotinylated for 1 h in labeling buffer, containing 5 mM biocytin-hydrazide (Pitsch Nucleic Acids AG, Switzerland) and 5 mM 2-Amino-5-methoxybenzoic acid (5-MA) in PBS, pH 7.4. Afterwards, cells were washed thrice with PBS pH 7.4, harvested by scraping, snap-frozen in liquid N₂ and stored at -80 °C.

Samples were lysed in 100 mM tris(hydroxymethyl)aminomethane (TRIS), 1% sodium deoxycholate (SDC), 10 mM tris(2-carboxyethyl)phosphine (TCEP), 15 mM 2-chloroacetamide, pH 8.0 at 95 °C for 10 min. Complete lysis was supported by 2 x 30 s sonication (Amplitude: 80 %, Cycle time: 80%) using a VialTweeter (Hielscher Ultrasonics). Proteins were digested using bovine trypsin (Sigma Aldrich) in a trypsin-protein ratio of 1:50 in complete lysis buffer at 37 °C for 16 h overnight. Afterwards, trypsin was inactivated by incubation at 95 °C for 5 min, and SDC was precipitated by acidification to pH 2-3 with 10 % formic acid (FA) followed by 10 min centrifugation. The peptide concentration was determined by A280 (Nanodrop, Thermo Fisher Scientific) and within each experiment normalized using 50 mM Ambic. For the affinity purification of the biotinylated cell surface glycopeptide species, an automated 96-well format pipetting robot (Versette, Thermo Fisher Scientific) was deployed and for each experiment equal amounts of peptide starting material were loaded. Enrichment, washing and elution process was conducted as described in (van Oostrum et al., 2019). Briefly, biotinylated glycopeptides

were enriched with Pierce™ Streptavidin Plus UltraLink™ Resin (Thermo Scientific) for 2.5 h and subsequently washed with 5 M NaCl, StimLys Buffer (100 mM NaCl, 100 mM glycerol, 50 mM Tris, 1% Triton X-100, pH 8.0), 50 mM ammonium bicarbonate, 100 mM NaHCO₃, pH 11 and with 50 mM ammonium bicarbonate equilibrated again. For the elution peptides were incubated overnight at 37 °C in 50 mM ammonium bicarbonate containing 1000 units PNGase F (New England Biolabs). Eluted peptides were cleaned with C18 UltraMicroSpin columns (The Nest Group) and dried to completeness in a SpeedVac concentrator (Thermo Scientific).

Total proteome analysis

For the total proteome analysis, an aliquot of approximately 50 µg peptide solution was taken from the tryptic digested sample after the above described normalization step. Peptides were cleaned with C18 UltraMicroSpin columns (The Nest Group) and dried to completeness in a SpeedVac concentrator (Thermo Scientific).

Library generation

For mass spectrometry-based surfaceome analysis in data-independent acquisition, an aliquot of each CSC sample was pooled condition-wise and each pooled condition sample was analysed beforehand in data-dependent acquisition mode with the below reported method details.

For mass spectrometry-based total proteome analysis a spectral library was generated based on a fractionated pooled sample. Wherefore, an aliquot of each sample was taken and the pooled sample fractionated by high pH reversed phase chromatography. Briefly, 100 µg pooled peptides were resuspended in buffer A (20 mM ammonium formate/ 2 % ACN/ H₂O) and loaded onto a 250 mm x 0.5 mm inner diameter C18 column (YMC Europe, 3 µm) with buffer A. Peptides were eluted with a buffer B (20 mM ammonium formate/ 80 % ACN/H₂O) with an increasing gradient ranging from 5 - 50 % buffer B in 70 min. Eluted peptides were row-wise collected in 36 fractions over 60 min. Subsequently, the 36 fractions were column-wise pooled in twelve fractions overall. These were dried to completeness using a SpeedVac concentrator. The twelve fractions were analysed in data-dependent acquisition mode with the below reported method details.

Stable cell line generation

Open reading frames for A40_VACCW and A14_VACCW proteins were optimized for human codon usage and synthesized by GeneArt Gene synthesis (Thermo Fisher Scientific). Present in the gateway compatible donor vector pDONR223, ORFs were transferred through LR recombination (Gateway LR Clonase II Enzyme mix, Invitrogen) in the destination vector pcDNA5/FRT/TO/SH/GW (Glatter et al., 2009). The final transfection vector contained the Flp Recombination Target (FRT) site, the hygromycin resistance as well as the doxycycline-inducible N-terminal HA-twin-Strep-(SH)-tagged bait protein ORF.

The respective ORF-containing vector was co-transfected with pOG44 Flp recombinase expression vector in T-REx-HeLa CCL2 Flp-In cells using jetPRIME transfection reagent (Polyplus-transfection) following the manufacturer's guidelines. After 24 h after transfection 50 % of full growth media was exchanged to selection medium. After 48 h full selection medium was applied, composed of 360 µg/ml Hygromycin B (Gibco) and 13 µg/ml Blasticidin S HCl (Invitrogen) in full growth medium. Stably integrated ORFs were selected for 2-3 weeks until colony formation.

Flow cytometry

For flow cytometry analysis, HeLa CCL2 cells were harvested with 5 mM EDTA in PBS for 5 min and subsequently washed twice with FACS buffer, containing 1 % FCS, 1 mM MgCl₂ and 1 mM CaCl₂ in PBS, pH 7.4. HeLa CCL2 cells were stained with the respective primary antibody in FACS buffer for 20 min shaking at 300 rpm. Afterwards, cells were washed twice with FACS buffer and stained with the secondary antibody for 20 min in the dark. Subsequently, cells were washed twice with FACS buffer before subjection to flow cytometry analysis using a BioLegend Accuri C6. Measured cell events were gated for singlets and dead-live staining using propidium iodide. Finally, flow cytometry data were analysed using FlowJo 10.0.

Antibody-SOG conjugation for LUX-MS

First, antibodies were cleaned using Zeba Spin columns (MWCO 40 kDa, Thermo Fisher Scientific) following the manufacturer's guidelines. For buffer exchange, the antibodies were eluted in a 50 mM carbonate buffer, pH 8.0. Cleaned antibodies were conjugated to singlet oxygen generators (SOGs) via NHS-based chemistry in an AB:SOG ratio of 1:3. Per sample 10 µg HA antibody was incubated with NHS-SOG for 1 h in carbonate buffer

at 25 °C in the dark. Subsequently, AB-SOG conjugates were cleaned using Zeba Spin columns and buffer exchanged to PBS, pH 7.4. Conjugates were stored for subsequent immediate usage at 4 °C in the dark.

Proximity biotinylation with LUX-MS

Expression of the viral protein of interest in HeLa CCL2 cells was induced at 70 % confluency with 1 µg/ml doxycycline in full growth medium. After 24 h, cells were washed with PBS and 10 µg AB-SOG conjugate in 5 ml PBS per 10 cm dish added and incubated for 30 min in the dark at 4 °C. All subsequent steps were always carried out with ice-cooled buffers and at 4 °C. Afterwards, cells were washed with PBS and 5 ml illumination buffer, composed of 5 mM biocytin-hydrazide (Pitch Nucleic Acid), phosphate-buffered in D2O, added. To generate singlet oxygen, cells were illuminated for 15 min with light of 590 nm wavelength. Afterwards, cells were washed with PBS and 10 ml 5 mM biocytin-hydrazide, 50 mM AMI in PBS was added. The biotinylation reaction was incubated for 1 h at 4 °C in the dark. Afterwards, cells were washed twice with ice-cold PBS and harvested by scraping.

Proximity biotinylation with SPPLAT

Expression of the viral protein of interest in HeLa CCL2 cells was induced at 70 % confluency with 1 µg/ml doxycycline in full growth medium for 24 h. Cells were washed twice with ice-cold PBS and incubated with 10 µg Streptactin-HRP in 5 ml PBS per 10 cm dish for 30 min at 4 °C. Afterwards, cells were washed twice with ice-cold PBS and 0.1 mM cell impermeable biotin-tyramide in 5 ml PBS added. The biotinylation reaction was started by gentle addition of final 10 mM H₂O₂ (prediluted in PBS). After 1 min incubation, the reaction was stopped by addition of 2x quenching buffer, composed of 10 mM sodium azide, 10 mM sodium ascorbate and 10,000 units catalase in PBS. Cells were additionally washed twice with quenching buffer and twice with PBS. Afterwards, cells were harvested by scraping and snap-frozen in liquid N₂.

Sample processing of Lux-MS and SPPLAT samples

HeLa CCL2 cells were lysed in 100 mM tris(hydroxymethyl)aminomethane (TRIS), 1% sodium deoxycholate (SDC), 10 mM tris(2-carboxyethyl)phosphine (TCEP), 15 mM 2-chloroacetamide, pH 8.0 at 95 °C for 10 min. Complete lysis was supported by 2 x 30 s sonication (Amplitude: 80 %, Cycle time: 80%) using a VialTweeter (Hielscher Ultrasonics). Subsequently, protein concentration was normalised across the samples and

5 mg per sample of biotinylated proteins were enriched using an automated pipetting robot Versette (ThermoFisherScientific). In brief, biotinylated proteins were enriched with self-filled Streptavidin resin tips (Pierce™ Streptavidin Plus UltraLink™ Resin (Thermo Scientific)) by continuous aspirating and dispensing for 2.5 h. Subsequently, the resin was washed with 5 M NaCl, StimLys Buffer (100 mM NaCl, 100 mM glycerol, 50 mM Tris, 1% Triton X-100, pH 8.0), 50 mM ammonium bicarbonate, 100 mM NaHCO₃, pH 11 and 3 M Urea buffer. Then, proteins were first digested with 1 µg Lyc-C (Fujifilm) for 1.5 h in 3 M urea and secondly with 2.5 µg trypsin (Promega Gold) for 16 h in 1.5 M urea. Afterwards, the tips were fully dispensed and washed once with 50 mM Ambic. Both eluates were jointly collected and desalted by C18 clean-up using C18 UltraMicroSpin columns (The Nest Group) following the manufacturer's guidelines. Peptides were dried to completeness in a SpeedVac concentrator (Thermo Scientific) and frozen at -80 °C until LC-MS/MS analysis.

Liquid chromatography-tandem mass spectrometry analysis of CSC samples

For CSC analysis, peptides were reconstituted in 3 % ACN/0.1 % FA/H₂O and the entire sample was subjected to liquid chromatography-tandem mass spectrometry. The infection time course was analysed using a nLC1000 (Thermo Scientific) coupled to an Orbitrap Fusion Tribrid mass spectrometer (Thermo Scientific). Peptides were loaded onto a 15 cm in-house packed column (New Objective) with mobile phase buffer A containing 0.1 % FA/H₂O and separated by reverse-phase chromatography with ReproSil-Pur 120 A C18-AQ 1.9 µm stationary phase (Dr. Maisch GmbH). Peptides were eluted with mobile phase buffer B, composed of 99 % ACN/0.1 % FA/H₂O starting from 5 % B and increasing up to 50 % B in 68 min. The pooled condition CSC samples for library generation were analysed in data-dependent acquisition mode. Therefore, MS₁ spectra were recorded at an AGC of 1e6 or after 50 ms from 350-1650 m/z with a resolution of 120,000 m/z at 200 m/z. For 3 s peptide precursor ions with charge state 2-7 were iteratively isolated with a 2 m/z isolation window and fragmented by high-energy collisional dissociation (HCD) with a normalized collision energy of $n_{ce} = 27$. Recording of MS₂ spectra was triggered at an AGC of 5e4 or after 54 ms with a first mass of 120. Fragmented peptides ions were dynamically excluded for further analysis for 15 s.

The individual CSC samples were analysed in data-independent acquisition mode. Therefore, MS₁ spectra recordings were triggered at an AGC of 1e6 or after 50 ms from 350-1650 m/z with a resolution of 120,000 m/z at 200 m/z. Subsequently, peptide ions

within 14 windows with dynamic width, summarized in table 2, were iteratively isolated and fragmented by HCD with an energy of $nce = 27$. MS2 scan recordings were triggered at an AGC of $1e6$ or after 118 ms from 200-2000 m/z with a resolution of 30000 m/z at 200 m/z.

Table 2 Isolation window properties for DIA-based CSC analysis

Center (m/z)	Isolation window width (m/z)
377.5	55
423.5	39
459.5	35
493	34
526.5	35
560.5	35
595.5	37
633	40
673	42
718	50
772	60
839	76
933	114
1319.5	661

CSC samples in localization experiments were analysed using a nLC1000 (Thermo Scientific) coupled to an Orbitrap QExactive Plus (Thermo Scientific). Peptides were loaded onto a 15 cm in-house packed column (New Objective) with mobile phase buffer A containing 0.1 % FA/H₂O and separated by reverse-phase chromatography with ReproSil-Pur 120 A C18-AQ 1.9 μ m stationary phase (Dr. Maisch GmbH). Peptides were eluted with mobile phase buffer B, composed of 99 % ACN/0.1 % FA/H₂O starting from 5 % B and increasing up to 50 % B in 80 min. MS1 spectra were recorded at an AGC of $3e6$ or after 64 ms from 350-1650 m/z with a resolution of 70,000 m/z at 200 m/z. Top twelve peptide precursor ions were iteratively isolated with a 1.5 m/z isolation window and fragmented by high-energy collisional dissociation (HCD) with a normalized collision energy of $nce = 27$. Recording of MS2 spectra were triggered at an AGC of $1e3$ or after 110 ms from 200 m/z

- 2000 m/z. Unassigned or single charge state peptide ions were excluded. Fragmented peptide ions were dynamically excluded for further analysis for 30 s.

Liquid chromatography-tandem mass spectrometry of total proteome samples

Peptides were reconstituted in 3 % ACN/0.1 % FA/H₂O. Within the infection time course experiment, for label-free total proteome analysis 1 µg peptides of each sample and for total proteome library generation 2 µg peptides of each fraction were subjected to liquid chromatography-tandem mass spectrometry analysis using a nLC1000 (Thermo Scientific) coupled to an Orbitrap Fusion Tribrid mass spectrometer (Thermo Scientific). Peptides were loaded onto a 45 cm in-house packed column with mobile phase buffer A containing 0.1 % FA/H₂O and separated by reverse-phase chromatography with ReproSil-Pur 120 A C18-AQ 1.9 µm stationary phase (Dr. Maisch GmbH). Peptides were eluted with mobile phase buffer B, consisting of 80 % ACN/0.1 % FA/H₂O, starting from 7 % B up to 62 % B in 235 min.

The fractionated total proteome samples for library generation were analysed in data-dependent acquisition mode. MS1 spectra were recorded at an AGC of 1e6 or after 50 ms from 350-1650 m/z with a resolution of 120,000 m/z at 200 m/z. For 3 s peptide precursor ions with charge state 2-6 were iteratively isolated with a 1.6 m/z isolation window and fragmented by high-energy collisional dissociation (HCD) with a normalized collision energy of $nce = 27$. Recording of MS2 spectra was triggered at an AGC of 5e4 or after 22 ms with a first mass of 120. Fragmented peptides ions were dynamically excluded for further analysis for 15 s.

The total proteome samples for label-free quantification were analysed in data-independent acquisition mode. Therefore, MS1 spectra recordings were triggered at an AGC of 3e6 or after 50 ms from 350-1650 m/z with a resolution of 120,000 m/z at 200 m/z. Subsequently, peptide ions within 24 windows with dynamic width, summarized in table 3, were iteratively isolated and fragmented by HCD with an energy of $nce = 27$. MS2 scan recordings were triggered at an AGC of 1e6 or after 54 ms from 200-2000 m/z with a resolution of 30000 m/z at 200 m/z.

Table 3: Isolation window properties for DIA-based total proteome analysis

Center (m/z)	Isolation window width (m/z)
367.5	35
398	28
422.5	23
444	22
464	20
483.5	21
503	20
522.5	21
542.5	21
562	20
582	22
603	22
624.5	23
647	24
670.5	25
695.5	27
723	30
754	34
789	38
827.5	41
873	52
932	68
1016.5	103
1358.5	583

Liquid chromatography-tandem mass spectrometry of total proteome samples

Lux-MS samples were reconstituted in 3 % ACN/0.1 % FA/H₂O and 0.6 µg per sample subjected to LC-MS/MS analysis using a nLC1200 (Thermo Scientific) coupled to an Orbitrap QExactive HF (Thermo Scientific). Peptides were loaded onto a 30 cm in-house packed column with mobile phase buffer A containing 0.1 % FA/H₂O and separated by reverse-phase chromatography with ReproSil-Pur 120 A C18-AQ 1.9 µm stationary phase (Dr. Maisch GmbH). Peptides were eluted with mobile phase buffer B, consisting of 80 % ACN/0.1 % FA/H₂O, starting from 7 % B up to 62 % B in 110 min. The Lux-MS samples were analysed in data-dependent mode. Eluted peptides were recorded in MS1 from 350 m/z to 1650 m/z with an AGC target of 1e6 and 50 ms injection time. Top 12 intense peptides were iteratively isolated with an isolation window of 1.3 m/z and fragmented with HCD at a normalized energy of $n_{ce} = 27$. MS2 spectra were recorded at an AGC of 5e4 or after 22 ms injection time. Only peptides with M/Z 2-6 were isolated and once fragmented peptides were excluded from further analysis for 30 s.

Bioinformatic analysis

Library generation

The library was built within Spectronaut (Biognosys, v.15). Spectra from DDA-acquired raw files were searched with Pulsar against UniprotKB/SwissProt Homo sapiens, VACV WR and common contaminations (retrieved 04/2018) for identification. Default parameters were applied with carbamidomethylation at cysteine as fixed modification, as well as oxidation at methionine as variable modification with maximum of two miss cleavages. The CSC samples were additionally searched with deamidation at asparagine as variable modification. The library was controlled for maximum 1 % false discovery identification by Pulsar.

Total and Surfaceome analysis

Identification and quantification of the total and surfaceome experiments was performed with Spectronaut (Biognosys, v15.) DIA-acquired .raw files were searched with the experiment-specific library using default parameters. Identified peptides were only considered for quantification if proteotypic. Normalization was performed by Spectronauts' built-in local normalization algorithm on host species' peptides only. For quantitative analysis QValue percentile 20 % mode with sample specific run-wise imputation was applied. For the vaccinia virus temporal class analysis, the QValue mode without imputation was used. Extracted features were exported and peptides derived from common contaminants removed. For the surfaceome analysis, only peptides containing the deamidated asparagine (+ 1 Da) in the consensus NXS/T sequence, where X is every amino acid except Proline, were considered. For total proteome data, minimum two, and for the surfaceome analysis minimum one proteotypic stripped peptide was required. The FDR was controlled within Spectronaut for 1 % on peptide as well as protein level. The statistical analysis for differentially regulated proteins between the infected timepoints and the mock-infected HeLa CCL2 cells was subsequently performed with MSstats. For total and surfaceome analysis, four replicates per condition were quantified. In brief, the fold change and significance testing was estimated with a linear mixed model. Multiple testing was corrected by Benjamini-Hochberg and proteins were considered significantly regulated with a fold change of > 2 or < 0.5 and an adjusted p-value < 0.05 .

Lux-MS/SPPLAT MS analysis

For the Lux-MS and SPPLAT MS analysis, peptides were identified with Proteome Discoverer 2.1 and subsequently quantified in Progenesis v.4.1. In brief, spectra were searched against the UniProtKB/SwissProt Homo sapiens, VACV WR and common contamination databases (retrieved 04/20218). Default parameters were applied with 10 ppm MS1 and 0.02 Da MS2 deviation allowance, carbamidomethylation at cysteine as fixed modification, as well as oxidation at methionine as variable modification with maximum two miss cleavages. FDR was controlled to 1 % on PSM level with Target Decoy PSM Validator. Identifications were subsequently transferred into Progenesis. Here, raw files were aligned on their MS1 traces feature intensity extracted on MS1 level. Common contaminants were removed and only proteins with minimum two proteotypic peptides were considered for quantification. The statistical analysis of differential regulation was performed with MSstats, as described above. Significance was reported for proteins with a fold change of > 2 or < 0.5 and an adjusted p-value of < 0.05 .

NK cytotoxicity assays

Secreted IFN- γ detection by ELISA

Stably transfected HeLa CCL2 cells with either A14 or A40 were seeded in a 24-well plate. Expression of the viral protein of interest was induced at 50 % confluency with 1 $\mu\text{g/ml}$ doxycycline in full growth medium for 24 h. NK-92 cells were centrifuged at 300 g for 5 min and subsequently resuspended in RPMI medium containing 1 % FCS, PenStrep and 100 u/ml IL-2. Afterwards, the full growth medium of HeLa CCL2 cells was removed and NK-92 cells were added in a ratio of 1:5 HeLa CCL2:NK-92 cells. After 12 h of incubation the supernatant of the cells was collected, centrifuged at 300 g for 5 min to remove all NK-92 cells in suspension and subsequently the supernatant was pressed through a filter. The supernatant was analyzed using a Human IFN gamma ELISA Kit (Abcam, ab174443) according to the manufacturer's protocol.

NK-killing assay

HeLa CCL2 cells were used as target cells and NK-92 cells were used as effector cells for the NK killing assay. Expression of the viral protein of interest in HeLa CCL2 cells was induced at 70 % confluency with 1 $\mu\text{g/ml}$ doxycycline in full growth medium for 24 h. HeLa CCL2 cells were harvested with 5 mM EDTA in PBS for 5 min and subsequently washed once with PBS. For each target cell condition, HeLa CCL2 cells expressing A14,

HeLa CCL2 cells expressing A40 and corresponding uninduced HeLa CCL2 cells, 1×10^6 cells were resuspended in 500 μ l 1 μ M CFSE (Biolegend) in PBS and incubated for 10 min at 37 °C in the dark. Staining was quenched by adding 500 μ l FCS. After centrifugation at 300 g for 5 min target cells were resuspended in RPMI medium containing 1 % FCS, PenStrep and 100 u/ml IL-2 to 0.1×10^6 cells per ml. NK-92 cells were centrifuged at 300 g for 5 min and subsequently resuspended in RPMI medium containing 1 % FCS, PenStrep and 100u/ml IL-2 to either 0.5×10^6 cells per ml or 1×10^6 cells per ml according to the effector to target ratio 5:1 and 10:1. The NK killing assay was performed in a 96-well plate (u-bottom) and 3 wells were used per condition. Wells were filled in total with 200 μ l according to the different target to effector ratios 1:0, 1:5, 1:10, 0:5 and 0:10 and incubated for 12 h at 37 °C in 5 % CO₂ atmosphere. After incubation all cells per condition were collected. Attached cells were harvested with 5 mM EDTA in PBS for 5 min and added to the collection tube. After centrifugation at 300 g for 5 min, cells were resuspended in RPMI medium containing 1 % FCS, PenStrep, 100 u/ml IL-2, 1 μ g/mL propidium iodide. Cells were analyzed using FACS Canto II. Finally, flow cytometry data were analysed using FlowJo 10.0.

3.6 Figures and figure legends

Figure 1: Temporal investigation of the proteotype upon VACV infection.

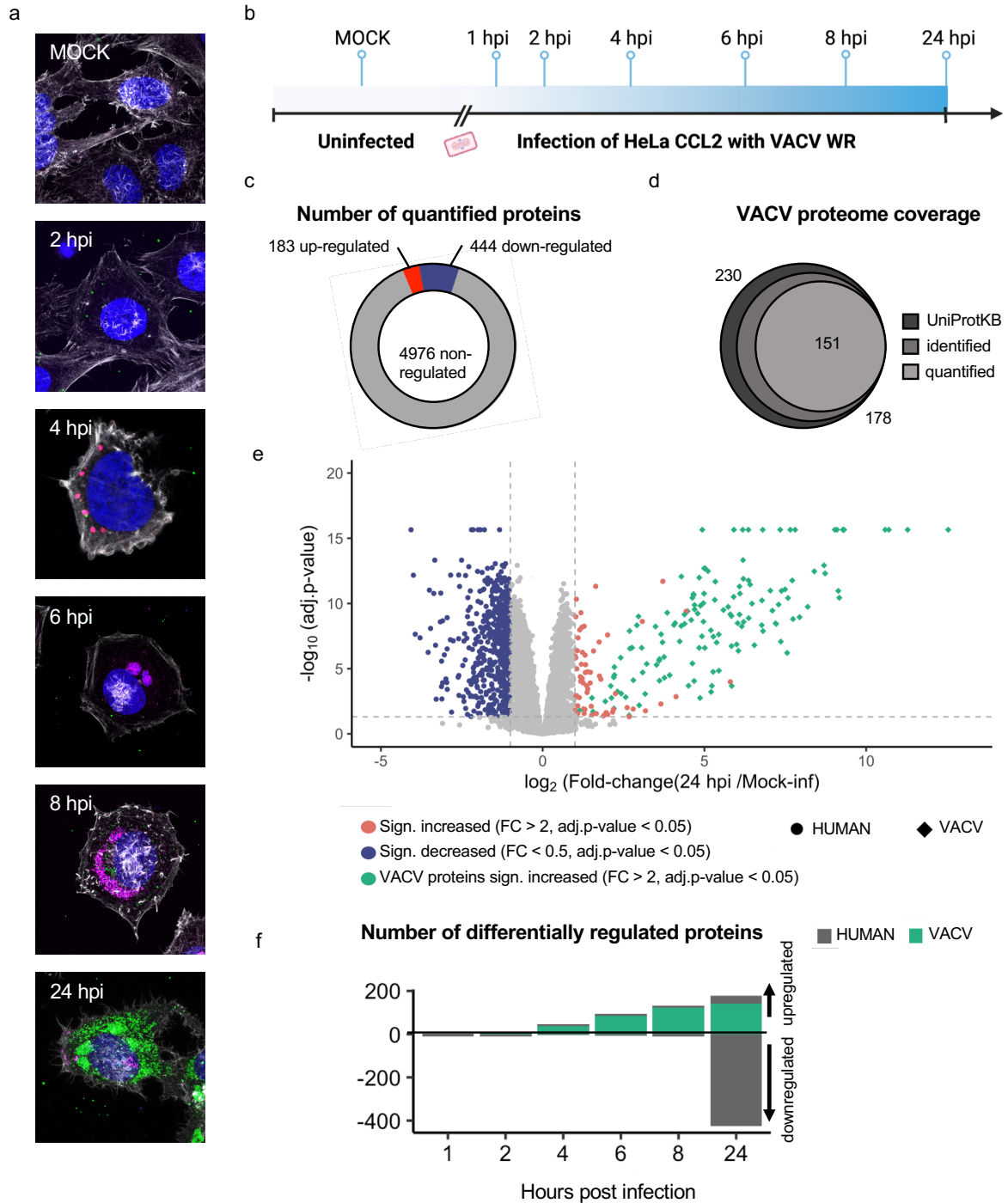


Figure 1: Temporal investigation of the proteotype upon VACV infection.

A. Immunofluorescence analysis of mock- and VACV-infected HeLa CCL2 cells after 2, 4, 6, 8 and 24 hpi representing the trajectory of the VACV life cycle, which were used for the total proteome analysis. Samples were stained with DAPI (nucleus), phalloidin (actin), anti-VACV-L1 (virion) and anti-VACV-I3 (ssDNA), followed by labeling with respective secondary fluorophore-conjugated antibodies.

B. Schematic representation of the experimental design for the temporal proteome analysis of HeLa CCL2 cells upon VACV infection. Quantitative total proteome analysis was conducted at the indicated time points in comparison to the mock-infected control.

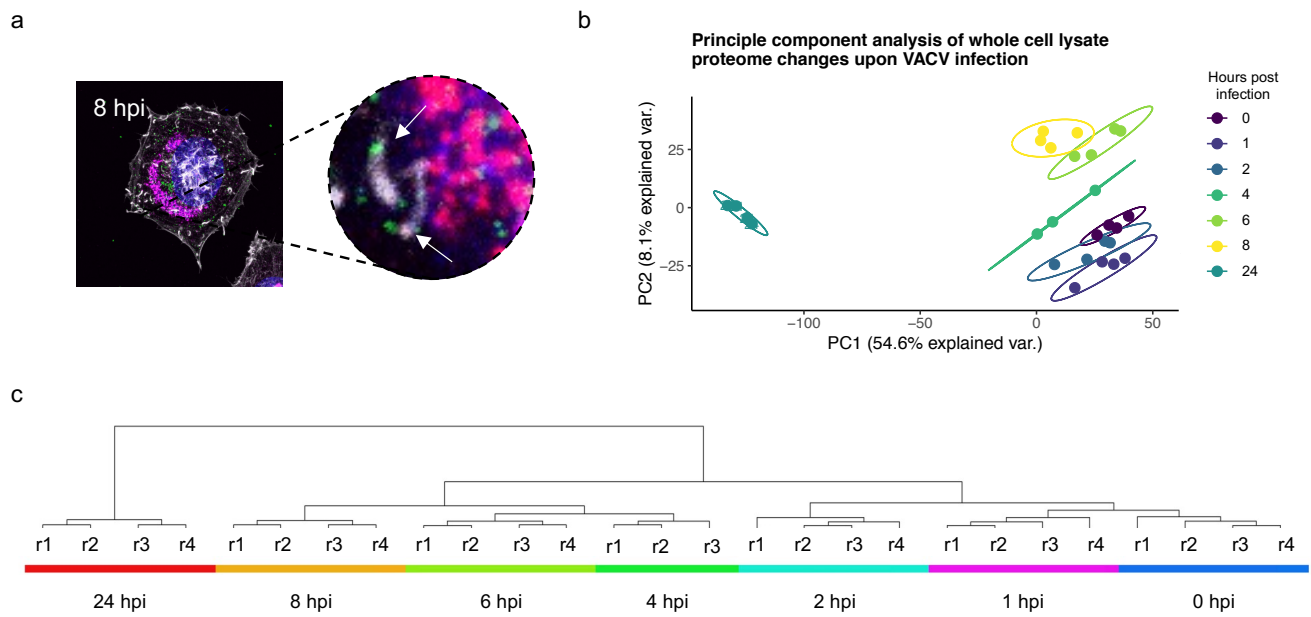
C. Pie chart representing the number of quantified proteins in the total proteome analysis. Significant differentially regulated proteins are colored (fold change > 2 or < 0.5 , and p-value < 0.05). Numbers of differentially regulated proteins were accumulated from mock-infected vs all VACV-infected time points containing host and viral proteins.

D. Venn diagram displaying the coverage of the identified and quantified VACV proteome in reference to the VACV proteins from the UniprotKB database. Identified VACV protein refers to the experiment specific hpH RP library. Quantified VACV proteins were quantified across the viral life cycle of VACV.

E. Volcano plot depicting protein abundance changes between mock-infected and VACV-infected HeLa CCL2 cells at 24 hpi. Quantification is based on a run-wise imputed data matrix. Significantly downregulated host proteins displayed in blue (fold change < 0.5 , and FDR-adjusted significance threshold p-value < 0.05) and significantly upregulated host proteins displayed in red (fold change > 2 , and FDR-adjusted significance threshold p-value < 0.05). Host proteins are sphere-shaped. Viral proteins are rhombus shaped and green-colored. For better visualization the FDR-adj. p-value capped at $P = 10^{-16}$.

F. Mirror plot representing the number of significant differentially regulated proteins for each VACV-infected timepoint (1, 2, 4, 6, 8 and 24 hpi) of HeLa CCL2 cells quantified against the mock-infected control (fold change of > 2 or < 0.5 , and FDR-adjusted significance threshold of p-value < 0.05).

Supplementary Figure 1



Supplementary Figure 1

A. Immunofluorescence analysis of HeLa CCL2 cells infected with VACV WR at 8 hpi. Stained with DAPI (nucleus), phalloidin (actin), anti-VACV-L1 (virion) and anti-VACV-I3 (ssDNA), followed by labeling with respective secondary fluorophore-conjugated antibodies. Zoom depicts VACV virions on actin protrusions during cell egress.

B. Principal component analysis of the temporal total proteome analysis of HeLa CCL2 cells upon VACV infection.

C. Hierarchical cluster analysis of the temporal total proteome analysis of HeLa CCL2 cells upon VACV infection.

Figure 2: VACV infection regulates transcription factors and extracellular matrix constituents

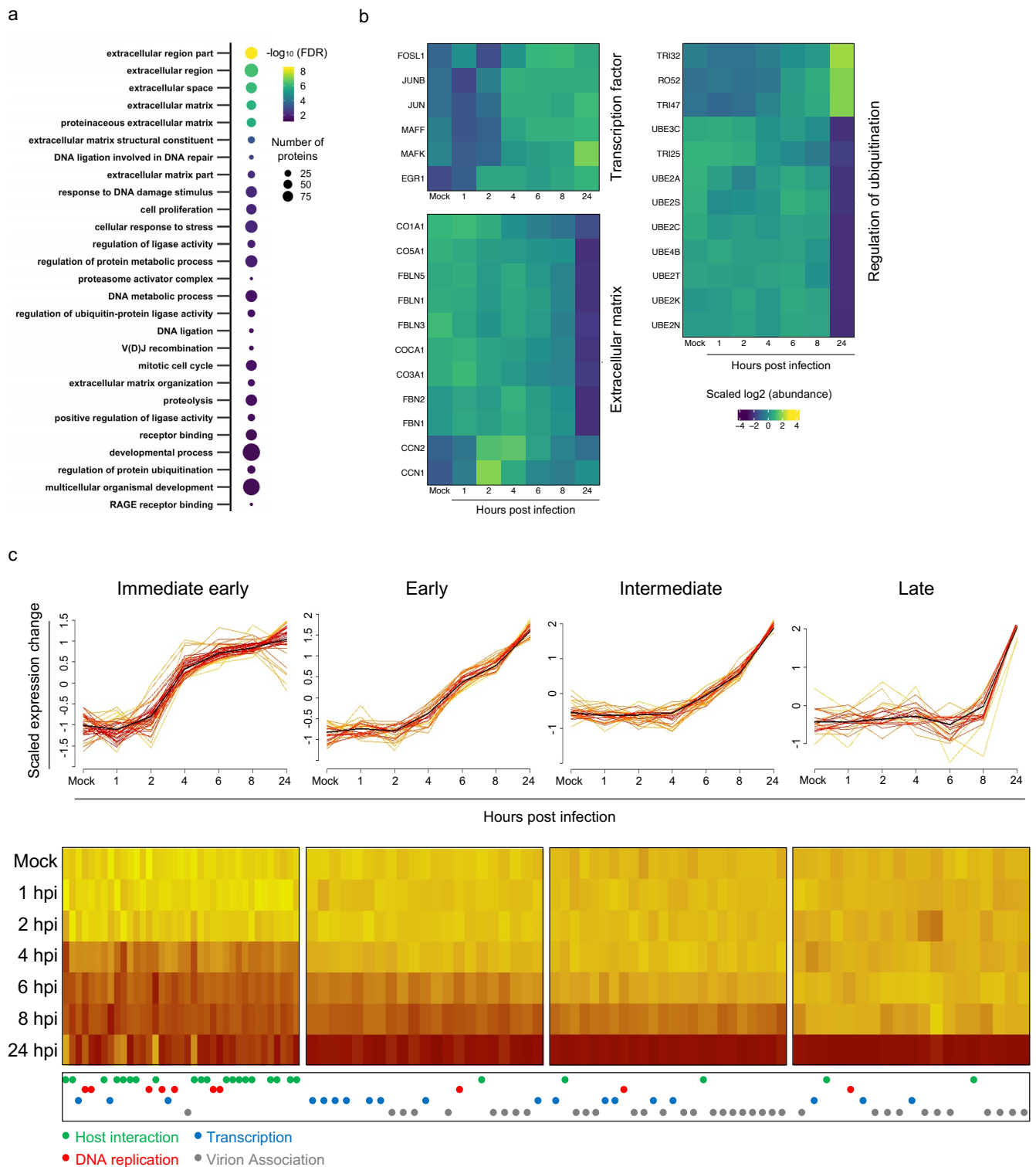


Figure 2: VACV infection regulates transcription factors and extracellular matrix constituents

A. Gene Ontology analysis (Biological Pathway, Molecular Function, Compartment analysis) of all differentially regulated host proteins using the network gene ontology tool Bingo within Cytoscape. Only statistically significant enriched GO terms with minimum 15 protein members are shown (FDR-adjusted p-value $P < 0.05$ and fold change > 2).

B. Heatmap visualisation of scaled \log_2 intensity of selected proteins from the temporal total proteome analysis of HeLa CCL2 cells upon VACV infection. Displayed candidates belong to the transcription factors function, the extracellular matrix and the regulation of ubiquitination.

C. Temporal analysis of viral protein synthesis from the temporal total proteome analysis of HeLa CCL2 cells upon VACV infection. Cluster analysis was conducted with Mfuzz soft clustering. Proteins are only included, if minimum cluster membership > 0.5 . Optimal number of clusters was determined using the Elbow method. Heatmap visualisation of scaled \log_2 abundance of viral proteins across the viral life cycle. Functional annotation of viral proteins was conducted literature-guided.

Figure 3: VACV hijacks the cell surface by modulation of host proteins and repopulation with viral proteins

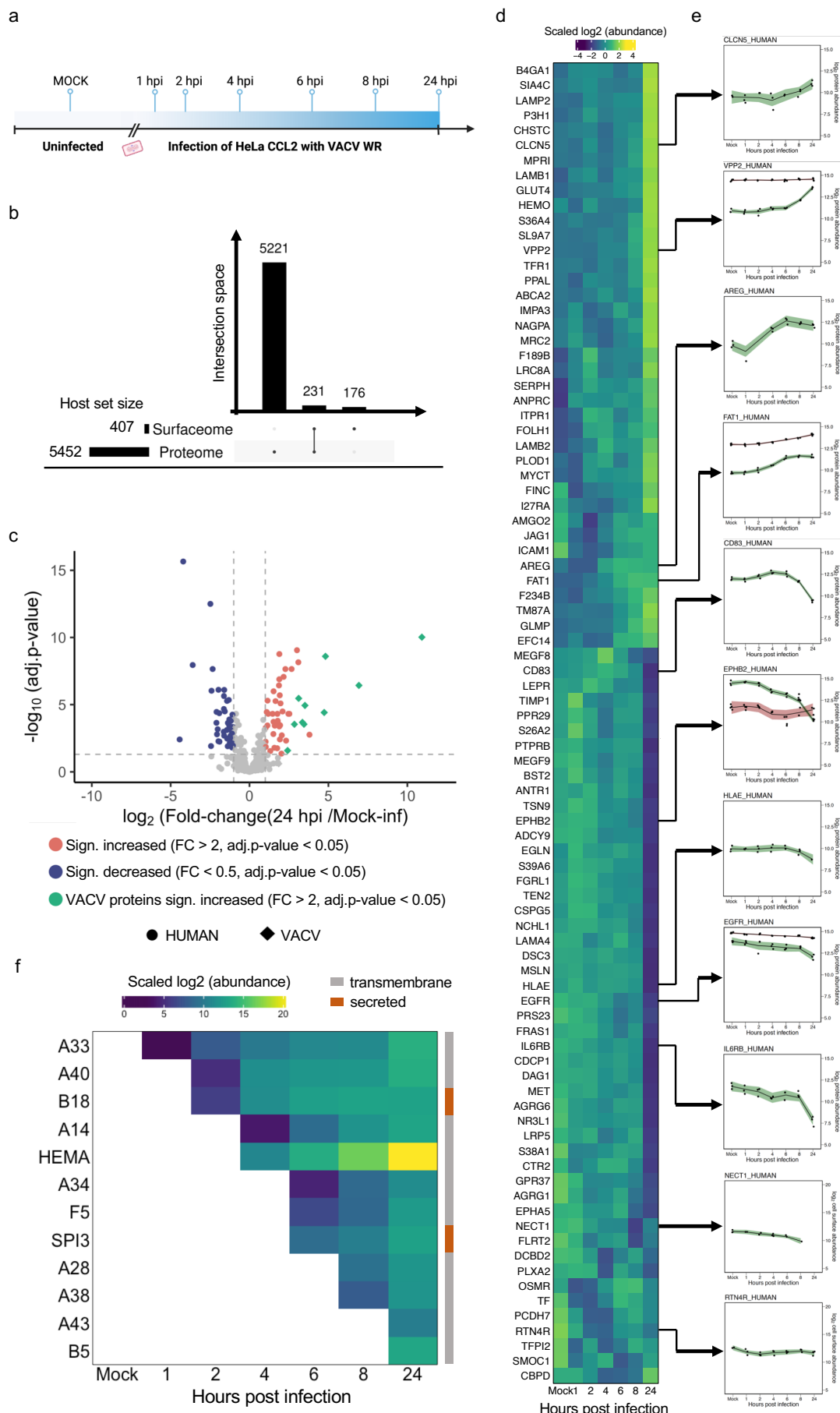


Figure 3: VACV hijacks the cell surface by modulation of host proteins and repopulation with viral proteins

A. Schematic representation of the experimental design for the temporal surfaceome analysis of HeLa CCL2 cells upon VACV infection. Quantitative total surfaceome analysis was conducted at the indicated time points against the mock-infected control.

B. Bar plots representing the summary of quantified proteins within the surfaceome, total proteome analysis and the intersection between both datasets of HeLa CCL2 cells upon VACV infection.

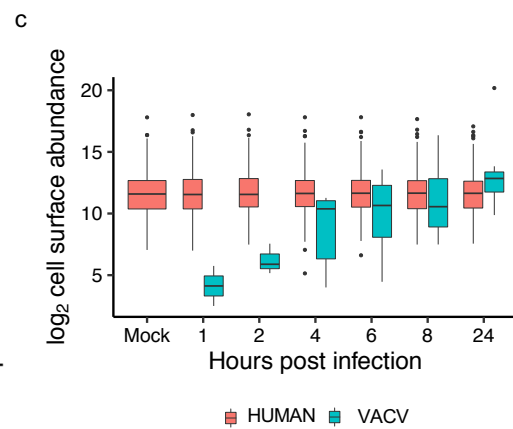
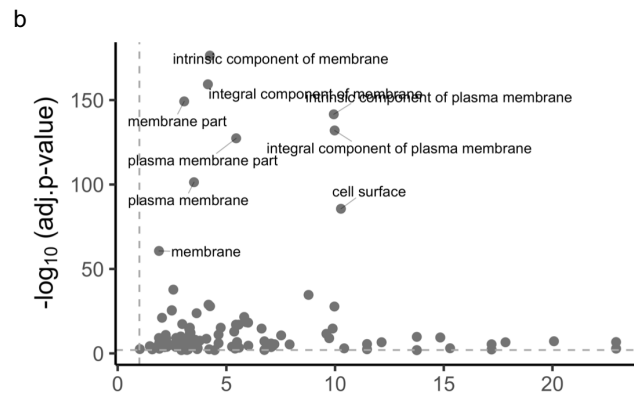
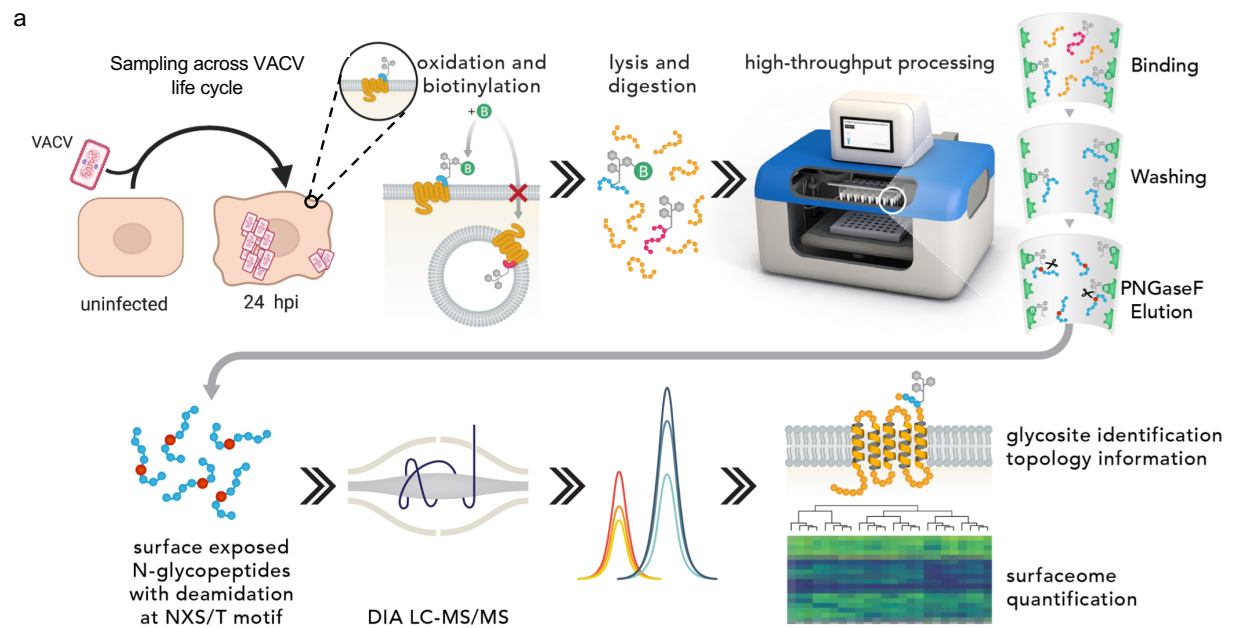
C. Volcano plot depicting protein abundance changes between mock-infected and VACV-infected HeLa CCL2 cells at 24 hpi from the surfaceome analysis. Quantification is based on a run-wise imputed data matrix. Significantly downregulated host proteins are displayed in blue and significantly upregulated host proteins are displayed in red (fold change < 0.5 , and FDR-adjusted significance threshold p -value < 0.05). Host proteins are sphere shaped. Viral proteins are rhombus shaped and green colored.

D. Heatmap visualization of scaled \log_2 intensity of all regulated host proteins from the temporal surfaceome analysis of HeLa CCL2 cells upon VACV infection. Quantification is based on a non-imputed data matrix.

E. Line plots displaying the \log_2 abundance of selected proteins along the temporal analysis of HeLa CCL2 cells upon VACV infection at the cell surface (green) and in the total proteome (red) datasets. Dots represent replicates per time point. Line is modelled along the changes. Width of the colored area represents standard error of the measurements per time point.

F. Heatmap visualization of scaled \log_2 intensity of viral proteins from the temporal surfaceome analysis of HeLa CCL2 cells upon VACV infection. Protein annotation as transmembrane and secreted based on UniprotKB database. Virion annotation based on literature. Quantification is based on non-imputed data matrix.

Supplementary Figure 3.1



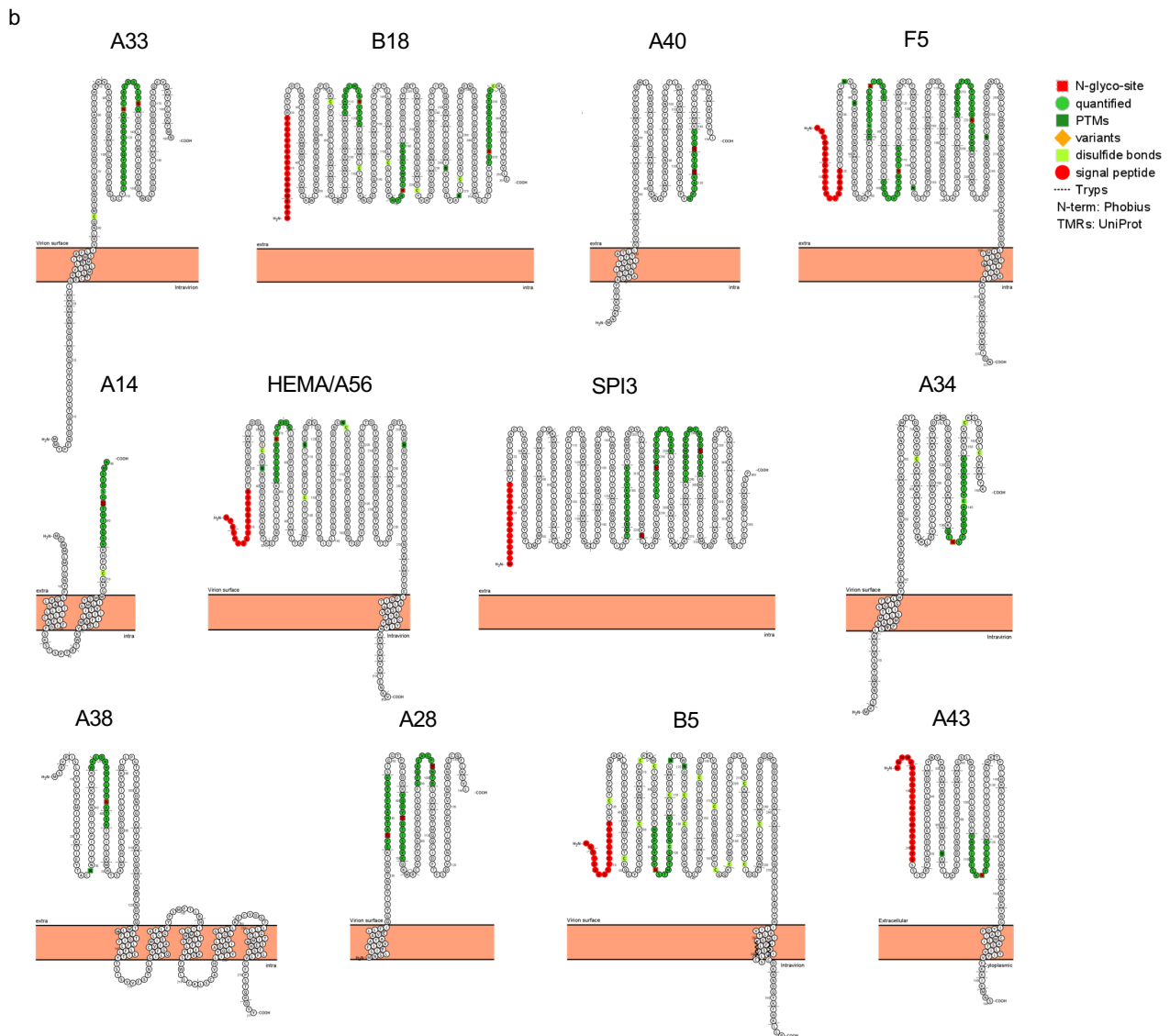
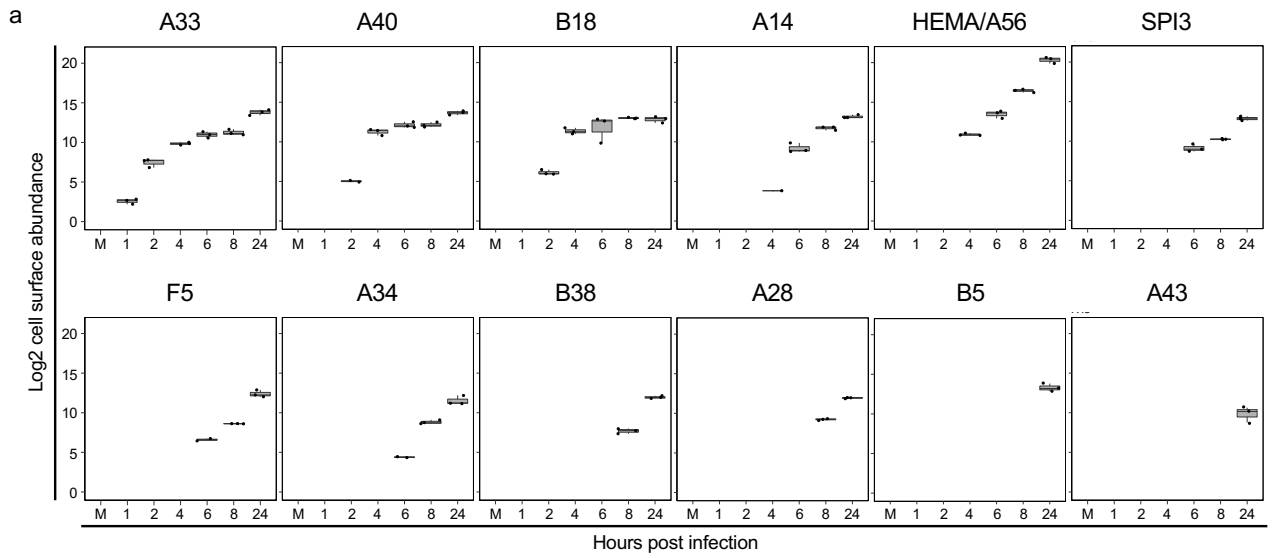
Supplementary Figure 3.1

A. Schematic representation of the autoCSC workflow for quantitative surfaceome snapshots, modified from (van Oostrum et al., 2019). Cell surface exposed N-glycoproteins are biotinylated with cell membrane impermeable biotin-probes on living cells. After cell lysis, proteins are digested with trypsin and biotinylated N-glycopeptides are enriched with immobilised streptavidin using an automated liquid handling system. Subsequently, enriched N-glycopeptides are washed and enzymatically eluted with PNGase F, cleaving the innermost glycan from the asparagine residue and causing a deamidation mass tag at the asparagine residue (-1 Da). Eluted peptides were analysed with DIA-based LC-MS/MS and formerly cell surface localisation of the respective protein is verified by filtering the quantified peptides for the deamidation within the NXS/T glycosylation motif with X being every amino acid except for proline. Surfaceome snapshots enable the identification of cell surface proteins, their quantitation across the viral life cycle and reveal topology information based on the deamidated N in the glycosylation motif.

B. Cell compartment analysis of quantified proteins using GO term analysis within Gorilla revealed the strong enrichment of plasma membrane and cell surface protein terms. Only FDR-adjusted, significantly enriched Go terms are considered.

C. Box plots representing the log₂ cell surface abundance range of all proteins from the surfaceome analysis of HeLa CCL2 cells upon VACV infection, separated by host and viral origin.

Supplementary Figure 3.2



Supplementary Figure 3.2

A. Box plots displaying the log₂ cell surface abundance of viral proteins from the surfaceome analysis of HeLa CCL2 cells upon VACV infection.

B. Protein sequence visualisation of viral proteins localising at the cell surface from the surfaceome analysis of HeLa CCL2 cells upon VACV infection, displayed with Protter. Transmembrane and signal peptide predictions are based on the UniprotKB and Phoebeius database. Identified N-glycopeptides per protein are coloured in green and the respective N-glycosite with squared red symbols. Further PTM annotations are based on Uniprot.

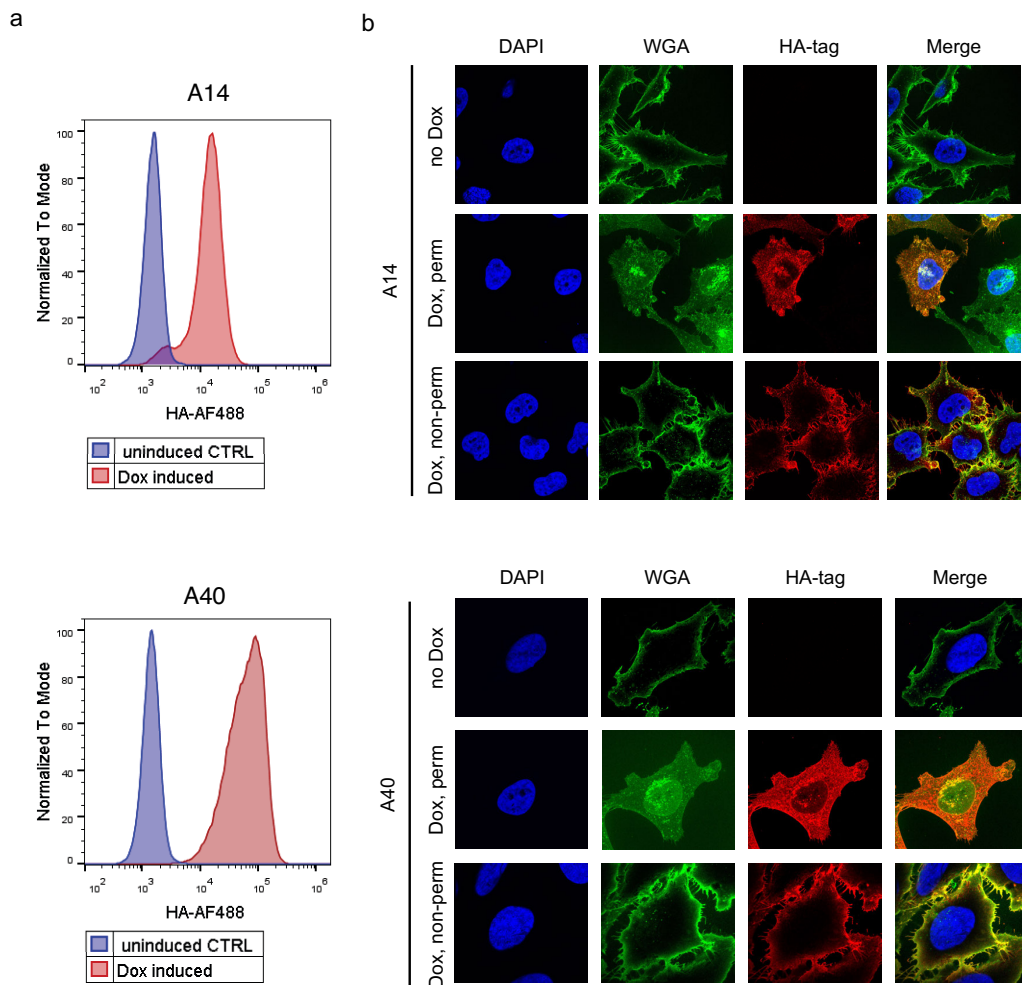
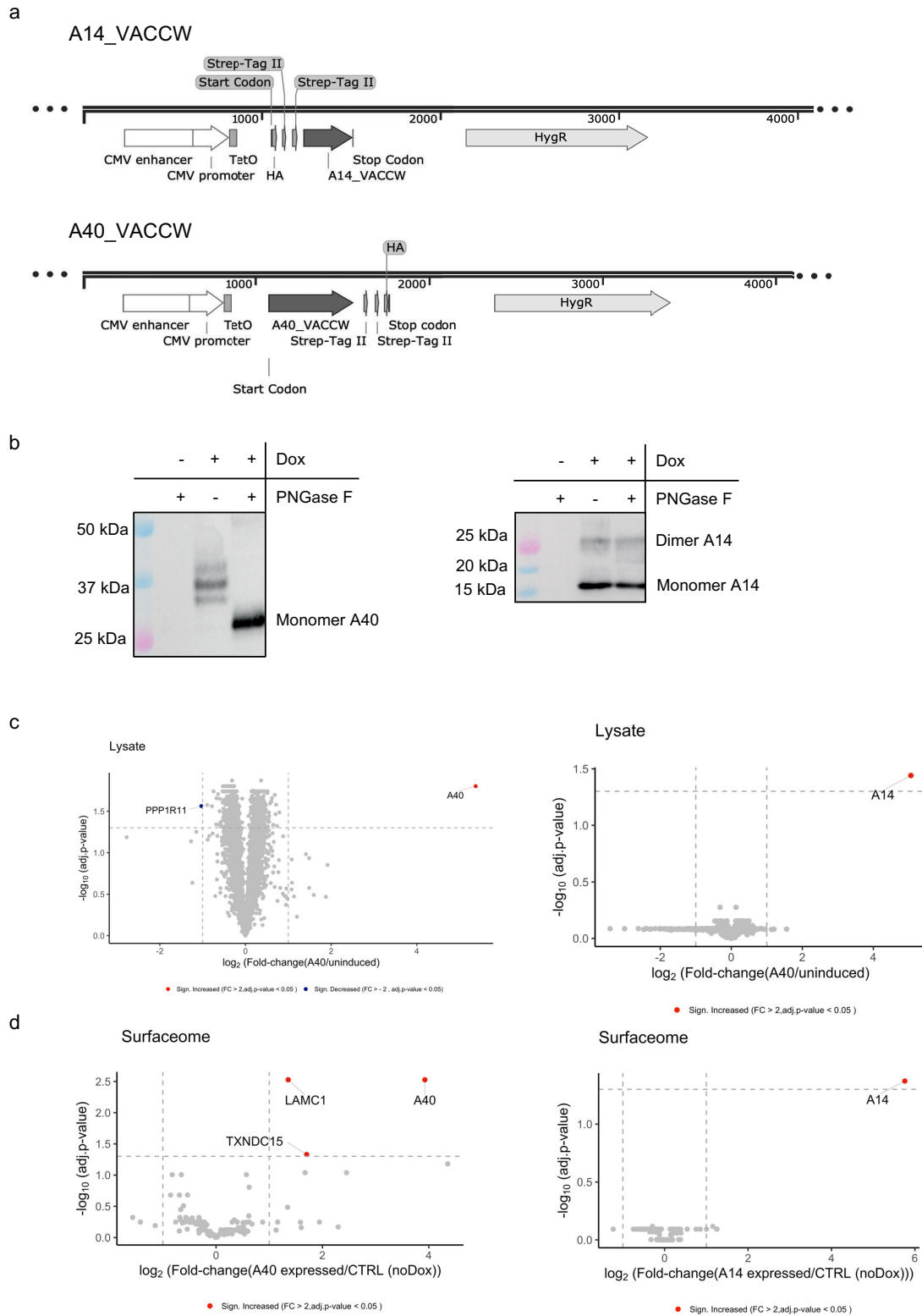
Figure 4: VACV-encoded A14 and A40 are N-glycosylated proteins localising to the host cell surface

Figure 4: VACV-encoded A14 and A40 are N-glycosylated proteins localising to the host cell surface

A. Flow cytometry analysis of untreated and doxycycline-induced SH-tagged A14 or A40 expressing HeLa CCL2 cells, stained with anti-HA-AF488.

B. Immunofluorescence analysis of untreated and doxycycline-induced A14 or A40 expressing HeLa CCL2 cells. Generic glycosylation stained with WGA-AF488 and SH-tagged viral proteins A14 and A40 with HA-AF650, on uninduced, non-permeabilized as well as induced permeabilized and non-permeabilized cells.

Supplementary Figure 4



Supplementary Figure 4

A. Feature annotation of A14 and A40 plasmid used for transfection and generation of stable cell lines. Viral protein ORFs were codon optimised for mammalian expression. A14 is N-terminally tagged with a Twin-Strep-HA tag. A40 is C-terminally tagged with a TWIN-Strep-HA tag.

B. Immunoblot analysis of untreated and doxycycline-induced A14 or A40 expressing HeLa CCL2 cells, where the cell lysate was left untreated or treated with PNGase F, detected with anti-HA-HRP-based chemiluminescence.

C. Volcano plots depicting protein abundance changes of untreated and doxycycline-induced A14 or A40 expressing HeLa CCL2 cells.

D. Volcano plots depicting cell surface protein abundance changes of untreated and doxycycline-induced A14 or A40 expressing HeLa CCL2 cells.

Figure 5: Functional and phenotypic analysis of A40

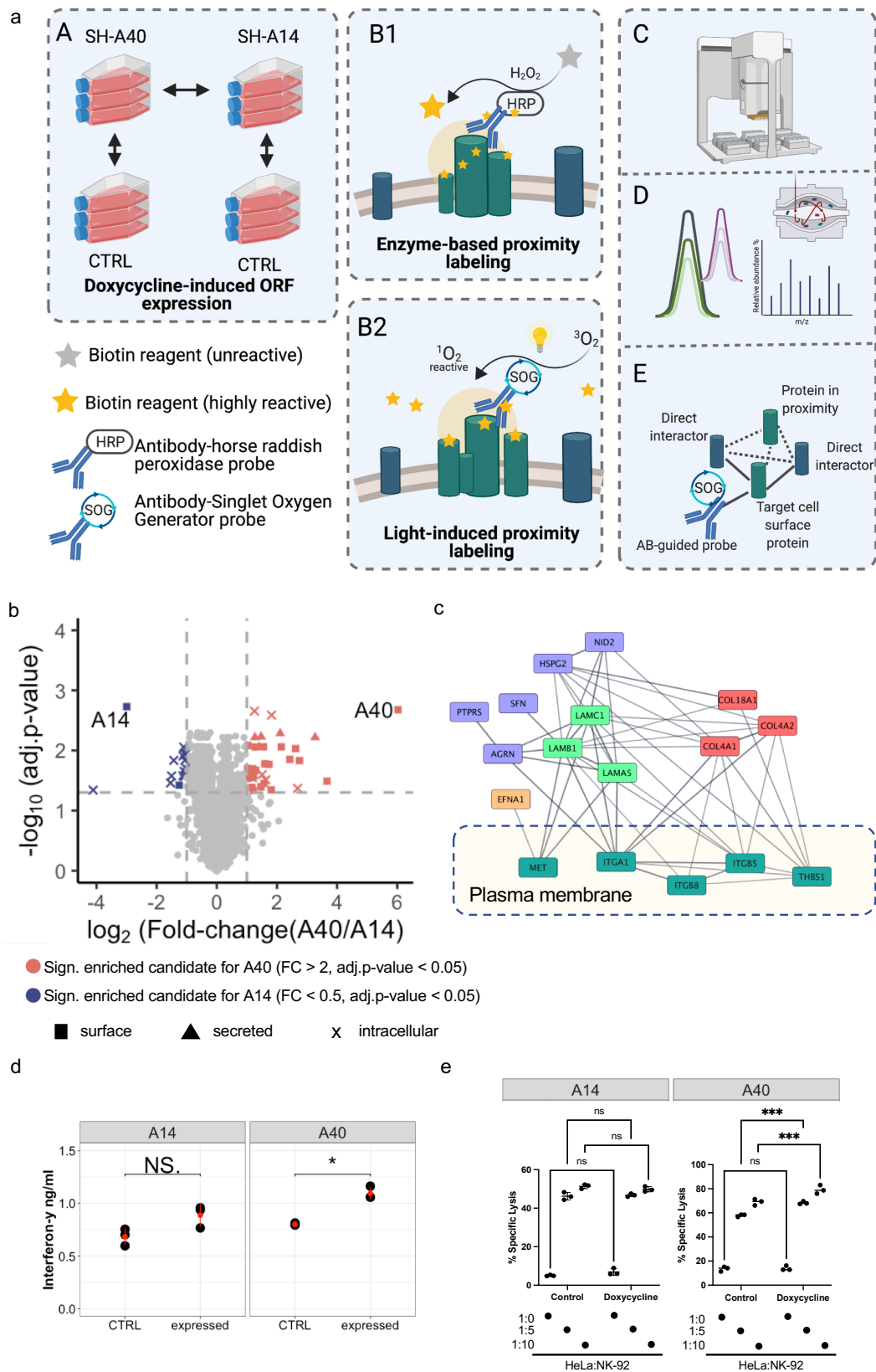


Figure 5: Functional and phenotypic analysis of A40

A. Schematic representation of the proximity labeling experiment. A40 & A14 expression was induced by doxycycline treatment and subsequently the protein neighbourhood was biotinylated using antibody-guided SPPLAT and LUX-MS methodologies. Modified from (Wendt et al. 2021)

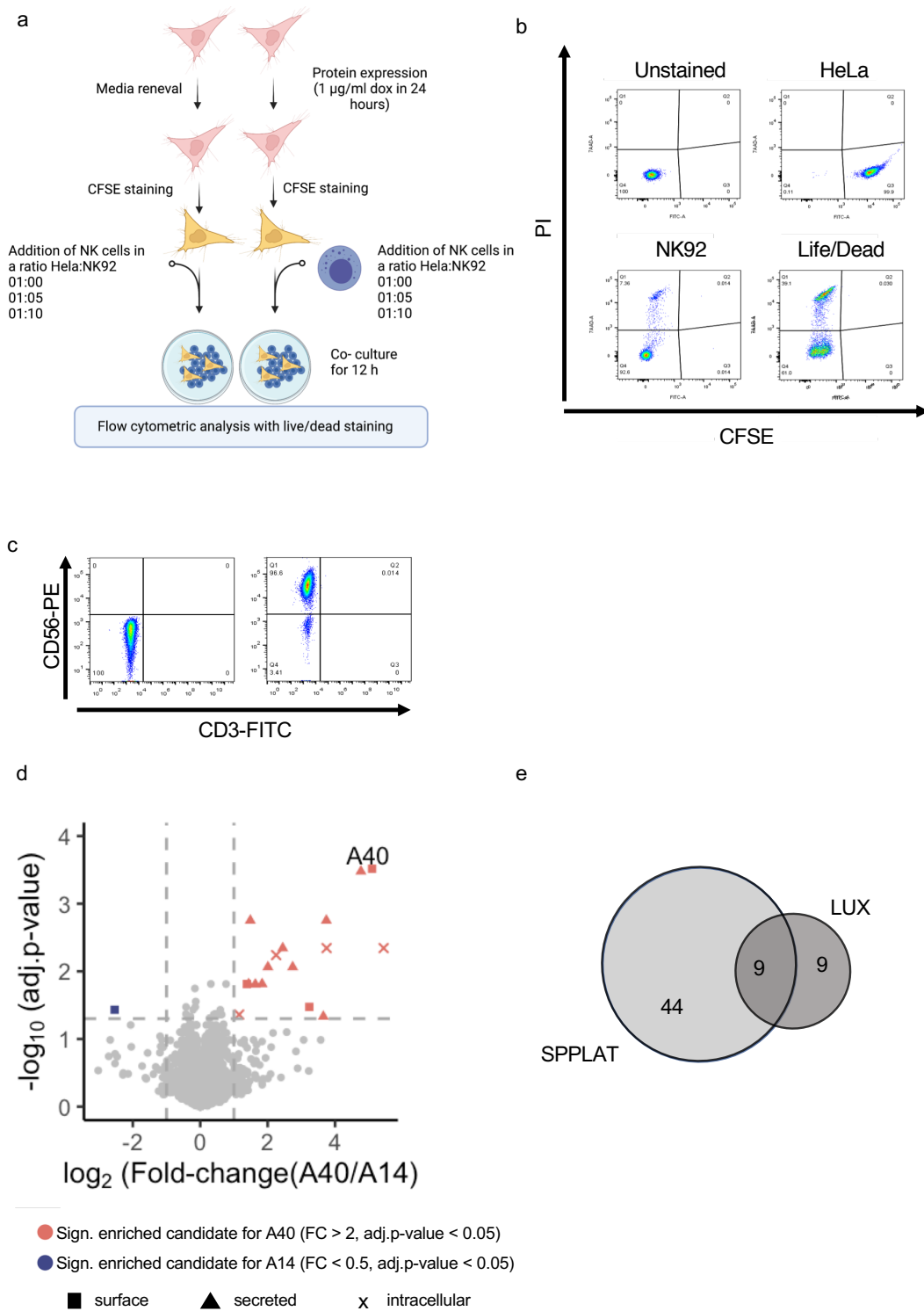
B. Volcano plot depicting enriched protein candidates between HeLa CCL2 cells expressing either A14 or A40 using SPPLAT-based proximity labeling. Proximity candidates for A14 are displayed in blue and proximity candidates for A40 are displayed in red (fold change < 0.5 , or > 2 , and FDR-adjusted significance threshold p-value < 0.05). Protein annotation based on UniprotKB database.

C. STRING-based network analysis of proteins enriched by SPPLAT-based proximity labeling approach of HeLa CCL2 cells expressing A40. Nodes represent candidate proteins, edges represent physical interactions based on literature with a confidence score of 0.7.

D. ELISA analysis of secreted IFN- γ from co-culture experiment of HeLa CCL2 and NK-92 cells after 12 h. Comparison between HeLa CCL2 expressing either A14 or A40 and their corresponding uninduced HeLa CCL2 cells control.

E. NK-mediated killing assay. Cytotoxicity was analysed with NK-92 as effector and HeLa CCL2 as target cells in T:E ratios of 1:0; 1:5; and 1:10. Comparison between HeLa CCL2 expressing either A14 or A40 and their corresponding uninduced HeLa CCL2 cells control.

Supplementary Figure 5



Supplementary Figure 5

A. Schematic representation of the NK killing assay. CFSE stained untreated or doxycycline-induced A14 and A40 expressing HeLa CCL2 cells were co-culture with NK-92 cells in T:E ratios of 1:0, 1:5 and 1:10 and analysed after 12 h by flow cytometry.

B. Gating scheme of NK killing assay.

C. Flow cytometry analysis of NK-92 cells, stained with anti-CD3 and anti-CD56, followed by labeling with respective secondary fluorophore-conjugated antibodies.

D. Volcano plot depicting enriched protein candidates between HeLa CCL2 cells expressing either A14 or A40 using LUX-MS-based proximity labeling. Proximity candidates for A14 are displayed in blue and proximity candidates for A40 are displayed in red (fold change < 0.5 , or > 2 , and FDR-adjusted significance threshold p-value < 0.05). Protein annotation based on UniprotKB database.

E. Venn diagram depicting the overlap of the candidate space of A40 in HeLa CCL2 cells from proximity labeling technologies SPPLAT and LUX-MS.

CHAPTER 4

Contributions to collaborative projects

This chapter contains collaborative work, I have contributed to during my PhD. The listed projects are in an advanced stage of the publication process, either published, accepted, submitted or with a manuscript in preparation. The presented collaborative work focuses around the characterization of proteotype and its modulation in health and disease. The underlying data illustrate the importance of characteristics such as localization, PTM profile and interaction of the proteotype as key regulator for the phenotype.

4.1 Light-mediated discovery of surfaceome nanoscale organization and intercellular receptor interaction networks

Maik Müller, Fabienne Gräbnitz, Nicolò Barandun, Yang Shen, **Fabian Wendt**, Sebastian N. Steiner, Yannik Severin, Stefan U. Vetterli, Milon Mondal, James R. Prudent, Raphael Hofmann, Marc van Oostrum, Roman C. Sarott, Alexey I. Nesvizhskii, Erick M. Carreira, Jeffrey W. Bode, Berend Snijder John A. Robinson, Martin J. Loessner, Annette Oxenius, Bernd Wollscheid

Nature Communications, accepted

Contribution

Fabian Wendt contributed to the method validation, by comparing antibody-guided LUX-MS and antibody-guided HRP-based proximity labeling. Here, he contributed ideas, planned, and conducted proteomic experiments including sample preparation, LC-MS/MS optimization, data acquisition and data analysis. Furthermore, he prepared CG1-HRP conjugates for cytotoxicity studies, and performed CD20 flow cytometry experiments. He edited the manuscript and gave critical input for the manuscript review.

Abstract

The molecular nanoscale organization of the surfaceome is a fundamental regulator of cellular signaling in health and disease. Technologies for mapping the spatial relationships of cell surface receptors and their extracellular signaling synapses would unlock theranostic opportunities to target protein communities and the possibility to engineer extracellular signaling. Here, we develop an optoproteomic technology termed LUX-MS that enables the targeted elucidation of acute protein interactions on and in between living cells using light controlled singlet oxygen generators (SOG). By using SOG-coupled antibodies, small molecule drugs, biologics and intact viral particles, we demonstrate the ability of LUX-MS to decode ligand receptor interactions across organisms and to discover surfaceome receptor nanoscale organization with direct implications for drug action. Furthermore, by coupling SOG to antigens we achieved light-controlled molecular mapping of intercellular signaling within functional immune synapses between antigen-presenting cells and CD8+ T cells providing insights into T cell activation with spatiotemporal specificity. LUX-MS based decoding of surfaceome signaling architectures thereby provides a molecular framework for the rational development of theranostic strategies.

4.2 PCprophet: a framework for protein complex prediction and differential analysis using proteomic data

Andrea Fossati*, Chen Li*, Federico Uliana, **Fabian Wendt**, Fabian Frommelt, Peter Sykacek, Moritz Heusel, Mahmoud Hallal, Isabell Bludau, Tümay Capraz, Peng Xue, Jiangning Song, Bernd Wollscheid, Anthony W. Purcell, Matthias Gstaiger and Ruedi Aebersold

** These authors contributed equally*

Nature Methods, 15 April 2021

DOI: 10.1038/s41592-021-01107-5

Contribution

Fabian Wendt contributed to the experimental validation of the computational method. He prepared the stable cell lines and collected the cellular starting material for the AP/MS experiments. He maintained the LC-MS/MS instrumentation for AP/MS data acquisition and was involved in initial data analysis. He visualized data and prepared figure panels. He edited the main manuscript and supplementary material in the context of the contributed data.

Abstract

Despite the availability of methods for analyzing protein complexes, systematic analysis of complexes under multiple conditions remains challenging. Approaches based on biochemical fractionation of intact, native complexes and correlation of protein profiles have shown promise. However, most approaches for interpreting cofractionation datasets to yield complex composition and rearrangements between samples depend considerably on protein–protein interaction inference. We introduce PCprophet, a toolkit built on size exclusion chromatography–sequential window acquisition of all theoretical mass spectrometry (SEC-SWATH-MS) data to predict protein complexes and characterize their changes across experimental conditions. We demonstrate improved performance of PCprophet over state-of-the-art approaches and introduce a Bayesian approach to analyze altered protein–protein interactions across conditions. We provide both command-line and graphical interfaces to support the application of PCprophet to any cofractionation MS dataset, independent of separation or quantitative liquid chromatography–MS workflow, for the detection and quantitative tracking of protein complexes and their physiological dynamics.

4.3 Diagnostics and correction of batch effects in large-scale proteomic studies: a tutorial

Jelena Cuklina, Chloe H Lee, Evan G Williams, Tatjana Sajic, Ben C Collins, Maria Rodriguez Martinez, Varun S Sharma, **Fabian Wendt**, Sandra Goetze, Gregory R Keele, Bernd Wollscheid, Ruedi Aebersold & Patrick G A Pedrioli

Molecular Systems Biology, 25 August 2021

DOI: 10.15252/msb.202110240

Contribution

Fabian Wendt contributed the bariatric surgery study dataset for the analysis with the R package proBatch. He conceived the proteomic study and conducted the proteomic sample preparation, measurements and analysis of the rat cohort lymph samples.

Abstract

Advancements in mass spectrometry-based proteomics have enabled experiments encompassing hundreds of samples. While these large sample sets deliver much-needed statistical power, handling them introduces technical variability known as batch effects. Here, we present a step-by-step protocol for the assessment, normalization, and batch correction of proteomic data. We review established methodologies from related fields and describe solutions specific to proteomic challenges, such as ion intensity drift and missing values in quantitative feature matrices. Finally, we compile a set of techniques that enable control of batch effect adjustment quality. We provide an R package, "proBatch", containing functions required for each step of the protocol. We demonstrate the utility of this methodology on five proteomic datasets each encompassing hundreds of samples and consisting of multiple experimental designs. In conclusion, we provide guidelines and tools to make the extraction of true biological signal from large proteomic studies more robust and transparent, ultimately facilitating reliable and reproducible research in clinical proteomics and systems biology.

4.4 PIM1 phosphorylation of GBP1 guards bystander cells during infection

Daniel Fisch, Moritz M. Pfeleiderer, **Fabian Wendt**, Eleni Anastasakou, Xiangyang Liu, Barbara Clough, Samuel Lara-Reyna, Vesela Encheva, Ambrosius P. Snijder, Hironori Bando, Masahiro Yamamoto, Avinash R. Shenoy, Jason P. Mercer, Bernd Wollscheid, Wojtek P. Galej, Eva-Maria Frickel

Manuscript in preparation

Contribution

Fabian Wendt contributed to the phosphoproteomic analysis of the GBP1 PTM sites. Here, he designed research, conducted the proteomic workflow, analyzed and visualized data, prepared figure panels and provided draft text for the manuscript regarding his contribution. Moreover, he conducted the phosphoproteomic experiments and analysis for a PIM1-kinase-dependent screen upon *Toxoplasma gondii* infection, which is not included in the manuscript but represents a valuable resource for future work.

Abstract

Interferon-gamma (IFN γ) produced during an infection upregulates cell-intrinsic host defense molecules to enable sensing and responses to invading microbes. The IFN γ -induced Guanylate Binding Protein (GBP) family are anti-microbial GTPases and the pathfinding family-member GBP1 localizes to some pathogen vacuolar membranes (e.g. the *Toxoplasma gondii* vacuole) to cause their disruption, programmed cell death and infection control. GBP1 also interacts with self-membranes but how uninfected bystander cells are protected from its potentially membrane-disruptive function is unknown. Here we discover the IFN γ -induced kinase PIM1 phosphorylates GBP1 serine 156 resulting in a GBP1 monomeric state with decreased Golgi association. Phosphorylated GBP1pS156 is sequestered in the cytosol by 14-3-3 σ and GBP1:14-3-3 σ complex visualization by cryo-electron microscopy confirms GBP1 being trapped as a GTPase-inactive monomer. Unphosphorylated GBP1 is GTPase active and leads to enhanced *Toxoplasma* vacuolar disruption, pathogen control and host cell death. Golgi targeting of unphosphorylated GBP1 causes organelle fragmentation and unprogrammed cell death. IFN γ -induced PIM1 has a half-life of minutes resulting in IFN γ -signaling blocking pathogens, such as *Toxoplasma*, to succumb to the PIM1-GBP1 trap whereby unphosphorylated GBP1 attacks the vacuolar membrane. At the same time, bystander cells with PIM1-guarded GBP1 are safe from enhanced disruptive Golgi targeting and cell death. This work reveals a novel concept of post-translational regulation driven by an IFN-dependent, yet labile protein as a rapidly tunable response to infection. More broadly it expands our knowledge of bystander cell safekeeping during infection.

4.5 Finding cellular receptors for gastrointestinal viruses

Annasara Lenman, **Fabian Wendt**, Ngan Thi Dong, Megha Khosla, Felix Meissner,
Bernd Wollsheid, Gisa Gerold

Manuscript in preparation

Contribution

Fabian Wendt designed and performed the proteomic experiments to find adenovirus and norovirus cognate receptors. He conducted the proteomic workflow, analyzed, visualized, and interpreted the data.

Abstract

Acute gastroenteritis (AGE) is a very frequent disease worldwide and a leading cause of child mortality with >500,000 deaths/year among children under the age of five (1). Within one year, no less than 1.7 billion cases of AGE was estimated to have occurred in young children (< 5 years) (2). Rotavirus (RV) has been a leading cause of AGE-associated death but the cases reduced from 453,000 deaths in 2008 to 193,000 deaths in 2011, thanks to the universal introduction of RV vaccines in 2007 (2, 3). RV, together with norovirus (NoV) and adenovirus (AdV) still constitute a leading cause of death in children under the age of five, and create a huge economic burden to society. Unfortunately, neither antiviral drugs nor vaccines are available for treatment and prevention of NoV and AdV infections. The aim of this project was to increase the basal knowledge about the molecules and mechanisms engaged in viral entry into target cells for NoV and AdV, and, to identify novel targets for antiviral drug development. For this purpose, we decoded the cognate receptor space using HATRIC-based ligand receptor (LRC) technology. Upon identification of potential binding partners, we verified their physiological relevance during virus entry using siRNA screens.

4.6 Multiplexed interactome analysis reveals the molecular architecture of the human prefoldin network

Fabian Frommelt, Andrea Fossati, Federico Uliana, **Fabian Wendt**, Xue Peng, Moritz Heusel, Bernd Wollscheid, Ruedi Aebersold, Rodolfo Ciuffa, and Matthias Gstaiger

Manuscript in preparation

Contribution

Fabian Wendt contributed to the LC-MS/MS analysis by preparing and maintaining the technical equipment during the cohort measurements.

Abstract

Most, if not all, proteins are organized in macromolecular assemblies, which represent key functional units regulating the majority of cellular processes. Heterogeneous in nature, protein complex subunits can partition in distinct assemblies with specialized functions. Affinity purification of the protein of interest combined with LC-MS/MS (AP-MS) still represents the method of choice to identify the set of proteins interacting with a bait protein but cannot resolve the composition of copurified complex isoforms. Data from multiple time- and resource-intensive reciprocal AP-MS experiments are currently needed to computationally infer the composition of concurrent complex isoforms. In this study we introduced Deep Interactome Profiling by Mass Spectrometry (DIP-MS), a novel approach combining affinity purification with biochemical fractionation and high-throughput data independent acquisition mass spectrometry (DIA-MS) to resolve bait containing complex isoforms in a single experiment. We applied our method to decipher multiple heterogeneous complexes and sub-complex assemblies to obtain a deep understanding of complex landscape for prefoldin subunits. Our findings describe an alternative PFD assembly and report associated client-complex interactions with PFD and the PAQosome.

4.7 ARTC1 enhances cancer cell proliferation through ADP-ribosylation and activation of c-MET, ErbB3 and IGF-IR signaling pathway

Kathrin Nowak, **Fabian Wendt**, Patrick Manetsch, Fabio Aimi, Jesus Glaus Garzón, Ann-Katrin Hopp, Tobias Suter, Peter Schraml, Holger Moch, Bernd Wollscheid, Deena M. Leslie Pedrioli and Michael O. Hottiger

Manuscript in preparation

Contribution

Fabian Wendt contributed the mass-spectrometry based total proteome and surfaceome analysis to the project for the characterization of the proteomic alterations upon ARTC1 expression. Here, he conceived the experimental strategy, and conducted the full proteomic workflow from sample preparation, data acquisition, and data analysis. He prepared figure panels, reviewed, and edited the experiment-associated text paragraphs.

Abstract

The GPI-anchored ADP-ribosyltransferase ARTC1 is expressed in a highly restricted manner in skeletal muscle and heart tissue. Although ARTC1 has been described to regulate tumorigenesis, the identification of ARTC1-modified targets and subsequent characterization of ARTC1-regulated signaling events remain elusive. Here, we observed by immunohistochemistry that increased ARTC1 expression negatively correlated with markers indicative of a better patient outcome in breast and brain cancers. Genetic complementation of A549 cells with wild type and an enzymatically inactive ARTC1 mutant revealed that the enzymatic activity of ARTC1 enhances cell proliferation *in vitro* as well as *in vivo*. While a mass spectrometry-based identification of the ADP-ribosylated proteins revealed that the modification profiles of A549 cells differed from complemented MDA-MB-231 cells or HCC2218 cells endogenously expressing ARTC1, a common set of modified ADP-ribosylated target proteins of the endomembrane system was detected in all tested cell lines. Surfaceome analysis of A549 cells indicated that overexpression of wild type ARTC1 altered the glycosylation status of defined surface proteins. Moreover, cell signaling analysis indicated that ARTC1 enhances phosphorylation of the HGFR, ErbB3 and IGF-1R. Exogenous NAD⁺ and subsequent hyper-ADP-ribosylation of these receptors abrogate this effect. Together, our results provide evidence that ARTC1 enhances in an enzymatic activity and NAD⁺-dependent manner the tumor intrinsic proliferation that is important for tumorigenesis.

CHAPTER 5

Conclusions and Future Perspective

With this thesis I provide a systematic view of the proteotype of the VACV infected host cell, focusing on the spatio-temporal investigation of the surfaceome. VACV infection leads to the cell surface abundance modulation of host proteins involved in proliferation and immune signaling, which most likely supports immune evasion. Integration of total proteome with subcellular surfaceome data revealed additional insights, such as differentiation between signaling and expression changes. Moreover, VACV proteins repopulate the host cell surface, being an extracellular marker for the intracellular infection stage. Using proximity-labeling strategies, viral protein A40 was found to be embedded in the vicinity of a network from integrin and ECM molecules. Based on my results and the published immune modulating phenotype, A40 may dysregulate ECM-immune cell interactions.

Our results illustrate the importance of spatial proteotype analysis, as the localisation of proteins dictates their potential interaction space and their functionality. Extracellular viral proteins can engage in signaling with uninfected bystander cells and immune cells, promoting the spread and immune evasion of the virus. However, their extracellular localisation makes them and their interactions attractive targets for antiviral therapeutics. In the following, I present further strategies to elucidate the extracellular interaction of viral proteins and its benefit for the development of antiviral strategies.

5.1 Refinement of the A40 interactome

Infection with Δ A40-VACV did not show impaired replication or plaque morphology *in vitro* but led to a reduced lesion size *in vivo* (Pérez et al., 2020; Tschärke et al., 2002). Hence, A40 is connected to an immunomodulating phenotype with unknown function during VACV infection. We have shown that A40 is in the proximity of integrins and their interaction partners of the ECM. The potential interaction is mediated by either protein-protein or protein-glycan-based interactions, conceivable since A40 is a C-type lectin-like family member. Although A40's carbohydrate-recognition domain (CRD) is only partially

conserved, it might still bind to glycans (Wilcock et al., 1999). The nature of the interaction mechanisms needs further investigation. We hypothesize that A40 dysregulates ECM-mediated immune cell functions. Consequently, we would like to investigate if the infiltration of immune cells at the infection site is altered with the Δ A40-VACV strain. We have shown that NK cells are stimulated by A40 expression in target cells. However, we cannot exclude that also other immune cells might be involved in the immune-modulating phenotype.

Furthermore, A40 could bind to immune cells directly. We probed the binding of the purified extracellular domain of A40 to various immortalized immune cell lines by flow cytometry binding experiments, but were not able to resolve the binding unambiguously (results not shown). Nevertheless, the interaction of A40 to immune cells could be of highly transient character and thus needs a more sensitive readout. In order to characterize weak protein-protein interactions, oligomerization of the ligand can improve the avidity of an interaction, a binding parameter often critical at the cell membrane (Erlendsson and Teilum, 2020).

Furthermore, A40 interaction with immune cells might need viral or host-derived co-receptors, which are missing in the above described binding experiments with the purified extracellular domain. Thus, cell-to-cell interactions studied between VACV, or Δ A40-VACV infected cells with immune cells could provide details to investigate this hypothesis and determine the involved immune cells.

5.2 Towards an *in vivo* resolved interaction network

The local infection site harbours a microenvironment composed of virus-infected and adjacent not yet infected cells as well as infiltrating immune cells of the innate and adaptive immune response (Bjarnsholt et al., 2021). Moreover, a heterogeneous mix of soluble ligands is present. All these extracellular factors stimulate and affect the cis/and trans interactions of cell surface-residing proteins, which is very challenging to simulate under *in vitro* conditions. Thus, *in vivo* resolved interaction networks are physiologically relevant and might be translatable to subsequent pre/clinical utilization. Hence, applying proximity labeling technologies in an *in vivo* setup is highly interesting. In order to study the interaction network of VACV proteins at the cell surface *in vivo*, the intradermal murine model would be very suitable. This model system enables the study of the local infection

including its microenvironment without inducing a systemic infection of the organism (Tscharke and Smith, 1999). Furthermore, the forming lesion at the inoculation site is located at the skin surface. This is advantageous for the light-induced reaction in the LUX-MS approach and makes it technically applicable, as light at the used wavelength of 590 nm penetrates the tissue with a depth of up to 4 mm (Ash et al., 2017). Furthermore, the necessary reagents such as the antibody-SOG probe could be supplied easily to the skin lesion. Since the *in vivo* model would take into consideration the microenvironment at the infection site it would be suitable to study cell-cell communication based on the interaction of viral proteins and their receptors on immune cells.

5.3 Investigation of VACV-induced paracrine signaling

Next to the surfaceome, secreted proteins are involved in extracellular signaling. VACV infection leads to the activation of the innate immune system by secretion of interferons, chemokines, and growth factors (Beerli et al., 2019; Liu et al., 2005). Moreover, glycoproteins can be shedded from the surface of infected cells. VACV counteracts the host response by secretion of viral proteins to alter receptor-mediated signaling in order to evade the immune response (Smith et al., 2018). However, the composition of the secretome has not been resolved systematically yet. Interestingly, we found metalloprotease inhibitors downregulated upon infection, which indicates dysregulated shedding of proteins. Hence, by investigation of the secretome upon VACV infection might reveal new insights into the modulation of the immune response, cell proliferation, mitogenesis, and cell motility.

In our present study, we used a high multiplicity of infection to achieve synchronous infection of the cells, due to the fact that we later process the average response across all cells in the sample. However, naturally occurring infections might be rather heterogeneous and harbour infected and non-infected bystander cells. The non-infected bystander cells are strongly perturbed by the virus-induced secretome, composed of many immune signaling relevant molecules such as cytokines, chemokines, and growth factors as well as viral secreted proteins. In order to investigate how these non-infected bystander cells respond to the virus-induced secretome, one would to either treat cells with conditioned media or one could infect cells with a lower multiplicity of infection. A cell sorting by flow cytometry prior to proteomic sample processing could resolve the infected and non-infected cell populations. Together, our surfaceome data, the secretome analysis and the bystander

analysis would facilitate the decoding of paracrine signaling and its effect on the outcome of the viral infection.

5.4 Utilizing extracellular viral proteins in immunotherapy

Cell surface proteins are a popular drug target due to their easy accessibility. Approximately 66% of all drugs are targeting membrane proteins at the cell surface (Bausch-Fluck et al., 2019). However, most antiviral drugs operate on intracellular host and viral proteins that are critical for viral replication. Recently, extracellular operating drugs gained interest. These target e.g. entry receptors and block the virus infection (MacArthur and Novak, 2008). Inhibition of cell entry works well for viruses with specific cognate receptors, but might be challenging for enveloped viruses such as VACV, which attach first to glycosaminoglycans (GAGs) and then enter the cell by macrocytosis. Thus, neutralizing antibodies against poxviruses were mostly developed against viral envelope proteins (Gilchuk et al., 2016).

We described the localisation of VACV proteins at the cell surface upon infection. These extracellular accessible viral proteins differentiate infected from non-infected cells and represent a promising target in antiviral therapy. In the last decade, biologics such as bispecific antibodies (bsAB) gained attention due to their success in anticancer therapy . The working principle of bsABs is based on the binding of two independent epitopes, which can be located on different cells and would engage the physical interaction of target cells with immune cells (Labrijn et al., 2019). The usage of bsAB binding the viral protein antigen and T cell epitope would redirect T cell-mediated cytotoxicity to infected tissue and support the immune response to the viral infection. Therefore, the development of bispecific antibodies against poxvirus x T cell epitopes would support the acute treatment of cowpox and monkeypox zoonoses. The suggested immunotherapy principles are transferable for other viral diseases such as HCMV infection, which also relocalise viral proteins to the cell surface of infected cells (Weekes et al., 2014).

As noted, bsABs are a promising oncolytic tool, as malignant tissue usually evades the immune system. However, the determination of the epitope dependencies is challenging. Whereas most immune cells are very well classified, knowledge of high abundant or even exclusive cell surface antigens on malignant cells of solid tumours is sparse. Thus, instead of utilizing endogenous differences between normal and malignant tissue, oncolytic viruses could be used to deliver the T cell antigens to tumour cells. Vaccinia virus is a promising

oncolytic agent, due to its short life cycle, broad cell tropism and cytosolic replication, minimizing the risk of genome integration (Al Yaghchi et al., 2015). Oncolytic VACV infects and replicates predominantly in cancer cells, expressing factors that ultimately lead to cell lysis and provoke a generic immune response. However, achievement of full tumour clearance is challenging. Thus, oncolytic VACV expressing T cell engagers would enhance the anticancer therapy. VACV expressing T cell antigens was successful in the first preclinical experiments, killing infected and non-infected cancer bystander cells effectively (Yu et al., 2014). Instead of expressing T cell engagers, one could also develop bispecific antibodies against the VACV proteins present at the host cell surface during the infection. This would have the advantage that one would not need to genetically modify the oncolytic virus itself and could administer a bsAB mix, engaging with different immune cells.

CHAPTER 6

References

- Abbas, W., and Herbein, G. (2014). Plasma membrane signaling in HIV-1 infection. *Biochim. Biophys. Acta* 1838, 1132–1142.
- Aebersold, R., and Mann, M. (2003). Mass spectrometry-based proteomics. *Nature* 422, 198–207.
- Aebersold, R., and Mann, M. (2016). Mass-spectrometric exploration of proteome structure and function. *Nature* 537, 347–355.
- Aebersold, R., Agar, J.N., Amster, I.J., Baker, M.S., Bertozzi, C.R., Boja, E.S., Costello, C.E., Cravatt, B.F., Fenselau, C., Garcia, B.A., et al. (2018). How many human proteoforms are there? *Nat. Chem. Biol.* 14, 206–214.
- Alcami, A., and Koszinowski, U.H. (2000). Viral mechanisms of immune evasion. *Trends Microbiol.* 8, 410–418.
- Alcami, A., Symons, J.A., and Smith, G.L. (2000). The vaccinia virus soluble alpha/beta interferon (IFN) receptor binds to the cell surface and protects cells from the antiviral effects of IFN. *J. Virol.* 74, 11230–11239.
- Alkhatib, G., Combadiere, C., Broder, C.C., Feng, Y., Kennedy, P.E., Murphy, P.M., and Berger, E.A. (1996). CC CKR5: a RANTES, MIP-1alpha, MIP-1beta receptor as a fusion cofactor for macrophage-tropic HIV-1. *Science* 272, 1955–1958.
- Almén, M.S., Nordström, K.J.V., Fredriksson, R., and Schiöth, H.B. (2009). Mapping the human membrane proteome: a majority of the human membrane proteins can be classified according to function and evolutionary origin. *BMC Biol.* 7, 50.
- Altenburg, A.F., Kreijtz, J.H.C.M., de Vries, R.D., Song, F., Fux, R., Rimmelzwaan, G.F., Sutter, G., and Volz, A. (2014). Modified vaccinia virus ankara (MVA) as production platform for vaccines against influenza and other viral respiratory diseases. *Viruses* 6, 2735–2761.
- Alvarez, R.A., Hamlin, R.E., Monroe, A., Moldt, B., Hotta, M.T., Rodriguez Caprio, G., Fierer, D.S., Simon, V., and Chen, B.K. (2014). HIV-1 Vpu antagonism of tetherin inhibits antibody-dependent cellular cytotoxic responses by natural killer cells. *J. Virol.* 88, 6031–6046.
- Al Yaghchi, C., Zhang, Z., Alusi, G., Lemoine, N.R., and Wang, Y. (2015). Vaccinia virus, a promising new therapeutic agent for pancreatic cancer. *Immunotherapy* 7, 1249–1258.

- Andrade, A.A., Silva, P.N.G., Pereira, A.C.T.C., De Sousa, L.P., Ferreira, P.C.P., Gazzinelli, R.T., Kroon, E.G., Ropert, C., and Bonjardim, C.A. (2004). The vaccinia virus-stimulated mitogen-activated protein kinase (MAPK) pathway is required for virus multiplication. *Biochem. J* *381*, 437–446.
- Arias, J.F., Heyer, L.N., von Bredow, B., Weisgrau, K.L., Moldt, B., Burton, D.R., Rakasz, E.G., and Evans, D.T. (2014). Tetherin antagonism by Vpu protects HIV-infected cells from antibody-dependent cell-mediated cytotoxicity. *Proc. Natl. Acad. Sci. U. S. A.* *111*, 6425–6430.
- Armingol, E., Officer, A., Harismendy, O., and Lewis, N.E. (2021). Deciphering cell-cell interactions and communication from gene expression. *Nat. Rev. Genet.* *22*, 71–88.
- Arrighi, J.-F., Pion, M., Garcia, E., Escola, J.-M., van Kooyk, Y., Geijtenbeek, T.B., and Piguet, V. (2004). DC-SIGN-mediated Infectious Synapse Formation Enhances X4 HIV-1 Transmission from Dendritic Cells to T Cells. *J. Exp. Med.* *200*, 1279–1288.
- Ash, C., Dubec, M., Donne, K., and Bashford, T. (2017). Effect of wavelength and beam width on penetration in light-tissue interaction using computational methods. *Lasers Med. Sci.* *32*, 1909–1918.
- Assarsson, E., Greenbaum, J.A., Sundström, M., Schaffer, L., Hammond, J.A., Pasquetto, V., Oseroff, C., Hendrickson, R.C., Lefkowitz, E.J., Tschärke, D.C., et al. (2008). Kinetic analysis of a complete poxvirus transcriptome reveals an immediate-early class of genes. *Proc. Natl. Acad. Sci. U. S. A.* *105*, 2140–2145.
- Baltimore, D. (1971). Expression of animal virus genomes. *Bacteriol. Rev.* *35*, 235–241.
- Bantscheff, M., Schirle, M., Sweetman, G., Rick, J., and Kuster, B. (2007). Quantitative mass spectrometry in proteomics: a critical review. *Anal. Bioanal. Chem.* *389*, 1017–1031.
- Bar, D.Z., Atkatsch, K., Tavares, U., Erdos, M.R., Gruenbaum, Y., and Collins, F.S. (2018). Biotinylation by antibody recognition—a method for proximity labeling. *Nat. Methods* *15*, 127.
- Barnard, A.L., Igakura, T., Tanaka, Y., Taylor, G.P., and Bangham, C.R.M. (2005). Engagement of specific T-cell surface molecules regulates cytoskeletal polarization in HTLV-1-infected lymphocytes. *Blood* *106*, 988–995.
- Barrass, S.V., and Butcher, S.J. (2020). Advances in high-throughput methods for the identification of virus receptors. *Med. Microbiol. Immunol.* *209*, 309–323.
- Bass, D.M., and Greenberg, H.B. (1992). Strategies for the identification of icosahedral virus receptors. *J. Clin. Invest.* *89*, 3–9.
- Bausch-Fluck, D., Hofmann, A., Bock, T., Frei, A.P., Cerciello, F., Jacobs, A., Moest, H., Omasits, U., Gundry, R.L., Yoon, C., et al. (2015). A mass spectrometric-derived cell surface protein atlas. *PLoS One* *10*, e0121314.

- Bausch-Fluck, D., Goldmann, U., Müller, S., van Oostrum, M., Müller, M., Schubert, O.T., and Wollscheid, B. (2018). The in silico human surfaceome. *Proc. Natl. Acad. Sci. U. S. A.* *115*, E10988–E10997.
- Bausch-Fluck, D., Milani, E.S., and Wollscheid, B. (2019). Surfaceome nanoscale organization and extracellular interaction networks. *Curr. Opin. Chem. Biol.* *48*, 26–33.
- Bayliss, R.J., and Piguet, V. (2018). Masters of manipulation: Viral modulation of the immunological synapse. *Cell. Microbiol.* *20*, e12944.
- Beck, S., and Barrell, B.G. (1988). Human cytomegalovirus encodes a glycoprotein homologous to MHC class-I antigens. *Nature* *331*, 269–272.
- Beerli, C., Yakimovich, A., Kilcher, S., Reynoso, G.V., Fläschner, G., Müller, D.J., Hickman, H.D., and Mercer, J. (2019). Vaccinia virus hijacks EGFR signalling to enhance virus spread through rapid and directed infected cell motility. *Nat Microbiol* *4*, 216–225.
- Berg, J.M., Tymoczko, J.L., and Stryer, L. (2002a). *Protein Structure and Function* (W H Freeman).
- Berg, J.M., Tymoczko, J.L., and Stryer, L. (2002b). *DNA, RNA, and the Flow of Genetic Information* (W H Freeman).
- Berg, J.M., Tymoczko, J.L., and Stryer, L. (2002c). *Amino Acids Are Encoded by Groups of Three Bases Starting from a Fixed Point* (W H Freeman).
- Berro, R., de la Fuente, C., Klase, Z., Kehn, K., Parvin, L., Pumfery, A., Agbottah, E., Vertes, A., Nekhai, S., and Kashanchi, F. (2007). Identifying the membrane proteome of HIV-1 latently infected cells. *J. Biol. Chem.* *282*, 8207–8218.
- Bidgood, S.R., and Mercer, J. (2015). Cloak and Dagger: Alternative Immune Evasion and Modulation Strategies of Poxviruses. *Viruses* *7*, 4800–4825.
- Bidgood, S.R., Novy, K., Collopy, A., Albrecht, D., Krause, M., Burden, J.J., Wollscheid, B., and Mercer, J. (2020). Poxviruses package viral redox proteins in lateral bodies and modulate the host oxidative response.
- Bjarnsholt, T., Whiteley, M., Rumbaugh, K.P., Stewart, P.S., Jensen, P.Ø., and Frimodt-Møller, N. (2021). The importance of understanding the infectious microenvironment. *Lancet Infect. Dis.*
- Blank, A., Markert, C., Hohmann, N., Carls, A., Mikus, G., Lehr, T., Alexandrov, A., Haag, M., Schwab, M., Urban, S., et al. (2016). First-in-human application of the novel hepatitis B and hepatitis D virus entry inhibitor myrcludex B. *Journal of Hepatology* *65*, 483–489.
- Bogomolov, P., Alexandrov, A., Voronkova, N., Macievich, M., Kokina, K., Petrachenkova, M., Lehr, T., Lempp, F.A., Wedemeyer, H., Haag, M., et al. (2016). Treatment of chronic hepatitis D with the entry inhibitor myrcludex B: First results of a phase Ib/IIa study. *J. Hepatol.* *65*, 490–498.

- Bonjardim, C.A. (2017). Viral exploitation of the MEK/ERK pathway - A tale of vaccinia virus and other viruses. *Virology* 507, 267–275.
- Boylston, A. (2012). The origins of inoculation. *J. R. Soc. Med.* 105, 309–313.
- Bozek, K., Eckhardt, M., Sierra, S., Anders, M., Kaiser, R., Kräusslich, H.-G., Müller, B., and Lengauer, T. (2012). An expanded model of HIV cell entry phenotype based on multi-parameter single-cell data. *Retrovirology* 9, 60.
- Breitbach, C.J., Burke, J., Jonker, D., Stephenson, J., Haas, A.R., Chow, L.Q.M., Nieva, J., Hwang, T.-H., Moon, A., Patt, R., et al. (2011). Intravenous delivery of a multi-mechanistic cancer-targeted oncolytic poxvirus in humans. *Nature* 477, 99–102.
- Brooks, C.R., Elliott, T., Parham, P., and Khakoo, S.I. (2006). The inhibitory receptor NKG2A determines lysis of vaccinia virus-infected autologous targets by NK cells. *J. Immunol.* 176, 1141–1147.
- Brown, K.A., Melby, J.A., Roberts, D.S., and Ge, Y. (2020). Top-down proteomics: challenges, innovations, and applications in basic and clinical research. *Expert Rev. Proteomics* 17, 719–733.
- Cairns, J. (1960). The initiation of vaccinia infection. *Virology* 11, 603–623.
- Carbonara, K., Andonovski, M., and Coorsen, J.R. (2021). Proteomes Are of Proteoforms: Embracing the Complexity. *Proteomes* 9.
- Casadevall, A., and Pirofski, L.A. (1999). Host-pathogen interactions: redefining the basic concepts of virulence and pathogenicity. *Infect. Immun.* 67, 3703–3713.
- Chen, C.-L., and Perrimon, N. (2017). Proximity-dependent labeling methods for proteomic profiling in living cells. *Wiley Interdiscip. Rev. Dev. Biol.* 6.
- Chen, W., Mou, K.Y., Solomon, P., Aggarwal, R., Leung, K.K., and Wells, J.A. (2021). Large remodeling of the Myc-induced cell surface proteome in B cells and prostate cells creates new opportunities for immunotherapy. *Proc. Natl. Acad. Sci. U. S. A.* 118.
- Chung, C.S., Hsiao, J.C., Chang, Y.S., and Chang, W. (1998). A27L protein mediates vaccinia virus interaction with cell surface heparan sulfate. *J. Virol.* 72, 1577–1585.
- Chung, C.-S., Chen, C.-H., Ho, M.-Y., Huang, C.-Y., Liao, C.-L., and Chang, W. (2006). Vaccinia virus proteome: identification of proteins in vaccinia virus intracellular mature virion particles. *J. Virol.* 80, 2127–2140.
- Colucci, F., Di Santo, J.P., and Leibson, P.J. (2002). Natural killer cell activation in mice and men: different triggers for similar weapons? *Nat. Immunol.* 3, 807–813.
- Condit, R.C., Moussatche, N., and Traktman, P. (2006). In A Nutshell: Structure and Assembly of the Vaccinia Virion. In *Advances in Virus Research*, (Academic Press), pp. 31–124.

- Cosman, D., Fanger, N., Borges, L., Kubin, M., Chin, W., Peterson, L., and Hsu, M.L. (1997). A novel immunoglobulin superfamily receptor for cellular and viral MHC class I molecules. *Immunity* *7*, 273–282.
- Croft, N.P., de Verteuil, D.A., Smith, S.A., Wong, Y.C., Schittenhelm, R.B., Tschärke, D.C., and Purcell, A.W. (2015). Simultaneous Quantification of Viral Antigen Expression Kinetics Using Data-Independent (DIA) Mass Spectrometry. *Mol. Cell. Proteomics* *14*, 1361–1372.
- Curtis, B.M., Scharnrowske, S., and Watson, A.J. (1992). Sequence and expression of a membrane-associated C-type lectin that exhibits CD4-independent binding of human immunodeficiency virus envelope glycoprotein gp120. *Proceedings of the National Academy of Sciences* *89*, 8356–8360.
- Cyrklaff, M., Risco, C., Fernández, J.J., Jiménez, M.V., Estéban, M., Baumeister, W., and Carrascosa, J.L. (2005). Cryo-electron tomography of vaccinia virus. *Proc. Natl. Acad. Sci. U. S. A.* *102*, 2772–2777.
- Dai, A., Cao, S., Dhungel, P., Luan, Y., Liu, Y., Xie, Z., and Yang, Z. (2017). Ribosome Profiling Reveals Translational Upregulation of Cellular Oxidative Phosphorylation mRNAs during Vaccinia Virus-Induced Host Shutoff. *J. Virol.* *91*.
- Dehaven, B.C., Gupta, K., and Isaacs, S.N. (2011). The vaccinia virus A56 protein: a multifunctional transmembrane glycoprotein that anchors two secreted viral proteins. *J. Gen. Virol.* *92*, 1971–1980.
- Dhungel, P., Cantu, F.M., Molina, J.A., and Yang, Z. (2020). Vaccinia Virus as a Master of Host Shutoff Induction: Targeting Processes of the Central Dogma and Beyond. *Pathogens* *9*.
- Di Giulio, D.B., and Eckburg, P.B. (2004). Human monkeypox: an emerging zoonosis. *Lancet Infect. Dis.* *4*, 15–25.
- Dobson, B.M., Procter, D.J., Hollett, N.A., Flesch, I.E.A., Newsome, T.P., and Tschärke, D.C. (2014). Vaccinia virus F5 is required for normal plaque morphology in multiple cell lines but not replication in culture or virulence in mice. *Virology* *456-457*, 145–156.
- Doceul, V., Hollinshead, M., van der Linden, L., and Smith, G.L. (2010). Repulsion of superinfecting virions: a mechanism for rapid virus spread. *Science* *327*, 873–876.
- Doll, S., Gnad, F., and Mann, M. (2019). The Case for Proteomics and Phospho-Proteomics in Personalized Cancer Medicine. *Proteomics Clin. Appl.* *13*, e1800113.
- Doms, R.W., and Trono, D. (2000). The plasma membrane as a combat zone in the HIV battlefield. *Genes Dev.* *14*, 2677–2688.
- Donkers, J.M., Zehnder, B., van Westen, G.J.P., Kwakkenbos, M.J., IJzerman, A.P., Oude Elferink, R.P.J., Beuers, U., Urban, S., and van de Graaf, S.F.J. (2017). Reduced hepatitis B and D viral entry using clinically applied drugs as novel inhibitors of the bile acid transporter NTCP. *Sci. Rep.* *7*, 15307.

- Dorr, P., Westby, M., Dobbs, S., and Griffin, P. (2005). Maraviroc (UK-427,857), a potent, orally bioavailable, and selective small-molecule inhibitor of chemokine receptor CCR5 with broad-spectrum anti-human *Antimicrob. Agents Chemother.*
- Duggan, A.T., Perdomo, M.F., Piombino-Mascali, D., Marciniak, S., Poinar, D., Emery, M.V., Buchmann, J.P., Duchêne, S., Jankauskas, R., Humphreys, M., et al. (2016). 17th Century Variola Virus Reveals the Recent History of Smallpox. *Curr. Biol.* *26*, 3407–3412.
- Durbin, K.R., Fornelli, L., Fellers, R.T., Doubleday, P.F., Narita, M., and Kelleher, N.L. (2016). Quantitation and Identification of Thousands of Human Proteoforms below 30 kDa. *J. Proteome Res.* *15*, 976–982.
- Durr, E., Yu, J., Krasinska, K.M., Carver, L.A., Yates, J.R., Testa, J.E., Oh, P., and Schnitzer, J.E. (2004). Direct proteomic mapping of the lung microvascular endothelial cell surface in vivo and in cell culture. *Nat. Biotechnol.* *22*, 985–992.
- Elia, G. (2008). Biotinylation reagents for the study of cell surface proteins. *Proteomics* *8*, 4012–4024.
- Ellner, P.D. (1998). Smallpox: gone but not forgotten. *Infection* *26*, 263–269.
- Elschenbroich, S., Kim, Y., Medin, J.A., and Kislinger, T. (2010). Isolation of cell surface proteins for mass spectrometry-based proteomics. *Expert Rev. Proteomics* *7*, 141–154.
- Ember, S.W.J., Ren, H., Ferguson, B.J., and Smith, G.L. (2012). Vaccinia virus protein C4 inhibits NF- κ B activation and promotes virus virulence. *J. Gen. Virol.* *93*, 2098–2108.
- Engelmayer, J., Larsson, M., Subklewe, M., Chahroudi, A., Cox, W.I., Steinman, R.M., and Bhardwaj, N. (1999). Vaccinia Virus Inhibits the Maturation of Human Dendritic Cells: A Novel Mechanism of Immune Evasion. *J. Immunol.* *163*, 6762–6768.
- Erlendsson, S., and Teilum, K. (2020). Binding Revisited-Avidity in Cellular Function and Signaling. *Front Mol Biosci* *7*, 615565.
- Ersing, I., Nobre, L., Wang, L.W., Soday, L., Ma, Y., Paulo, J.A., Narita, Y., Ashbaugh, C.W., Jiang, C., Grayson, N.E., et al. (2017). A Temporal Proteomic Map of Epstein-Barr Virus Lytic Replication in B Cells. *Cell Rep.* *19*, 1479–1493.
- Esparza, J., Schrick, L., Damaso, C.R., and Nitsche, A. (2017). Equination (inoculation of horsepox): An early alternative to vaccination (inoculation of cowpox) and the potential role of horsepox virus in the origin of the smallpox vaccine. *Vaccine* *35*, 7222–7230.
- Fang, L., Cheng, J.-C., Chang, H.-M., Sun, Y.-P., and Leung, P.C.K. (2013). EGF-like growth factors induce COX-2-derived PGE2 production through ERK1/2 in human granulosa cells. *J. Clin. Endocrinol. Metab.* *98*, 4932–4941.
- Fenner, F., Henderson, D.A., Arita, I., Jezek, Z., Ladnyi, I.D., and World Health Organization (1988). *Smallpox and its eradication* / F. Fenner ... [et al.] (World Health Organization).

- Fleming, A. (1929). On the Antibacterial Action of Cultures of a Penicillium, with Special Reference to their Use in the Isolation of B. influenzae. *Br. J. Exp. Pathol.* *10*, 226.
- Forsyth, K.S., and Eisenlohr, L.C. (2016). Giving CD4+ T cells the slip: viral interference with MHC class II-restricted antigen processing and presentation. *Curr. Opin. Immunol.* *40*, 123–129.
- Frei, A.P., Jeon, O.-Y., Kilcher, S., Moest, H., Henning, L.M., Jost, C., Plückthun, A., Mercer, J., Aebersold, R., Carreira, E.M., et al. (2012). Direct identification of ligand-receptor interactions on living cells and tissues. *Nat. Biotechnol.* *30*, 997–1001.
- Galaway, F., and Wright, G.J. (2020). Rapid and sensitive large-scale screening of low affinity extracellular receptor protein interactions by using reaction induced inhibition of *Gussia luciferase*. *Sci. Rep.* *10*, 10522.
- Gaynes, R.P. (2020). *Germ theory: Medical pioneers in infectious diseases* (ASM Press).
- Geijtenbeek, T.B.H., Kwon, D.S., Torensma, R., van Vliet, S.J., van Duijnhoven, G.C.F., Middel, J., Cornelissen, I.L.M.H.A., Nottet, H.S.L.M., KewalRamani, V.N., Littman, D.R., et al. (2000). DC-SIGN, a Dendritic Cell-Specific HIV-1-Binding Protein that Enhances trans-Infection of T Cells. *Cell* *100*, 587–597.
- Geri, J.B., Oakley, J.V., Reyes-Robles, T., Wang, T., McCarver, S.J., White, C.H., Rodriguez-Rivera, F.P., Parker, D.L., Jr, Hett, E.C., Fadeyi, O.O., et al. (2020). Microenvironment mapping via Dexter energy transfer on immune cells. *Science* *367*, 1091–1097.
- Gisa Gerold, *Proteomics Approaches to Unravel Virus - Vertebrate Host Interactions* (Elsevier).
- Gerold, G., Bruening, J., and Pietschmann, T. (2016). Decoding protein networks during virus entry by quantitative proteomics. *Virus Res.* *218*, 25–39.
- Gilchuk, I., Gilchuk, P., Sapparapu, G., Lampley, R., Singh, V., Kose, N., Blum, D.L., Hughes, L.J., Satheshkumar, P.S., Townsend, M.B., et al. (2016). Cross-Neutralizing and Protective Human Antibody Specificities to Poxvirus Infections. *Cell* *167*, 684–694.e9.
- Glatter, T., Wepf, A., Aebersold, R., and Gstaiger, M. (2009). An integrated workflow for charting the human interaction proteome: insights into the PP2A system. *Mol. Syst. Biol.* *5*, 237.
- Gordon, D.E., Hiatt, J., Bouhaddou, M., Rezelj, V.V., Ulferts, S., Braberg, H., Jureka, A.S., Obernier, K., Guo, J.Z., Batra, J., et al. (2020). Comparative host-coronavirus protein interaction networks reveal pan-viral disease mechanisms. *Science* *370*.
- Granados, A.A., Pietsch, J.M.J., Cepeda-Humerez, S.A., Farquhar, I.L., Tkačik, G., and Swain, P.S. (2018). Distributed and dynamic intracellular organization of extracellular information. *Proc. Natl. Acad. Sci. U. S. A.* *115*, 6088–6093.

- Gray, R.D.M., Beerli, C., Pereira, P.M., Scherer, K.M., Samolej, J., Bleck, C.K.E., Mercer, J., and Henriques, R. (2016). VirusMapper: open-source nanoscale mapping of viral architecture through super-resolution microscopy. *Sci. Rep.* *6*, 29132.
- Gray, R.D.M., Albrecht, D., Beerli, C., Huttunen, M., Cohen, G.H., White, I.J., Burden, J.J., Henriques, R., and Mercer, J. (2019). Nanoscale polarization of the entry fusion complex of vaccinia virus drives efficient fusion. *Nat Microbiol* *4*, 1636–1644.
- Greco, T.M., and Cristea, I.M. (2017). Proteomics Tracing the Footsteps of Infectious Disease. *Mol. Cell. Proteomics* *16*, S5–S14.
- Greve, J.M., Davis, G., Meyer, A.M., Forte, C.P., Yost, S.C., Marlor, C.W., Kamarck, M.E., and McClelland, A. (1989). The major human rhinovirus receptor is ICAM-1. *Cell* *56*, 839–847.
- Grosche, L., Knippertz, I., König, C., Royzman, D., Wild, A.B., Zinser, E., Sticht, H., Muller, Y.A., Steinkasserer, A., and Lechmann, M. (2020). The CD83 Molecule - An Important Immune Checkpoint. *Front. Immunol.* *11*, 721.
- Gudleski-O'Regan, N., Greco, T.M., Cristea, I.M., and Shenk, T. (2012). Increased expression of LDL receptor-related protein 1 during human cytomegalovirus infection reduces virion cholesterol and infectivity. *Cell Host Microbe* *12*, 86–96.
- Haga, I.R., and Bowie, A.G. (2005). Evasion of innate immunity by vaccinia virus. *Parasitology* *130 Suppl*, S11–S25.
- Hassan, Z., Kumar, N.D., Reggiori, F., and Khan, G. (2021). How Viruses Hijack and Modify the Secretory Transport Pathway. *Cells* *10*.
- Heo, J., Reid, T., Ruo, L., Breitbach, C.J., Rose, S., Bloomston, M., Cho, M., Lim, H.Y., Chung, H.C., Kim, C.W., et al. (2013). Randomized dose-finding clinical trial of oncolytic immunotherapeutic vaccinia JX-594 in liver cancer. *Nat. Med.* *19*, 329–336.
- Hoffmann, M., Kleine-Weber, H., Schroeder, S., Krüger, N., Herrler, T., Erichsen, S., Schiergens, T.S., Herrler, G., Wu, N.-H., Nitsche, A., et al. (2020). SARS-CoV-2 Cell Entry Depends on ACE2 and TMPRSS2 and Is Blocked by a Clinically Proven Protease Inhibitor. *Cell* *181*, 271–280.e8.
- Holmes, V.M., Maluquer de Motes, C., Richards, P.T., Roldan, J., Bhargava, A.K., Orange, J.S., and Krummenacher, C. (2019). Interaction between nectin-1 and the human natural killer cell receptor CD96. *PLoS One* *14*, e0212443.
- Homann, S., Smith, D., Little, S., Richman, D., and Guatelli, J. (2011). Upregulation of BST-2/Tetherin by HIV infection in vivo. *J. Virol.* *85*, 10659–10668.
- Hopkins, D. (2002). *The greatest killer: Smallpox in history* (Chicago, IL: University of Chicago Press).
- Hosur, V., Farley, M.L., Burzenski, L.M., Shultz, L.D., and Wiles, M.V. (2018). ADAM17 is essential for ectodomain shedding of the EGF-receptor ligand amphiregulin. *FEBS Open Bio* *8*, 702–710.

- Hsiao, J.C., Chung, C.S., and Chang, W. (1999). Vaccinia virus envelope D8L protein binds to cell surface chondroitin sulfate and mediates the adsorption of intracellular mature virions to cells. *J. Virol.* *73*, 8750–8761.
- Hsu, J.L. (2013). A brief history of vaccines: smallpox to the present. *S. D. Med. Spec no*, 33–37.
- Hsu, J.-L., van den Boomen, D.J.H., Tomasec, P., Weekes, M.P., Antrobus, R., Stanton, R.J., Ruckova, E., Sugrue, D., Wilkie, G.S., Davison, A.J., et al. (2015). Plasma membrane profiling defines an expanded class of cell surface proteins selectively targeted for degradation by HCMV US2 in cooperation with UL141. *PLoS Pathog.* *11*, e1004811.
- Husain, B., Ramani, S.R., Chiang, E., Lehoux, I., Paduchuri, S., Arena, T.A., Patel, A., Wilson, B., Chan, P., Franke, Y., et al. (2019). A Platform for Extracellular Interactome Discovery Identifies Novel Functional Binding Partners for the Immune Receptors B7-H3/CD276 and PVR/CD155. *Mol. Cell. Proteomics* *18*, 2310–2323.
- Hutchings, M.I., Truman, A.W., and Wilkinson, B. (2019). Antibiotics: past, present and future. *Curr. Opin. Microbiol.* *51*, 72–80.
- Huttunen, M., Samolej, J., Evans, R.J., Yakimovich, A., White, I.J., Kriston-Vizi, J., Martin-Serrano, J., Sundquist, W.I., Frickel, E.-M., and Mercer, J. (2021). Vaccinia virus hijacks ESCRT-mediated multivesicular body formation for virus egress. *Life Sci Alliance* *4*.
- Igakura, T., Stinchcombe, J.C., Goon, P.K.C., Taylor, G.P., Weber, J.N., Griffiths, G.M., Tanaka, Y., Osame, M., and Bangham, C.R.M. (2003). Spread of HTLV-I between lymphocytes by virus-induced polarization of the cytoskeleton. *Science* *299*, 1713–1716.
- International Human Genome Sequencing Consortium (2004). Finishing the euchromatic sequence of the human genome. *Nature* *431*, 931–945.
- Jacobs, B.L., Langland, J.O., Kibler, K.V., Denzler, K.L., White, S.D., Holechek, S.A., Wong, S., Huynh, T., and Baskin, C.R. (2009). Vaccinia virus vaccines: past, present and future. *Antiviral Res.* *84*, 1–13.
- Jacobson, K., Liu, P., and Lagerholm, B.C. (2019). The Lateral Organization and Mobility of Plasma Membrane Components. *Cell* *177*, 806–819.
- Janeway, C.A., Jr, Travers, P., Walport, M., and Shlomchik, M.J. (2001). *Infectious agents and how they cause disease* (Garland Science).
- Jarahian, M., Fiedler, M., Cohnen, A., Djandji, D., Hämmerling, G.J., Gati, C., Cerwenka, A., Turner, P.C., Moyer, R.W., Watzl, C., et al. (2011). Modulation of NKp30- and NKp46-mediated natural killer cell responses by poxviral hemagglutinin. *PLoS Pathog.* *7*, e1002195.
- Jean Beltran, P.M., Mathias, R.A., and Cristea, I.M. (2016). A Portrait of the Human Organelle Proteome In Space and Time during Cytomegalovirus Infection. *Cell Syst* *3*, 361–373.e6.

- Jenner, E. (1798). An inquiry into the causes and effects of the variolae vaccinae: a disease discovered in some of the western counties of England, particularly Gloucestershire, and known by the name of the cow pox (Springfield).
- Jiang, S., Kotani, N., Ohnishi, T., Miyagawa-Yamaguchi, A., Tsuda, M., Yamashita, R., Ishiura, Y., and Honke, K. (2012). A proteomics approach to the cell-surface interactome using the enzyme-mediated activation of radical sources reaction. *Proteomics* *12*, 54–62.
- Jolly, C., Mitar, I., and Sattentau, Q.J. (2007). Requirement for an intact T-cell actin and tubulin cytoskeleton for efficient assembly and spread of human immunodeficiency virus type 1. *J. Virol.* *81*, 5547–5560.
- Jolly, C., Welsch, S., Michor, S., and Sattentau, Q.J. (2011). The regulated secretory pathway in CD4(+) T cells contributes to human immunodeficiency virus type-1 cell-to-cell spread at the virological synapse. *PLoS Pathog.* *7*, e1002226.
- Jouvenet, N., Neil, S.J.D., Zhadina, M., Zang, T., Kratovac, Z., Lee, Y., McNatt, M., Hatzioannou, T., and Bieniasz, P.D. (2009). Broad-spectrum inhibition of retroviral and filoviral particle release by tetherin. *J. Virol.* *83*, 1837–1844.
- Kalxdorf, M., Gade, S., Eberl, H.C., and Bantscheff, M. (2017). Monitoring Cell-surface N-Glycoproteome Dynamics by Quantitative Proteomics Reveals Mechanistic Insights into Macrophage Differentiation. *Mol. Cell. Proteomics* *16*, 770–785.
- Karhemo, P.-R., Ravela, S., Laakso, M., Ritamo, I., Tatti, O., Mäkinen, S., Goodison, S., Stenman, U.-H., Hölttä, E., Hautaniemi, S., et al. (2012). An optimized isolation of biotinylated cell surface proteins reveals novel players in cancer metastasis. *J. Proteomics* *77*, 87–100.
- Karin, M., Liu, Z. g., and Zandi, E. (1997). AP-1 function and regulation. *Curr. Opin. Cell Biol.* *9*, 240–246.
- King, A.M.Q., Adams, E.B., Carstens, E.B, Lefkowitz, E.G. Family - Poxviridae. In *Virus Taxonomy* (San Diego: Elsevier), pp. 291–309. (2012)
- Kärre, K., Ljunggren, H.G., Piontek, G., and Kiessling, R. (1986). Selective rejection of H-2-deficient lymphoma variants suggests alternative immune defence strategy. *Nature* *319*, 675–678.
- Kelly, R.T. (2020). Single-cell Proteomics: Progress and Prospects. *Mol. Cell. Proteomics* *19*, 1739–1748.
- Kelstrup, C.D., Bekker-Jensen, D.B., Arrey, T.N., Högbe, A., Harder, A., and Olsen, J.V. (2018). Performance Evaluation of the Q Exactive HF-X for Shotgun Proteomics. *J. Proteome Res.* *17*, 727–738.
- Kennedy, S.P., Hastings, J.F., Han, J.Z.R., and Croucher, D.R. (2016). The Under-Appreciated Promiscuity of the Epidermal Growth Factor Receptor Family. *Front Cell Dev Biol* *4*, 88.
- Kleinpeter, P., Remy-Ziller, C., Winter, E., Gantzer, M., Nourtier, V., Kempf, J., Hortelano, J., Schmitt, D., Schultz, H., Geist, M., et al. (2019). By Binding CD80 and

CD86, the Vaccinia Virus M2 Protein Blocks Their Interactions with both CD28 and CTLA4 and Potentiates CD80 Binding to PD-L1. *J. Virol.* *93*.

Koutsakos, M., McWilliam, H.E.G., Aktepe, T.E., Fritzlar, S., Illing, P.T., Mifsud, N.A., Purcell, A.W., Rockman, S., Reading, P.C., Vivian, J.P., et al. (2019). Downregulation of MHC Class I Expression by Influenza A and B Viruses. *Front. Immunol.* *10*, 1158.

Krause, M., Leslie, J.D., Stewart, M., Lafuente, E.M., Valderrama, F., Jagannathan, R., Strasser, G.A., Rubinson, D.A., Liu, H., Way, M., et al. (2004). Lamellipodin, an Ena/VASP ligand, is implicated in the regulation of lamellipodial dynamics. *Dev. Cell* *7*, 571–583.

Kuhlmann, L., Cummins, E., Samudio, I., and Kislinger, T. (2018). Cell-surface proteomics for the identification of novel therapeutic targets in cancer. *Expert Rev. Proteomics* *15*, 259–275.

Labrijn, A.F., Janmaat, M.L., Reichert, J.M., and Parren, P.W.H.I. (2019). Bispecific antibodies: a mechanistic review of the pipeline. *Nat. Rev. Drug Discov.* *18*, 585–608.

Lander, E.S., Linton, L.M., Birren, B., Nusbaum, C., Zody, M.C., Baldwin, J., Devon, K., Dewar, K., Doyle, M., FitzHugh, W., et al. (2001). Initial sequencing and analysis of the human genome. *Nature* *409*, 860–921.

Landi, A., Iannucci, V., Van Nuffel, A., Meuwissen, P., and Verhasselt, B. (2011). One protein to rule them all: modulation of cell surface receptors and molecules by HIV Nef. *Curr. HIV Res.* *9*, 496–504.

Leite, F.G.G., Torres, A.A., De Oliveira, L.C., Da Cruz, A.F.P., Soares-Martins, J.A.P., Pereira, A.C.T.C., Trindade, G.S., Abrahão, J.S., Kroon, E.G., Ferreira, P.C.P., et al. (2017). c-Jun integrates signals from both MEK/ERK and MKK/JNK pathways upon vaccinia virus infection. *Arch. Virol.* *162*, 2971–2981.

Leong, C.C., Chapman, T.L., Bjorkman, P.J., Formankova, D., Mocarski, E.S., Phillips, J.H., and Lanier, L.L. (1998). Modulation of natural killer cell cytotoxicity in human cytomegalovirus infection: the role of endogenous class I major histocompatibility complex and a viral class I homolog. *J. Exp. Med.* *187*, 1681–1687.

Li, J., Han, S., Li, H., Udeshi, N.D., Svinkina, T., Mani, D.R., Xu, C., Guajardo, R., Xie, Q., Li, T., et al. (2020a). Cell-Surface Proteomic Profiling in the Fly Brain Uncovers Wiring Regulators. *Cell* *180*, 373–386.e15.

Li, W., Moore, M.J., Vasilieva, N., Sui, J., Wong, S.K., Berne, M.A., Somasundaran, M., Sullivan, J.L., Luzuriaga, K., Greenough, T.C., et al. (2003). Angiotensin-converting enzyme 2 is a functional receptor for the SARS coronavirus. *Nature* *426*, 450–454.

Li, Y., Carroll, D.S., Gardner, S.N., Walsh, M.C., Vitalis, E.A., and Damon, I.K. (2007). On the origin of smallpox: correlating variola phylogenies with historical smallpox records. *Proc. Natl. Acad. Sci. U. S. A.* *104*, 15787–15792.

Li, Y., Qin, H., and Ye, M. (2020b). An overview on enrichment methods for cell surface proteome profiling. *J. Sep. Sci.* *43*, 292–312.

- Liu, L., Xu, Z., Fuhlbrigge, R.C., Peña-Cruz, V., Lieberman, J., and Kupper, T.S. (2005). Vaccinia virus induces strong immunoregulatory cytokine production in healthy human epidermal keratinocytes: a novel strategy for immune evasion. *J. Virol.* *79*, 7363–7370.
- Liu, L., Cooper, T., Howley, P.M., and Hayball, J.D. (2014). From crescent to mature virion: vaccinia virus assembly and maturation. *Viruses* *6*, 3787–3808.
- Liu, Q., Zheng, J., Sun, W., Huo, Y., Zhang, L., Hao, P., Wang, H., and Zhuang, M. (2018). A proximity-tagging system to identify membrane protein-protein interactions. *Nat. Methods* *15*, 715–722.
- Liu, X., Salokas, K., Weldatsadik, R.G., Gawriyski, L., and Varjosalo, M. (2020). Combined proximity labeling and affinity purification-mass spectrometry workflow for mapping and visualizing protein interaction networks. *Nat. Protoc.* *15*, 3182–3211.
- Liu, Y., Beyer, A., and Aebersold, R. (2016). On the Dependency of Cellular Protein Levels on mRNA Abundance. *Cell* *165*, 535–550.
- Lopez-Botet, M., Llano, M., and Ortega, M. (2001). Human cytomegalovirus and natural killer-mediated surveillance of HLA class I expression: a paradigm of host-pathogen adaptation. *Immunological Reviews* *181*, 193–202.
- Ludwig, C., Gillet, L., Rosenberger, G., Amon, S., Collins, B.C., and Aebersold, R. (2018). Data-independent acquisition-based SWATH-MS for quantitative proteomics: a tutorial. *Mol. Syst. Biol.* *14*, e8126.
- Lund, R., Leth-Larsen, R., Jensen, O.N., and Ditzel, H.J. (2009). Efficient isolation and quantitative proteomic analysis of cancer cell plasma membrane proteins for identification of metastasis-associated cell surface markers. *J. Proteome Res.* *8*, 3078–3090.
- MacArthur, R.D., and Novak, R.M. (2008). Reviews of anti-infective agents: maraviroc: the first of a new class of antiretroviral agents. *Clin. Infect. Dis.* *47*, 236–241.
- Mackett, M., Smith, G.L., and Moss, B. (1982). Vaccinia virus: a selectable eukaryotic cloning and expression vector. *Proc. Natl. Acad. Sci. U. S. A.* *79*, 7415–7419.
- Maity, P.C., Yang, J., Klaesener, K., and Reth, M. (2015). The nanoscale organization of the B lymphocyte membrane. *Biochim. Biophys. Acta* *1853*, 830–840.
- Mansouri, M., Viswanathan, K., Douglas, J.L., Hines, J., Gustin, J., Moses, A.V., and Früh, K. (2009). Molecular mechanism of BST2/tetherin downregulation by K5/MIR2 of Kaposi's sarcoma-associated herpesvirus. *J. Virol.* *83*, 9672–9681.
- Martell, J.D., Yamagata, M., Deerinck, T.J., Phan, S., Kwa, C.G., Ellisman, M.H., Sanes, J.R., and Ting, A.Y. (2016). A split horseradish peroxidase for the detection of intercellular protein–protein interactions and sensitive visualization of synapses. *Nat. Biotechnol.* *34*, 774–780.
- Martinez-Martin, N. (2017). Technologies for Proteome-Wide Discovery of Extracellular Host-Pathogen Interactions. *J Immunol Res* *2017*, 2197615.

- Martinez-Martin, N., Ramani, S.R., Hackney, J.A., Tom, I., Wranik, B.J., Chan, M., Wu, J., Paluch, M.T., Takeda, K., Hass, P.E., et al. (2016). The extracellular interactome of the human adenovirus family reveals diverse strategies for immunomodulation. *Nat. Commun.* *7*, 11473.
- Matheson, N.J., Sumner, J., Wals, K., Rapiteanu, R., Weekes, M.P., Vigan, R., Weinelt, J., Schindler, M., Antrobus, R., Costa, A.S.H., et al. (2015). Cell Surface Proteomic Map of HIV Infection Reveals Antagonism of Amino Acid Metabolism by Vpu and Nef. *Cell Host Microbe* *18*, 409–423.
- Mattila, P.K., Batista, F.D., and Treanor, B. (2016). Dynamics of the actin cytoskeleton mediates receptor cross talk: An emerging concept in tuning receptor signaling. *J. Cell Biol.* *212*, 267–280.
- Maverakis, E., Kim, K., Shimoda, M., Gershwin, M.E., Patel, F., Wilken, R., Raychaudhuri, S., Ruhaak, L.R., and Lebrilla, C.B. (2015). Glycans in the immune system and The Altered Glycan Theory of Autoimmunity: a critical review. *J. Autoimmun.* *57*, 1–13.
- McFadden, G. (2005). Poxvirus tropism. *Nat. Rev. Microbiol.* *3*, 201–213.
- Meier, F., Brunner, A.-D., Frank, M., Ha, A., Bludau, I., Voytik, E., Kaspar-Schoenefeld, S., Lubeck, M., Raether, O., Bache, N., et al. (2020). diaPASEF: parallel accumulation-serial fragmentation combined with data-independent acquisition. *Nat. Methods* *17*, 1229–1236.
- Melnick, M., Abichaker, G., Htet, K., Sedghizadeh, P., and Jaskoll, T. (2011). Small molecule inhibitors of the host cell COX/AREG/EGFR/ERK pathway attenuate cytomegalovirus-induced pathogenesis. *Exp. Mol. Pathol.* *91*, 400–410.
- Mercer, J., and Helenius, A. (2008). Vaccinia virus uses macropinocytosis and apoptotic mimicry to enter host cells. *Science* *320*, 531–535.
- Mercer, J., and Traktman, P. (2003). Investigation of structural and functional motifs within the vaccinia virus A14 phosphoprotein, an essential component of the virion membrane. *J. Virol.* *77*, 8857–8871.
- Mercer, J., Snijder, B., Sacher, R., Burkard, C., Bleck, C.K.E., Stahlberg, H., Pelkmans, L., and Helenius, A. (2012). RNAi screening reveals proteasome- and Cullin3-dependent stages in vaccinia virus infection. *Cell Rep.* *2*, 1036–1047.
- Meseda, C.A., Kuhn, J., Atukorale, V., Campbell, J., and Weir, J.P. (2014). Glycosylated and nonglycosylated complement control protein of the lister strain of vaccinia virus. *Clin. Vaccine Immunol.* *21*, 1330–1338.
- Mocarski, E.S., Jr, Shenk, T., Griffiths, P.D., and Pass, R.F. (2013). Cytomegaloviruses. 1960–2014.
- Morens, D.M., and Fauci, A.S. (2020). Emerging Pandemic Diseases: How We Got to COVID-19. *Cell*.

- Morens, D.M., Folkers, G.K., and Fauci, A.S. (2004). The challenge of emerging and re-emerging infectious diseases. *Nature* *430*, 242–249.
- Morens, D.M., Folkers, G.K., and Fauci, A.S. (2008). Emerging infections: a perpetual challenge. *Lancet Infect. Dis.* *8*, 710–719.
- Morgis, R.A., Haan, K., Schrey, J.M., Zimmerman, R.M., and Hersperger, A.R. (2021). The epidermal growth factor ortholog of ectromelia virus activates EGFR/ErbB1 and demonstrates mitogenic function in vitro. *Virology* *564*, 1–12.
- Morizono, K., Xie, Y., Olafsen, T., Lee, B., Dasgupta, A., Wu, A.M., and Chen, I.S.Y. (2011). The soluble serum protein Gas6 bridges virion envelope phosphatidylserine to the TAM receptor tyrosine kinase Axl to mediate viral entry. *Cell Host Microbe* *9*, 286–298.
- Moss, B. (2004). Foreword to *Vaccinia Virus and Poxvirology* (Humana Press Inc.).
- Moss, B. (2006). Poxvirus entry and membrane fusion. *Virology* *344*, 48–54.
- Müller, M., Gräbnitz, F., Barandun, N., Shen, Y., Vetterli, S.U., Mondal, M., Prudent, J.R., Severin, Y., van Oostrum, M., Hofmann, R., et al. (2020). Light-mediated discovery of surfaceome nanoscale organization and intercellular receptor interaction networks.
- Muntel, J., Gandhi, T., Verbeke, L., Bernhardt, O.M., Treiber, T., Bruderer, R., and Reiter, L. (2019). Surpassing 10 000 identified and quantified proteins in a single run by optimizing current LC-MS instrumentation and data analysis strategy. *Mol Omics* *15*, 348–360.
- Neil, S.J.D., Zang, T., and Bieniasz, P.D. (2008). Tetherin inhibits retrovirus release and is antagonized by HIV-1 Vpu. *Nature* *451*, 425–430.
- Nejmeddine, M., and Bangham, C.R.M. (2010). The HTLV-1 Virological Synapse. *Viruses* *2*, 1427–1447.
- Nejmeddine, M., Barnard, A.L., Tanaka, Y., Taylor, G.P., and Bangham, C.R.M. (2005). Human T-lymphotropic virus, type 1, tax protein triggers microtubule reorientation in the virological synapse. *J. Biol. Chem.* *280*, 29653–29660.
- Nesvizhskii, A.I., and Aebersold, R. (2005). Interpretation of shotgun proteomic data: the protein inference problem. *Mol. Cell. Proteomics* *4*, 1419–1440.
- Nilsen, T.W., and Graveley, B.R. (2010). Expansion of the eukaryotic proteome by alternative splicing. *Nature* *463*, 457–463.
- Njeumi, F., Taylor, W., Diallo, A., Miyagishima, K., Pastoret, P.-P., Vallat, B., and Traore, M. (2012). The long journey: a brief review of the eradication of rinderpest. *Rev. Sci. Tech.* *31*, 729–746.
- Novy, K., Kilcher, S., Omasits, U., Bleck, C.K.E., Beerli, C., Vowinckel, J., Martin, C.K., Syedbasha, M., Maiolica, A., White, I., et al. (2018). Proteotype profiling unmasks a viral signalling network essential for poxvirus assembly and transcriptional competence. *Nat Microbiol* *3*, 588–599.

- Nusinow, D.P., Szpyt, J., Ghandi, M., Rose, C.M., McDonald, E.R., 3rd, Kalocsay, M., Jané-Valbuena, J., Gelfand, E., Schweppe, D.K., Jedrychowski, M., et al. (2020). Quantitative Proteomics of the Cancer Cell Line Encyclopedia. *Cell* *180*, 387–402.e16.
- Olaya-Abril, A., Jiménez-Munguía, I., Gómez-Gascón, L., and Rodríguez-Ortega, M.J. (2014). Surfomics: shaving live organisms for a fast proteomic identification of surface proteins. *J. Proteomics* *97*, 164–176.
- van Oostrum, M., Müller, M., Klein, F., Bruderer, R., Zhang, H., Pedrioli, P.G.A., Reiter, L., Tsapogas, P., Rolink, A., and Wollscheid, B. (2019). Classification of mouse B cell types using surfaceome proteotype maps. *Nat. Commun.* *10*, 5734.
- van Oostrum, M., Campbell, B., Seng, C., Müller, M., Tom Dieck, S., Hammer, J., Pedrioli, P.G.A., Földy, C., Tyagarajan, S.K., and Wollscheid, B. (2020). Surfaceome dynamics reveal proteostasis-independent reorganization of neuronal surface proteins during development and synaptic plasticity. *Nat. Commun.* *11*, 4990.
- Orange, J.S., Fasset, M.S., Koopman, L.A., Boyson, J.E., and Strominger, J.L. (2002). Viral evasion of natural killer cells. *Nat. Immunol.* *3*, 1006–1012.
- Ou, X., Liu, Y., Lei, X., Li, P., Mi, D., Ren, L., Guo, L., Guo, R., Chen, T., Hu, J., et al. (2020). Characterization of spike glycoprotein of SARS-CoV-2 on virus entry and its immune cross-reactivity with SARS-CoV. *Nat. Commun.* *11*, 1620.
- Overington, J.P., Al-Lazikani, B., and Hopkins, A.L. (2006). How many drug targets are there? *Nat. Rev. Drug Discov.* *5*, 993–996.
- Palacios, S., Perez, L.H., Welsch, S., Schleich, S., Chmielarska, K., Melchior, F., and Locker, J.K. (2005). Quantitative SUMO-1 modification of a vaccinia virus protein is required for its specific localization and prevents its self-association. *Mol. Biol. Cell* *16*, 2822–2835.
- Palm, W., and Thompson, C.B. (2017). Nutrient acquisition strategies of mammalian cells. *Nature* *546*, 234–242.
- Parkinson, J.E., Sanderson, C.M., and Smith, G.L. (1995). The vaccinia virus A38L gene product is a 33-kDa integral membrane glycoprotein. *Virology* *214*, 177–188.
- Paul, S., and Lal, G. (2017). The Molecular Mechanism of Natural Killer Cells Function and Its Importance in Cancer Immunotherapy. *Front. Immunol.* *8*, 1124.
- Pegram, H.J., Andrews, D.M., Smyth, M.J., Darcy, P.K., and Kershaw, M.H. (2011). Activating and inhibitory receptors of natural killer cells. *Immunol. Cell Biol.* *89*, 216–224.
- Pérez, P., Marín, M.Q., Lázaro-Frías, A., Sorzano, C.Ó.S., Gómez, C.E., Esteban, M., and García-Arriaza, J. (2020). Deletion of Vaccinia Virus A40R Gene Improves the Immunogenicity of the HIV-1 Vaccine Candidate MVA-B. *Vaccines (Basel)* *8*.
- Petersen, J.L., Morris, C.R., and Solheim, J.C. (2003). Virus evasion of MHC class I molecule presentation. *J. Immunol.* *171*, 4473–4478.

- Peterson, V.M., Zhang, K.X., Kumar, N., Wong, J., Li, L., Wilson, D.C., Moore, R., McClanahan, T.K., Sadekova, S., and Klappenbach, J.A. (2017). Multiplexed quantification of proteins and transcripts in single cells. *Nat. Biotechnol.* *35*, 936–939.
- Pham, T.N.Q., Lukhele, S., Dallaire, F., Perron, G., and Cohen, É.A. (2016). Enhancing Virion Tethering by BST2 Sensitizes Productively and Latently HIV-infected T cells to ADCC Mediated by Broadly Neutralizing Antibodies. *Scientific Reports* *6*.
- Pietra, G., Romagnani, C., Moretta, L., and Mingari, M.C. (2009). HLA-E and HLA-E-bound peptides: recognition by subsets of NK and T cells. *Curr. Pharm. Des.* *15*, 3336–3344.
- Piret, J., and Boivin, G. (2020). Pandemics Throughout History. *Front. Microbiol.* *11*, 631736.
- Pollara, J.J., Spesock, A.H., Pickup, D.J., Laster, S.M., and Petty, I.T.D. (2012). Production of prostaglandin E₂ in response to infection with modified vaccinia Ankara virus. *Virology* *428*, 146–155.
- Prod'homme, V., Griffin, C., Aicheler, R.J., Wang, E.C.Y., McSharry, B.P., Rickards, C.R., Stanton, R.J., Borysiewicz, L.K., López-Botet, M., Wilkinson, G.W.G., et al. (2007). The human cytomegalovirus MHC class I homolog UL18 inhibits LIR-1+ but activates LIR-1- NK cells. *J. Immunol.* *178*, 4473–4481.
- Ravenhill, B.J., Soday, L., Houghton, J., Antrobus, R., and Weekes, M.P. (2020). Comprehensive cell surface proteomics defines markers of classical, intermediate and non-classical monocytes. *Sci. Rep.* *10*, 4560.
- Rees, J.S., Li, X.-W., Perrett, S., Lilley, K.S., and Jackson, A.P. (2015). Selective Proteomic Proximity Labeling Assay Using Tyramide (SPPLAT): A Quantitative Method for the Proteomic Analysis of Localized Membrane-Bound Protein Clusters. *Curr. Protoc. Protein Sci.* *80*, 19.27.1–18.
- Resch, W., Hixson, K.K., Moore, R.J., Lipton, M.S., and Moss, B. (2007). Protein composition of the vaccinia virus mature virion. *Virology* *358*, 233–247.
- Reyburn, H.T., Mandelboim, O., Valés-Gómez, M., Davis, D.M., Pazmany, L., and Strominger, J.L. (1997). The class I MHC homologue of human cytomegalovirus inhibits attack by natural killer cells. *Nature* *386*, 514–517.
- Reynolds, M.G., Guagliardo, S.A.J., Nakazawa, Y.J., Doty, J.B., and Mauldin, M.R. (2018). Understanding orthopoxvirus host range and evolution: from the enigmatic to the usual suspects. *Curr. Opin. Virol.* *28*, 108–115.
- Riedel, S. (2005). Edward Jenner and the history of smallpox and vaccination. *Proc.* *18*, 21–25.
- Rodriguez Boulan, E., and Pendergast, M. (1980). Polarized distribution of viral envelope proteins in the plasma membrane of infected epithelial cells. *Cell* *20*, 45–54.
- Röst, H.L., Malmström, L., and Aebersold, R. (2015). Reproducible quantitative proteotype data matrices for systems biology. *Mol. Biol. Cell* *26*, 3926–3931.

Sakuma, T., Noda, T., Urata, S., Kawaoka, Y., and Yasuda, J. (2009). Inhibition of Lassa and Marburg virus production by tetherin. *J. Virol.* *83*, 2382–2385.

Sander, W.J., O'Neill, H.G., and Pohl, C.H. (2017). Prostaglandin E2 As a Modulator of Viral Infections. *Front. Physiol.* *8*, 89.

Sattentau, Q. (2008). Avoiding the void: cell-to-cell spread of human viruses. *Nat. Rev. Microbiol.* *6*, 815–826.

Schmidt, F.I., Bleck, C.K.E., Helenius, A., and Mercer, J. (2011). Vaccinia extracellular virions enter cells by macropinocytosis and acid-activated membrane rupture. *EMBO J.* *30*, 3647–3661.

Schubert, O.T., Röst, H.L., Collins, B.C., Rosenberger, G., and Aebersold, R. (2017). Quantitative proteomics: challenges and opportunities in basic and applied research. *Nat. Protoc.* *12*, 1289–1294.

Schust, D.J., Tortorella, D., Seebach, J., Phan, C., and Ploegh, H.L. (1998). Trophoblast class I major histocompatibility complex (MHC) products are resistant to rapid degradation imposed by the human cytomegalovirus (HCMV) gene products US2 and US11. *J. Exp. Med.* *188*, 497–503.

Silva, P.N.G., Soares, J.A.P., Brasil, B.S.A.F., Nogueira, S.V., Andrade, A.A., de Magalhães, J.C., Bonjardim, M.B., Ferreira, P.C.P., Kroon, E.G., Bruna-Romero, O., et al. (2006). Differential role played by the MEK/ERK/EGR-1 pathway in orthopoxviruses vaccinia and cowpox biology. *Biochem. J* *398*, 83–95.

Smith, G.L., and Law, M. (2004). The exit of vaccinia virus from infected cells. *Virus Res.* *106*, 189–197.

Smith, G.L., Talbot-Cooper, C., and Lu, Y. (2018). Chapter Fourteen - How Does Vaccinia Virus Interfere With Interferon? In *Advances in Virus Research*, M. Kielian, T.C. Mettenleiter, and M.J. Roossinck, eds. (Academic Press), pp. 355–378.

Smith, H.R.C., Heusel, J.W., Mehta, I.K., Kim, S., Dorner, B.G., Naidenko, O.V., Iizuka, K., Furukawa, H., Beckman, D.L., Pingel, J.T., et al. (2002). Recognition of a virus-encoded ligand by a natural killer cell activation receptor. *Proc. Natl. Acad. Sci. U. S. A.* *99*, 8826–8831.

Smith, L.M., Kelleher, N.L., and Consortium for Top Down Proteomics (2013). Proteoform: a single term describing protein complexity. *Nat. Methods* *10*, 186–187.

Sobotzki, N., Schafroth, M.A., Rudnicka, A., Koetemann, A., Marty, F., Goetze, S., Yamauchi, Y., Carreira, E.M., and Wollscheid, B. (2018). HATRIC-based identification of receptors for orphan ligands. *Nat. Commun.* *9*, 1–8.

Soday, L., Lu, Y., Albarnaz, J.D., Davies, C.T.R., Antrobus, R., Smith, G.L., and Weekes, M.P. (2019). Quantitative Temporal Proteomic Analysis of Vaccinia Virus Infection Reveals Regulation of Histone Deacetylases by an Interferon Antagonist. *Cell Rep.* *27*, 1920–1933.e7.

- Soh, T.K., Davies, C.T.R., Muenzner, J., Hunter, L.M., Barrow, H.G., Connor, V., Bouton, C.R., Smith, C., Emmott, E., Antrobus, R., et al. (2020). Temporal Proteomic Analysis of Herpes Simplex Virus 1 Infection Reveals Cell-Surface Remodeling via pUL56-Mediated GOPC Degradation. *Cell Rep.* *33*, 108235.
- Sood, C.L., and Moss, B. (2010). Vaccinia virus A43R gene encodes an orthopoxvirus-specific late non-virion type-1 membrane protein that is dispensable for replication but enhances intradermal lesion formation. *Virology* *396*, 160–168.
- Speth, C., and Dierich, M.P. (1999). Modulation of cell surface protein expression by infection with HIV-1. *Leukemia* *13 Suppl 1*, S99–S105.
- Srivastava, M., Zhang, Y., Chen, J., Sirohi, D., Miller, A., Zhang, Y., Chen, Z., Lu, H., Xu, J., Kuhn, R.J., et al. (2020). Chemical proteomics tracks virus entry and uncovers NCAM1 as Zika virus receptor. *Nat. Commun.* *11*, 3896.
- Stergiou, L., Bauer, M., Mair, W., Bausch-Fluck, D., Drayman, N., Wollscheid, B., Oppenheim, A., and Pelkmans, L. (2013). Integrin-mediated signaling induced by simian virus 40 leads to transient uncoupling of cortical actin and the plasma membrane. *PLoS One* *8*, e55799.
- Sterner, C.S. (1948). A brief history of miasmatic theory. *Bull. Hist. Med.* *22*, 747.
- Stoeckius, M., Hafemeister, C., Stephenson, W., Houck-Loomis, B., Chattopadhyay, P.K., Swerdlow, H., Satija, R., and Smibert, P. (2017). Simultaneous epitope and transcriptome measurement in single cells. *Nat. Methods* *14*, 865–868.
- Sugden, S., and Cohen, É.A. (2015). Attacking the Supply Lines: HIV-1 Restricts Alanine Uptake to Prevent T Cell Activation. *Cell Host Microbe* *18*, 514–517.
- Summers, W.C. (2009). Virus Infection. *Encyclopedia of Microbiology* 546.
- Townsley, A.C., Weisberg, A.S., Wagenaar, T.R., and Moss, B. (2006). Vaccinia virus entry into cells via a low-pH-dependent endosomal pathway. *J. Virol.* *80*, 8899–8908.
- Tscharke, D.C., and Smith, G.L. (1999). A model for vaccinia virus pathogenesis and immunity based on intradermal injection of mouse ear pinnae. *J. Gen. Virol.* *80 (Pt 10)*, 2751–2755.
- Tscharke, D.C., Reading, P.C., and Smith, G.L. (2002). Dermal infection with vaccinia virus reveals roles for virus proteins not seen using other inoculation routes. *J. Gen. Virol.* *83*, 1977–1986.
- Turner, P.C., and Moyer, R.W. (2008). The vaccinia virus fusion inhibitor proteins SPI-3 (K2) and HA (A56) expressed by infected cells reduce the entry of superinfecting virus. *Virology* *380*, 226–233.
- Tyanova, S., Temu, T., Sinitcyn, P., Carlson, A., Hein, M.Y., Geiger, T., Mann, M., and Cox, J. (2016). The Perseus computational platform for comprehensive analysis of (prote)omics data. *Nat. Methods* *13*, 731–740.

- Van Damme, N., Goff, D., Katsura, C., Jorgenson, R.L., Mitchell, R., Johnson, M.C., Stephens, E.B., and Guatelli, J. (2008). The interferon-induced protein BST-2 restricts HIV-1 release and is downregulated from the cell surface by the viral Vpu protein. *Cell Host Microbe* 3, 245–252.
- Vasiliver-Shamis, G., Cho, M.W., Hioe, C.E., and Dustin, M.L. (2009). Human immunodeficiency virus type 1 envelope gp120-induced partial T-cell receptor signaling creates an F-actin-depleted zone in the virological synapse. *J. Virol.* 83, 11341–11355.
- Venter, J.C., Adams, M.D., Myers, E.W., Li, P.W., Mural, R.J., Sutton, G.G., Smith, H.O., Yandell, M., Evans, C.A., Holt, R.A., et al. (2001). The sequence of the human genome. *Science* 291, 1304–1351.
- Vermeire, K., Zhang, Y., Princen, K., Hatse, S., Samala, M.F., Dey, K., Choi, H.-J., Ahn, Y., Sodoma, A., Snoeck, R., et al. (2002). CADA inhibits human immunodeficiency virus and human herpesvirus 7 replication by down-modulation of the cellular CD4 receptor. *Virology* 302, 342–353.
- Veyer, D.L., Carrara, G., Maluquer de Motes, C., and Smith, G.L. (2017). Vaccinia virus evasion of regulated cell death. *Immunol. Lett.* 186, 68–80.
- Viswanathan, K., Verweij, M.C., John, N., Malouli, D., and Früh, K. (2017). Quantitative membrane proteomics reveals a role for tetraspanin enriched microdomains during entry of human cytomegalovirus. *PLoS One* 12, e0187899.
- Vivier, E., Tomasello, E., Baratin, M., Walzer, T., and Ugolini, S. (2008). Functions of natural killer cells. *Nat. Immunol.* 9, 503–510.
- Volz, A., and Sutter, G. (2017). Chapter Five - Modified Vaccinia Virus Ankara: History, Value in Basic Research, and Current Perspectives for Vaccine Development. In *Advances in Virus Research*, M. Kielian, T.C. Mettenleiter, and M.J. Roossinck, eds. (Academic Press), pp. 187–243.
- Volz, T., Allweiss, L., Ben MBarek, M., Warlich, M., Lohse, A.W., Pollok, J.M., Alexandrov, A., Urban, S., Petersen, J., Lütgehetmann, M., et al. (2013). The entry inhibitor Myrcludex-B efficiently blocks intrahepatic virus spreading in humanized mice previously infected with hepatitis B virus. *J. Hepatol.* 58, 861–867.
- Washburn, M.P. (2016). There is no human interactome. *Genome Biol.* 17, 48.
- Weekes, M.P., Antrobus, R., Lill, J.R., Duncan, L.M., Hör, S., and Lehner, P.J. (2010). Comparative analysis of techniques to purify plasma membrane proteins. *J. Biomol. Tech.* 21, 108–115.
- Weekes, M.P., Tomasec, P., Huttlin, E.L., Fielding, C.A., Nusinow, D., Stanton, R.J., Wang, E.C.Y., Aicheler, R., Murrell, I., Wilkinson, G.W.G., et al. (2014). Quantitative temporal viromics: an approach to investigate host-pathogen interaction. *Cell* 157, 1460–1472.
- Wendt, F., Milani, E.S., and Wollscheid, B. (2021). Elucidation of host-virus surfaceome interactions using spatial proteotyping. *Adv. Virus Res.* 109, 105–134.

- Wilcock, D., Duncan, S.A., Traktman, P., Zhang, W.H., and Smith, G.L. (1999). The vaccinia virus A4OR gene product is a nonstructural, type II membrane glycoprotein that is expressed at the cell surface. *J. Gen. Virol.* *80* (Pt 8), 2137–2148.
- Wilder-Smith, A., and Freedman, D.O. (2020). Isolation, quarantine, social distancing and community containment: pivotal role for old-style public health measures in the novel coronavirus (2019-nCoV) outbreak. *J. Travel Med.* *27*.
- Wilkins, M.R., Sanchez, J.C., Gooley, A.A., Appel, R.D., Humphery-Smith, I., Hochstrasser, D.F., and Williams, K.L. (1996). Progress with proteome projects: why all proteins expressed by a genome should be identified and how to do it. *Biotechnol. Genet. Eng. Rev.* *13*, 19–50.
- Williamson, R. (1955). The germ theory of disease. Neglected precursors of Louis Pasteur. *Ann. Sci.* *11*, 44–57.
- Wollscheid, B., Bausch-Fluck, D., Henderson, C., O'Brien, R., Bibel, M., Schiess, R., Aebersold, R., and Watts, J.D. (2009). Mass-spectrometric identification and relative quantification of N-linked cell surface glycoproteins. *Nat. Biotechnol.* *27*, 378–386.
- Xie, J., Sok, D., Wu, N.C., Zheng, T., Zhang, W., Burton, D.R., and Lerner, R.A. (2017). Immunochemical engineering of cell surfaces to generate virus resistance. *Proc. Natl. Acad. Sci. U. S. A.* *114*, 4655–4660.
- Yamauchi, Y., and Helenius, A. (2013). Virus entry at a glance. *J. Cell Sci.* *126*, 1289–1295.
- Yan, H., Zhong, G., Xu, G., He, W., Jing, Z., Gao, Z., Huang, Y., Qi, Y., Peng, B., Wang, H., et al. (2012). Sodium taurocholate cotransporting polypeptide is a functional receptor for human hepatitis B and D virus. *Elife* *1*, e00049.
- Yang, W., Gu, Z., Zhang, H., and Hu, H. (2020). To TRIM the immunity: From innate to adaptive immunity. *Front. Immunol.* *11*, 02157.
- Yang, Z., Bruno, D.P., Martens, C.A., Porcella, S.F., and Moss, B. (2010). Simultaneous high-resolution analysis of vaccinia virus and host cell transcriptomes by deep RNA sequencing. *Proc. Natl. Acad. Sci. U. S. A.* *107*, 11513–11518.
- Yang, Z., Gray, M., and Winter, L. (2021). Why do poxviruses still matter? *Cell Biosci.* *11*, 96.
- Yin, H., and Flynn, A.D. (2016). Drugging Membrane Protein Interactions. *Annu. Rev. Biomed. Eng.* *18*, 51–76.
- Yu, F., Wang, X., Guo, Z.S., Bartlett, D.L., Gottschalk, S.M., and Song, X.-T. (2014). T-cell engager-armed oncolytic vaccinia virus significantly enhances antitumor therapy. *Mol. Ther.* *22*, 102–111.
- Zhang, Y., Shen, Y., Yin, L., Qi, T., Jia, X., Lu, H., and Zhang, L. (2019). Plasma Membrane Proteomic Profile Discovers Macrophage-capping Protein Related to Latent HIV-1. *Curr. HIV Res.* *17*, 42–52.

Zhen, Y., Haugsten, E.M., Singh, S.K., and Wesche, J. (2018). Proximity Labeling by a Recombinant APEX2-FGF1 Fusion Protein Reveals Interaction of FGF1 with the Proteoglycans CD44 and CSPG4. *Biochemistry* 57, 3807–3816.

Zhou, Z., Ye, C., Wang, J., and Zhang, N.R. (2020). Surface protein imputation from single cell transcriptomes by deep neural networks. *Nat. Commun.* 11, 651.

Acknowledgment

My doctorate would have not been possible without the contribution and support of my colleagues, old as well as new friends, and my family. I am grateful for all the continuous interactions, which made the doctorate a rewarding journey in and outside of the laboratory.

First of all, I would like to thank my doctoral supervisor Bernd Wollscheid for your loyal support and scientific advice during this time. But more importantly, you empowered me to grow into a critically-thinking scientist. Thank you, Bernd, for creating a motivating laboratory atmosphere, which enabled me to pursue my scientific interest successfully.

Moreover, I would like to thank my committee, namely Jason Mercer, Paola Picotti, and Berend Snyder for their scientific advice and feedback along the way to my graduation.

A special thank-you is due to the Wollscheid group with all its past and present members. You made the laboratory a feel-good place, and have been giving me a great start and stay in Switzerland. Thank you, Anika, for the countless discussions and valuable feedback on my research work, pushing me in the right direction. Thanks to Kathrin, for always motivating me to bite through with your contagious joyful spirit. Moreover, I really enjoyed the fun apéros.

A huge thank-you goes also to Ema. I am happy, that you showed me the Ticino way of life and additionally for partnering up to write a “too-long” review. Thank you, Marc and Maik, for teaching me the secrets of cell surface capturing and proximity labeling, as well as sharing the after-lunch coffees. I would like to thank Sandra for helping out with technical knowledge when mine reached its limits. Maria, your advice in and outside of the lab was always on point. Sebastian and Jonas, thank you for bringing a fresh perspective to the group and being great lab mates. I enjoyed our numerous conversations about camping and bicycle equipment. Audrey, thank you for providing me with your large knowledge about cloning and cell line generation. Moreover, I would like to thank Patrick for always trying to answer all my bioinformatic questions. Last but not least, a big thanks goes to Damaris, Adithi, Julia, Heidi, Arend, Martin G., Silvana, and Jens for creating a pleasant atmosphere, and always keeping the spirit up.

Furthermore, I would like to thank my collaboration partners, who taught me their expert knowledge and contributed to this journey. I need to thank Moona for her patience while training me in practical virology. You made my time in London a great change from everyday life. Additionally, I thank Richard Kammerer for the expression and purification of viral proteins. Yannik, Ben, Julien, and Thijs, thank you for teaching me the isolation of primary cells and running experiments in a large scale-format.

Over the years, I have had the chance to contribute to many projects with my expertise. In this regard, I am very grateful to all my collaboration partners who trusted me to work with their precious samples and enabled me to grow while running the projects successfully.

A big thank-you needs to go to the Aebersold group for being the best floor mates one could wish for. Especially, thank you, Fabian, Federico, Martin, and Andrea for the scientific exchange. Beyond this, I will miss the after-work time with you!

I would like to thank my parents, Roswitha and Eckhard, for teaching me the meaningful values in life, which form the foundation for this success. Moreover, Mathias, thank you for being a fun and caring brother, always present when needed!

Finally, let me express my deepest gratitude to the person, who shared this journey with me, closely experiencing the happy, as well as hard, but rewarding times. Thank you, Kathrin, for your loving support and joy throughout the years. Your indispensable belief in me and encouragement to believe in myself made it possible. Thank you!

Curriculum vitae

FABIAN WENDT

EDUCATION

09/2016 – 12/2021 **Ph.D. Candidate in Molecular Systems Biology**, ETH Zurich, Switzerland
Department of Health Sciences & Technology, Prof. Dr. Bernd Wollscheid

Thesis: Spatio-temporal elucidation of the vaccinia virus-induced host proteotype

10/2013 – 12/2015 **Master of Science in Biochemistry**, Ruhr-University Bochum, Germany
Medical Proteome Center, Prof. Dr. Kathrin Marcus

Thesis: Body fluid identification with protein mass spectrometry for forensic purposes

10/2010 – 09/2013 **Bachelor of Science in Biochemistry**, Ruhr-University Bochum, Germany

Faculty of Chemistry and Biochemistry, Prof. Dr. Raphael Stoll
Thesis: NMR-based binding studies of Rheb with small organic ligands

EXTRACURRICULAR ACTIVITIES

- **Established the BioMed Travel Grant** (10 x 1000 CHF), financially supported by the Biomed Program at the LSZGS to support Ph.D. students visiting conferences. Est. since 2020.
- **Conference volunteer** at the LS2 Annual Proteomics Meeting Switzerland, 2018
- **Assistant at Scientifica fair** for Nexus Booth Personalized Medicine in Cancer, 2017
- **Tutored pupil groups** at the Public Science Laboratory Day at ETH Zurich, annually, 2016 – 2019

SCHOLARSHIPS

- **LS2 Switzerland Travel Grant** for Ph.D. students (1000 CHF)
- **HUPO 2019 Student/ ECR Travel Award** (1000 AUD)
- **Travel Grant** from the German Society of Chemistry (GDCh) (300 €)
- **Travel Fellowship** from the German Society of Proteome Research (DGPF) (500 €)

PUBLIC TALKS/OUTREACH

- **Talk** at Human Proteome Organization (HUPO), Adelaide, Australia, 2019
- **Talk** at Weil-Cornell-Medicine Qatar symposia, Doha, Qatar, 2019 (invited speaker)
- **Flash talk** at LS2 Annual Swiss Proteomics meeting, Switzerland, Thun, 2017, and Montreux, 2019
- **Poster presentations** at scientific meetings Advanced Proteomics Summer School Brixen 2015, LS2 Annual Meeting 2017, Department Biology Symposium 2018, LSZGS Molecular Translational Biomedicine Meeting 2018 & 2019

LANGUAGES

- German native
- English proficient

PUBLICATIONS

Wendt, F., Milani, E. S., & Wollscheid, B. (2021). Elucidation of host-virus surfaceome interactions using spatial proteotyping. *Advances in Virus Research*, 109, 105–134.

Müller, M., Gräbnitz, F., Barandun, N., Shen, Y., **Wendt, F.**, Steiner, S. N., Severin, Y., Vetterli, S. U., Mondal, M., Prudent, J. R., Hofmann, R., van Oostrum, M., Sarott, R., Nesvizhskii, A. I., Carreira, E. M., Bode, J., Snijder, B., Robinson, J. A., Loessner, M. J., Oxenius, A., & Wollscheid, B. (2021). Light-mediated discovery of surfaceome nanoscale organization and intercellular receptor interaction networks. *Nature Communications*, accepted.

Čuklina, J., Lee, C. H., Williams, E. G., Sajic, T., Collins, B. C., Rodríguez Martínez, M., Sharma, V. S., **Wendt, F.**, Goetze, S., Keele, G. R., Wollscheid, B., Aebersold, R., & Pedrioli, P. G. A. (2021). Diagnostics and correction of batch effects in large-scale proteomic studies: a tutorial. *Molecular Systems Biology*, 17(8), e10240.

Fossati, A., Li, C., Uliana, F., **Wendt, F.**, Frommelt, F., Sykacek, P., Heusel, M., Hallal, M., Bludau, I., Capraz, T., Xue, P., Song, J., Wollscheid, B., Purcell, A. W., Gstaiger, M., & Aebersold, R. (2021). PCprophet: a framework for protein complex prediction and differential analysis using proteomic data. *Nature Methods*, 18(5), 520–527.